The PHILOSOPHICAL MAGAZINE

FIRST PUBLISHED IN 1798

L. 45 SEVENTH SERIES No. 370 November 1954

UNIVERSITY OF HAWAII LIBRARY
DEC 17 '54

A Journal of Theoretical Experimental and Applied Physics

EDITOR
PROFESSOR N F. MOTT, M.A., D.Sc., F.R.S.

EDITORIAL BOARD
SIR LAWRENCE BRAGG, O.B.E., M.C., M.A., D.Sc., F.R.S.
SIR GEORGE THOMSON, M.A., D.Sc., F.R.S.
PROFESSOR A. M. TYNDALL, C.B.E., D.Sc., F.R.S.

PRICE 15s. 0d.
Annual Subscription £8 0s. 0d. payable in advance

D AND PUBLISHED BY TAYLOR & FRANCIS LTD., RED LION COURT, FLEET ST., LONDON, E.C.4.

ERRATUM

The Scattering of Deuterons and Protons by Alpha-Particles, by R. G. Freemantle, T. Grotdal, W. M. Gibson, R. McKeague, D. J. Prowse, and J. Rotblat, 1954, *Phil. Mag.*, **45**, 1093.

An incorrect Q-value for the reaction ^{4}He(d, p)^{5}He was included inadvertently; the value actually obtained was $3{\cdot}3 \pm 0{\cdot}1$ Mev.

CXXII. *A Search for Natural Radioactivity in Neodymium, Rhenium and Osmium*

By D. Dixon and A. McNair
Department of Natural Philosophy, University of Glasgow*

[Received May 6, 1954]

Abstract

The element neodymium and the naturally occurring isobaric pair Rhenium 187 and Osmium 187 are investigated, as internally mounted sources in a well-shielded proportional counter, for evidence of natural radioactivity. The β-decay probability of Neodymium 150 corresponds to a half-life of not less than 10^{16} yr. No beta instability of rhenium is observed and 10^{15} yr. is suggested as the minimum possible half-life for the isotope ^{187}Re. The emission of L x-rays from osmium is observed, but it is found that dense materials show similar emission, and it is attributed to the photoelectric absorption of γ-rays (residual background) in the materials. It is concluded that there is no evidence of decay in osmium and the estimated minimum possible half-life by electron capture exceeds 10^{15} yr.

§ 1. Introductory

There have been various conflicting reports concerning the radioactivity of naturally occurring neodymium. In 1934 Libby attributed a β^--activity of half-life $1{\cdot}5\times10^{12}$ yr. and maximum energy 11 kev to neodymium and in later years evidence, reviewed by Mulholland and Kohman (1952), began to accumulate in favour of β^--activity. More recently Curran *et al.* (1952), in a preliminary survey of neodymium failed to detect any instability within the limits of the sensitivity of their apparatus, and a similar investigation by Mulholland and Kohman (1952), who laid stress on the need for chemical purification in the preparation of sources, increased the minimum possible half-life of ^{150}Nd to 2×10^{15} yr. It was suggested that the β^--decay of ^{150}Nd, which might be expected from a study of nuclear β-stability limits (Kohman 1948), was highly forbidden, due to a large spin change involved in the transition. Interest in the possible instability of naturally occurring ^{145}Nd was heightened on account of its position in the nuclear table with regard to the possible ‘ missing ’ stable isotopes of promethium. Considerations of the systematics of stable nuclei of odd Z (>7) restrict the occurrence of β-stable isotopes of promethium ($Z=61$) to odd A values and further limitations are expressed by the position of known artificially produced radioactive isotopes of Pm. The occurrence of a β^--stable isotope, ^{145}Pm, was considered, and in such circumstances the β^--decay of its neighbouring naturally occurring isobar ^{145}Nd should have been energetically possible (Feather 1952). The discovery, however, by Butement in 1951 of the captive-activity of ^{145}Pm, established indirectly the β^--stability of ^{145}Nd. The isotopes ^{145}Nd and ^{147}Sm thus remain as one of three instances of pairs of β-stable nuclei having the same odd number of neutrons ($Z>7$), stability being achieved seemingly by a single even number of protons in all other nuclei of odd N values. Evidence of alpha-instability in isotopes in the region $N=84$, is provided in several instances among artificially produced radio-isotopes (Thompson *et al.* 1949, Rasmussen *et al.* 1950) and the possibility of α-emission from naturally occurring neodymium isotopes (as suggested by Kohman 1949), was investigated by Mulholland and Kohman (1952) and an activity of less than 0·02 α's per sec per g was obtained, compared with 0·3 α's per sec per g obtained by Bestenreiner and Broda in 1949. Recently Waldron, Schultz and Kohman (1953) using impregnated nuclear plates, have found a natural α-activity in neodymium and have ascribed it to the isotope ^{144}Nd ($N=84$). This report on the investigation of the possible radioactivity of neodymium was completed in March 1953, with the exception of a renewed search for α-activity, which was undertaken following a private communication from Kohman reporting an α-activity of ^{144}Nd of $1{\cdot}9\pm0{\cdot}1$ Mev energy and of half-life $1{\cdot}5\times10^{15}$ yr. In our earlier experiments a very weak α-activity of 1·6 c.p.m. from 1·18 g of Nd was observed and was thought to arise mainly from slight radioactive contamination.

---

* Communicated by S. C. Curran, F.R.S.

§ 2. EXPERIMENTAL ARRANGEMENT

Previous investigations of the radioactivity of some natural radio-elements (Curran *et al.* 1952) showed that the maximum possible efficiency of detection was required, and our experimental equipment has been improved towards this end. The system now in operation (and to be described in detail in a subsequent paper) consists essentially of a large specially designed proportional tube spectrometer completely surrounded by two rings of G.M. counters (72 cm in length) in anticoincidence, and shielded by 8 in. of lead and 1 in. of iron on all sides. This system is situated in the most shielded part of the building, some 10 ft. below ground level. The proportional counter is of the end-corrected type (Cockroft and Curran 1951) with 10 in. of its cathode fully operative and with a diameter of 5·65 in. giving a maximum internal source area of 1100 cm^2. The inner walls of the counter are lined with stainless steel and, together with other refinements, this helped to reduce the total background count rate to less than 16 c.p.m., a value of the same order (for comparative counting volumes) as that observed by Libby *et al.* (1951) and Kulp and Tryon (1952) in their experiments on ^{14}C. This has made possible the more successful investigation of certain radioelements (Dixon *et al.* 1954) and represents a reduction in the background by a factor of 20 relative to that observed in most of our earlier experiments. The pulses from any possible radioactive source are displayed oscillographically and a photographic record is analysed in amplitude to yield the pulse energy spectrum. The proportional counter, used with the anticoincidence system described above, is insensitive to the detection of radiations for only 1% of the time operated. The K x-rays of silver were used for energy calibrating purposes and the resolution, at high gas pressures, corresponded to a full width at half-height equal to 12% of the pulse amplitude. This resolution was maintained throughout the period of operation of the counter and energy calibrations made at intervals during the course of experimental runs up to 12 h duration, invariably remained constant.

Fig. 1

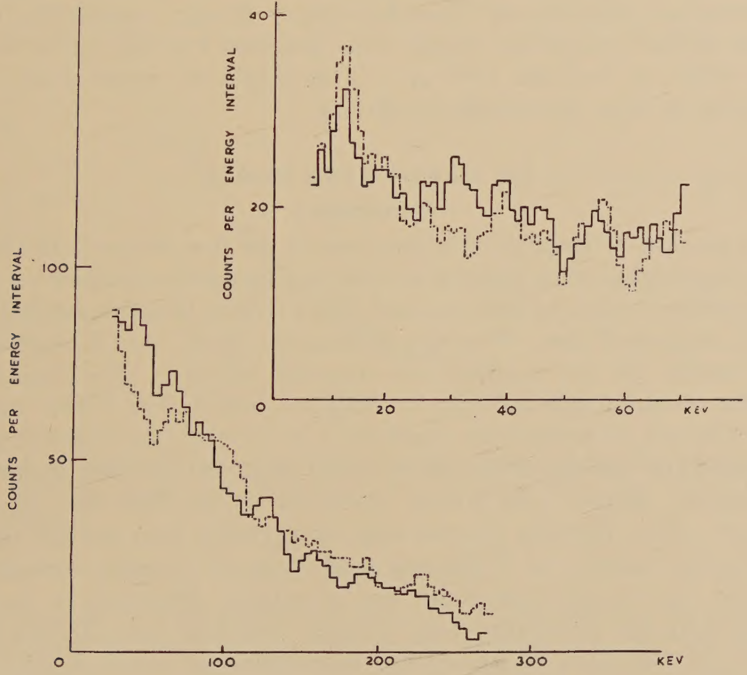

Spectra of background (indicated by broken histogram) and background +1·18 g of neodymium (full histogram).

§ 3. Neodymium

The source of neodymium was mounted on the steel inner lining of the counter in the form of $NdCl_3$, of thickness 2·1 mg/cm^2, obtained from the pure metal. The results of the spectrum analysis for the energy ranges 6–60 kev and 20–300 kev are shown in fig. 1. The counting rates of the total background and background+source at lower energies suggest that if the material is radioactive the half-life is not less than 10^{15} yr. In view of the complete absence of any appreciable difference in the pulse spectra of background and background+source it is likely to be much longer. We conclude that ^{150}Nd is effectively β-stable, a conclusion which is not in contradiction with any known nuclear stability rules. Following the communication from Kohman concerning the suggested α-activity of ^{144}Nd, an attempt was made to measure the energies of the α-rays previously observed in the experiments described above. Due to the unfavourable nature of the source and its thickness (2·1 mg/cm^2) our results, which did however indicate the presence of α-rays of energy $<2{\cdot}0$ Mev ($\sim$1·5 c.p.m.) must, in the main, be regarded as inconclusive. Earlier investigations of low energy α-rays following the natural decay of ^{147}Sm (Dixon 1953) illustrated the success that can be achieved in energy measurements of α-activities of long life-time, using thin uniform sources of finely divided powder internally mounted in proportional spectrometers. Energy resolution of 5% (width at half maximum height) was obtained for the 2·22 Mev α-rays from ^{147}Sm of half-life 10^{11} yr. It is hoped to re-examine Nd for α-activity in more favourable conditions.

§ 4. RHENIUM AND OSMIUM

Introductory

The isotopes ^{187}Re and ^{187}Os form one of the few instances of naturally occurring neighbouring isobars, so that one should be radioactive. Some of the earlier studies by Scherrer and Zingg (1939), Lougher and Rowlands (1944), suggested that ^{187}Os was radioactive by K- and L-capture, but later results did not confirm this reported activity. The examination of both rhenium and osmium by Naldrett and Libby (1948) indicated that ^{187}Re was β^--active with a half-life, τ, $4 \pm 1 \times 10^{12}$ yr., whilst Sugerman estimated the half-life to be almost twice as great. In their examination of osmium, Seliger and Bradt (1948) failed to find any significant activity. More recently Gauthé and Blum (1953) used nuclear plates to confirm the activity of ^{187}Re and work done in Glasgow seemed to do likewise, but in our case there was a notable difference in the value obtained for the maximum β-ray energy. Naldrett and Libby proposed 43 kev on the basis of absorption measurements, while a preliminary report by Curran (1952) on our own investigation of the form of the spectrum suggested that the β-rays had a limiting energy of about 400 kev. Since that time we have considerably reduced our ‘ background ’ as indicated above, and in the process found that most of the β-particles previously thought by us to be emitted from ^{187}Re were due entirely to the differing radioactive contamination of the aluminium sheets on which the source had been mounted, and that which was used as the inner lining of the proportional counter. This result indicates the need for very careful and constant checking of all materials used in the mounting of sources.

Experimental Arrangement

The same apparatus was used as in the earlier neodymium experiments. Two sources of thickness 0·686 mg/cm² and 0·423 mg/cm² were prepared using spectrographically pure rhenium metal and both were mounted in turn on the steel lining of the counter in the form of finely divided metallic powder held in suspension in a solution of amyl acetate, in which was dissolved a trace of nylon to act as an adhesive agent. The source areas were 900 cm².

Fig. 2

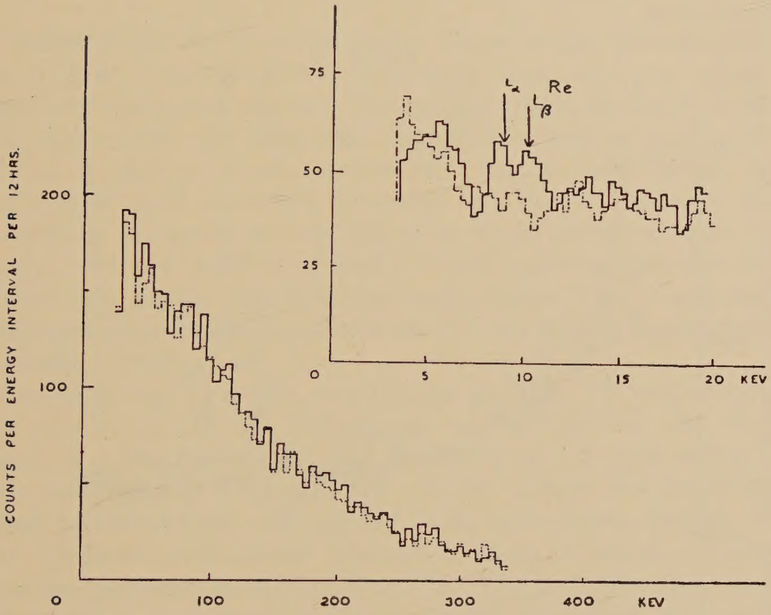

Spectra of background (indicated by broken histogram) and background+source (full histogram) for rhenium (0·62 g in main curve and 0·38 g in inset figure).

Spectrum Analysis

The results of this more thorough search for activity in ^{187}Re are shown in fig. 2, which covers two energy ranges. The spectra show no evidence of activity from the element, as hitherto assumed, and in the two energy ranges the counting rates of background and background+source were :

Wt. of source	Range in kev	Background counts/12 h	Background +source/12 h	Increase per 12 h
0·617 g	30–350	13038 ± 115	12853 ± 113	-185 ± 227
0·3805 g	3·3–20	2204 ± 47	2292 ± 48	$+ 88 \pm 95$

The corresponding minimum half-lives calculated from the above results for ^{187}Re are $1{\cdot}3 \times 10^{16}$ yr. and $1{\cdot}5 \times 10^{15}$ yr. respectively, but the complete absence of any trend in the curves leads us to conclude that 10^{16} yr. is a conservative estimate of the minimum possible half-life unless the energy of the β-rays is exceptionally low. Counting rates at lower energies confirmed the absence of β-particles down to about 1·0 kev. The occurrence of L x-rays of Re was noted on the lower energy curve and reference to this is made later in the paper. If allowance for the presence of these L x-rays is made, the above calculated half-lives of ^{187}Re will both be approximately $1{\cdot}4 \times 10^{16}$ yr. for the two energy ranges covered.

Fig. 3

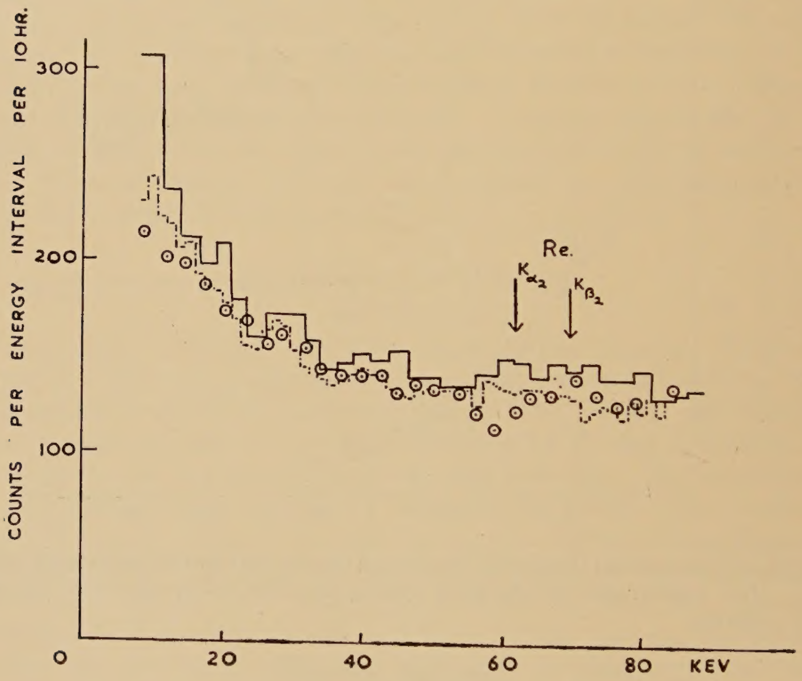

Spectra for osmium. (1) Background, marked ⊙. (2) Background+1·5 g Os, indicated by broken histogram and (3) background+7·5 g Os, shown by full histogram.

§ 5. Osmium

The negative results for rhenium given above led us to examine osmium in the form of a chemically stable oxide of purity greater than 99%. The sources employed contained 1·5 g and 7·5 g of osmium and a particularly close search was made for both K and L x-radiation, as it seemed not unlikely that decay by electron capture would take place. It had previously been verified that no γ-radiation, including annihilation quanta, was emitted so positron decay was eliminated.

Nylon in amyl acetate was used as a holding material for the sources and the results of the spectrum analysis in the region of the K x-rays of Re are tabulated below.

Background per 12 hours	Background +1·5 g Os per 12 hours	Background +7·5 g Os per 12 hours
1987±44	2127±46	2264±47

The spectrum for this K x-ray region, fig. 3, shows no evidence of a peak so that we conclude that if K-capture occurs it is not clearly set in evidence by these experiments. The gas absorption for the Re K x-rays was not high at the gas pressures employed (4 atm of argon) so the question of K-capture remains uncertain. In the lower energy region positive results were seemingly obtained and fig. 4 illustrates clearly the occurrence of x-rays in the region of Re L x-ray energies. Two separately observed difference spectra using different sources of the same mass gave similar peaks in the energy range 7 to 11 kev and the counting rates between the limits 6·0 and 13·3 kev were in good agreement over a period of 12 h.

The origin of the L x-rays was studied further. It was noted that a slight general rise in the background was obtained on the insertion of osmium into the counter and the possibility of L x-rays arising from external conversion of γ-rays in the osmium source was investigated. The effect of introducing a 20 mg/cm^2 lining of tungsten powder and a sheet of platinum 54·6 mg/cm^2 are shown in fig. 5 where L x-rays of tungsten and platinum are clearly observed. We must, therefore, presume that most of L x-rays observed, using the osmium source, are produced in the photoelectric interaction in the K and L shells, of γ-rays passing through the proportional counter, undetected by the G.M. anticoincidence system. Accurate quantitative data regarding the comparative number of L x-rays produced by osmium and tungsten as sources is lacking owing to an unavoidable change of site for the equipment. It would seem, however, from the following table, giving the number of L x-rays produced by three different elements, that by far the greater fraction of L x-rays arising from the osmium must be attributed to this photo-effect.

Element	Source of thickness mg/cm^2	No. of L x-rays observed per hour
Os	8·3	38
W	10·2	43
Pt	54·6	80

It is hoped to re-examine osmium in the near future, comparing the emission of L x-rays with those arising from a similar mass of tungsten under identical conditions.

A search for K x-rays from Os was made with a scintillation counter heavily shielded from background radiation. The NaI crystal was surrounded first with tungsten powder to obtain the background spectrum

Fig. 4

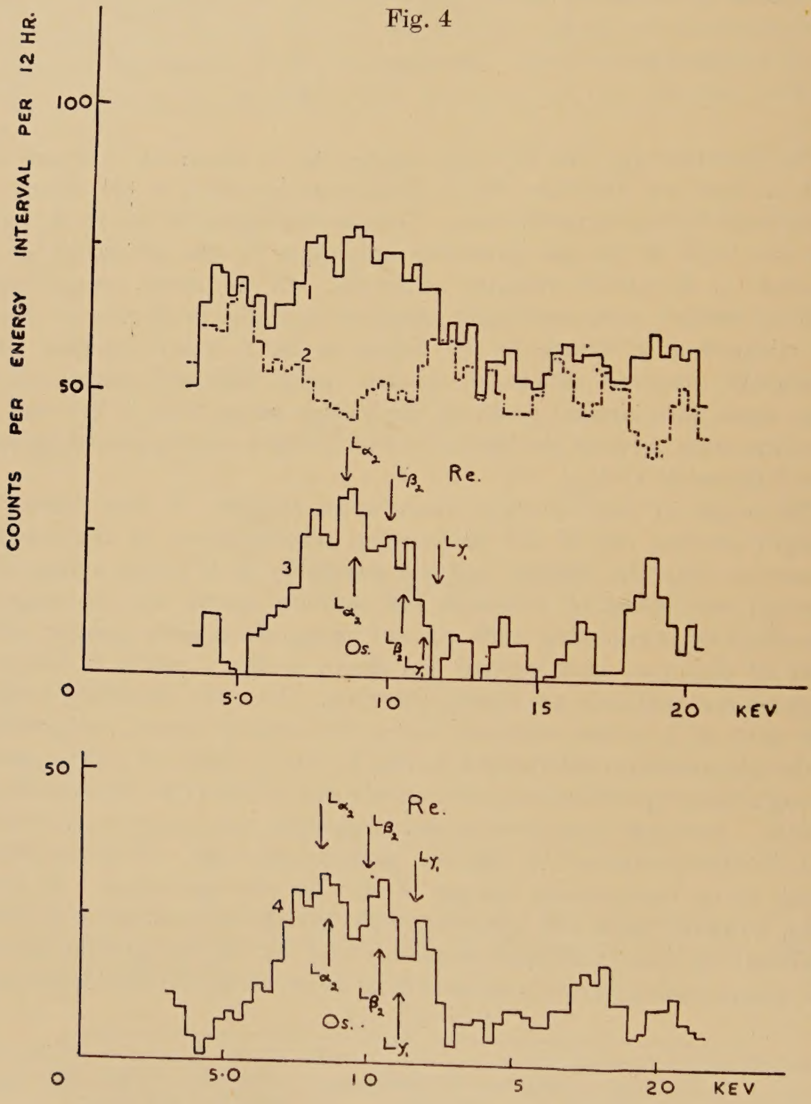

Low energy region of osmium spectra. Histogram 2 represents the background, 1 the background+source of 7·5 g Os and 3 the difference of 1 and 2. Histogram 4 is the difference spectrum of another source of 7·5 g osmium. The peak due to L x-radiation is clearly shown between 7–11 kev.

Fig 5

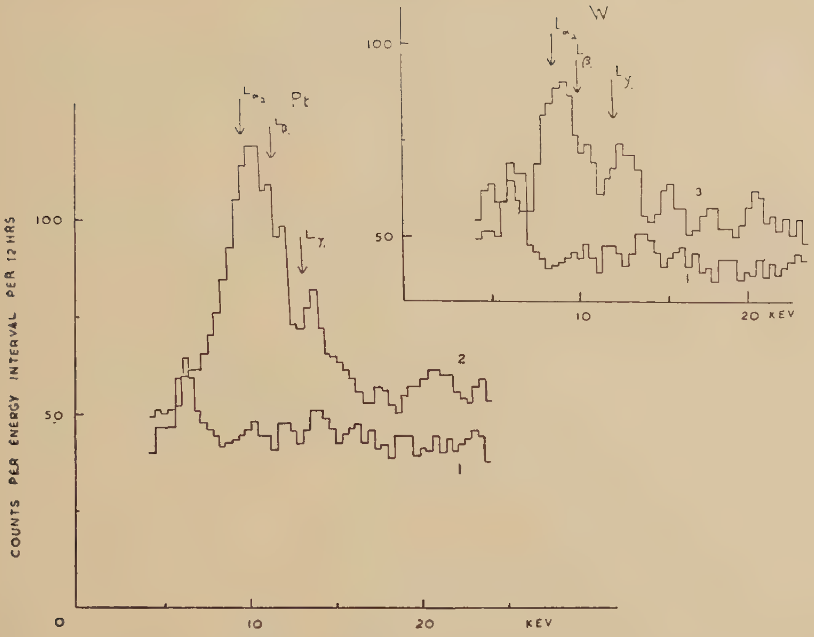

Low energy region of platinum and tungsten spectra. Histogram 1 represents the background, 2 the background+platinum source 54·6 mg/cm^2 and 3 the background+tungsten source 10·2 mg/cm^2.

Fig. 6

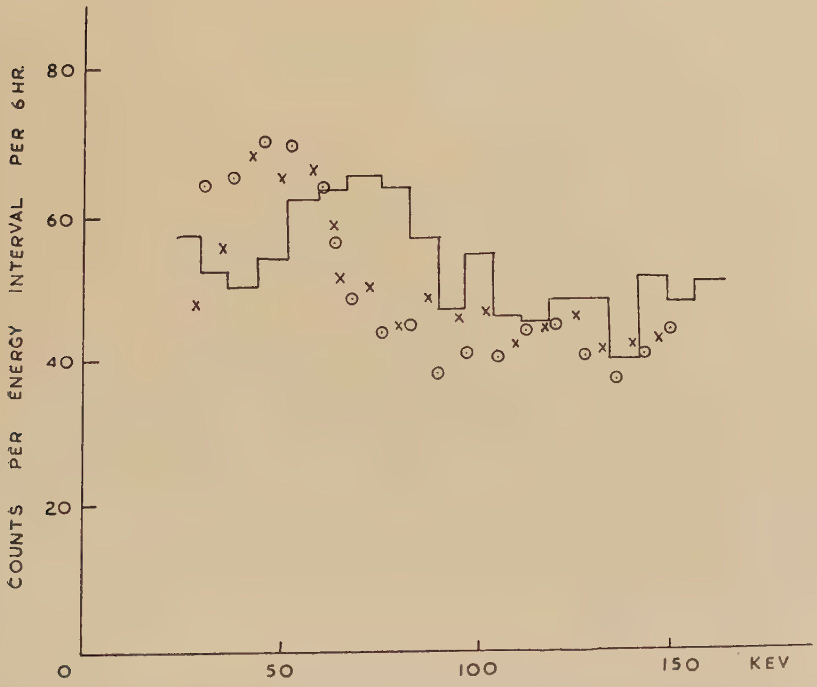

Spectra obtained with scintillation counter surrounded by tungsten and osmium. (1) Background represented by full histogram, (2) background+tungsten source marked ×, and (3) background+osmium source marked ⊙.

and subsequently with a similar mass of osmium >10 g. The results of this investigation are shown in fig. 6, from which we conclude that if K-capture does occur in ^{187}Os its decay probability is very small.

§ 6. DISCUSSION

The search for radioactivity in rhenium and osmium shows that the minimum value of the half-life, for whichever is unstable, exceeds 10^{15} yr. The very small decay probability that must be associated with either suggests that the energy release is small, a conclusion in agreement with the energetic studies of Jensen and Suess (1951). It is unlikely that there exists a naturally occurring stable isobaric pair and it is assumed that the instability associated with either one of these isotopes is beyond the limits of detection of our apparatus.

ACKNOWLEDGMENTS

We should like to take this opportunity to thank Professor P. I. Dee for his interest and encouragement and Dr. S. C. Curran for many helpful discussions throughout the course of this research. One of us (A. M.) is indebted to the Department of Scientific and Industrial Research for a financial grant.

REFERENCES

ANDERSON, E. C., ARNOLD, J. R., and LIBBY, W. F., 1951, *Rev. Sci. Instrum.*, **22,** 225.
BESTENREINER, F., and BRODA, E., 1949, *Nature, Lond.*, **164,** 919.
BUTEMENT, F. D. S., 1951, *Nature, Lond.*, **167,** 400.
COCKROFT, A. L., and CURRAN, S. C., 1951, *Rev. Sci. Instrum.*, **22,** 37.
CURRAN, S. C., 1952, *Physica*, **18,** 1161.
CURRAN, S. C., DIXON, D., and WILSON, H. W., 1952, *Phil. Mag.*, **43,** 82.
DIXON, D., 1953 (unpublished).
DIXON, D., MCNAIR, A., and CURRAN, S. C., 1954, *Phil. Mag.*, **45,** 683.
FEATHER, N., 1952, *Nuclear Stability Rules C.U.P.*
GAUTHÉ, B., and BLUM, J. M., 1953, *C. R. Acad. Sci. Paris*, **236,** 1255.
KOHMAN, T. P., 1948, *Phys. Rev.*, **73,** 16; 1949, *Ibid.*, **76,** 448.
KULP, J. L., and TRYON, L. E., 1952, *Rev. Sci. Instrum.*, **23,** 296.
LIBBY, W. F., 1934, *Phys. Rev.*, **45,** 845.
LOUGHER, E. T., and ROWLANDS, S., 1944, *Nature, Lond.*, **153,** 374.
MULHOLLAND, G. I., and KOHMAN, T. P., 1952, *Phys. Rev.*, **85,** 144.
NALDRETT, S. M., and LIBBY, W. F., 1948, *Phys. Rev.*, **73,** 487.
RASMUSSEN, J. O., REYNOLDS, F. L., THOMPSON, S. G., and GHIORSO, A., 1950, *Phys. Rev.*, **80,** 475.
SCHERRER, P., and ZINGG, E., 1939, *Helv. Phys. Acta*, **12,** 283.
SELIGER, H. H., and BRADT, H. L., 1948, *Phys. Rev.*, **73,** 1408.
SUESS, H. E., and JENSEN, J. H. D., 1951, *Ark. Fys.*, **3,** 577.
SUGERMAN, N., 1948, *Phys. Rev.*, **73,** 1410.
SUGERMAN, N., and RICHTER, M., 1948, *Phys. Rev.*, **73,** 1411.
THOMPSON, S. G., GHIORSO, A., RASMUSSEN, J. O., and SEABORG, G. T., 1949, *Phys. Rev.*, **76,** 1406.
WALDRON, E. C., SCHULTZ, V. A., and KOHMAN, T. P., 1953 (unpublished).

CXXIII. *Time Variations of Extensive Air Showers and the Origin of Cosmic Rays*

By T. E. Cranshaw and W. Galbraith
Atomic Energy Research Establishment, Harwell*

[Received May 28, 1954]

Abstract

An experiment is described in which sixteen Geiger counters each of area 200 cm² arranged on a square lattice of 54 m pitch were used in coincidence to count showers of energies about 10^{16}, 2×10^{16}, 5×10^{16} and 10^{17} ev. From the shower rates, no evidence of a deviation from the power law spectrum, $R(>E)\propto E^{-1\cdot7}$, was found. The results are analysed in solar and sidereal time. In solar time no variations greater than 1% for the 10^{16} ev showers or 10% for the 10^{17} ev showers were found, and these amplitudes could easily arise as a result of statistical fluctuations. In sidereal time, no variation greater than 0·6% was observed at an energy of 10^{16} ev. At 2×10^{16} and 5×10^{16} ev, small variations were observed which had about 1% chance of being due to random fluctuations. The bearing of these results on theories of the origin of cosmic rays is discussed.

§ 1. Introduction

Experiments have been reported in which the rates of recording cosmic ray events as a function of time were studied, and when variations were observed, attempts have been made to assign the cause. Two types of variation can be distinguished, and these have been called primary and secondary variations. Primary variations are variations which have to be ascribed to a property of the primary radiation at some distance from the earth, whereas secondary variations can be ascribed to local meteorological or geomagnetic conditions. At low primary energies ($\sim10^{10}$ ev) such as can be studied by counting neutrons or the total ionizing radiation, both types of variation have been observed (Elliot 1952). It appears that at these low energies, most of the primary variation can be described as a distortion by electromagnetic fields in the solar system of an external isotropic distribution, together with the emission of particles by the sun. Large increases in this emission have been shown to occur during solar flares (Adams 1950, Simpson 1953). The data for these energies have been analysed in sidereal time by Elliot and Dolbear (1951), who conclude that a variation of about 0·02% with a maximum at 0500 h L.S.T. is probable.

---

*Communicated by W. J. Whitehouse.

At somewhat higher energies (10^{12} ev), effects due to electromagnetic fields in the solar system may be expected to be much reduced, and primary variations would then be observed in sidereal time, and would relate to the radiation outside the solar system. Primary particles of energy about 10^{13}–10^{14} ev have been studied in attempts to observe such effects by counting μ-mesons underground. In an experiment of this type Cocconi (1951) found no correlation with either solar or sidereal time to within a statistical accuracy of 3% in the rate of arrival of μ-mesons. Barrett and Eisenberg (1952) and Sherman (1953) also found no evidence for anisotropy greater than 2% and 0·5% respectively. In a similar experiment, Sekido *et al.* (1951) reported an effect of 10% with a 2% significance level, the maximum being at 0500 h L.S.T. Other observations at this and higher energies have been made by counting the extensive air showers produced by interactions of the primaries with air nuclei. Hodson (1951) recording showers of estimated energy 5×10^{14} ev found a variation in sidereal time of $(1{\cdot}15\pm0{\cdot}61)\%$ with the maximum at 2330 h L.S.T. Daudin and Daudin (1953) found a sidereal variation of about 2% with the maximum between 20 and 23 h for showers of estimated energy about 10^{15} ev. Citron (1952) however found no significant sidereal effect, but a small solar effect of about 1%. Recently, Farley and Storey (1954) have reported a small but apparently significant sidereal variation for showers of energy probably between 10^{13}–10^{14} ev. When corrected for a seasonal effect, the amplitude of the first harmonic of the sidereal variation is $1{\cdot}5\pm0{\cdot}23\%$ with a maximum at 1700 h L.S.T.

It seems that the only conclusion which can be drawn from these results is that the radiation of energy less than 10^{15} ev is isotropic to within 1% or 2%. The dissentient results can hardly be considered as statistically significant when considered as part of the total number of experiments.

In the present experiment we have extended this result to an estimated energy of 10^{16} ev by counting extensive air showers. At an estimated energy of 5×10^{16} ev some indication of a sidereal variation is reported, and a possible interpretation suggested. The secondary variations observed during the course of this work appear to be due almost entirely to changes in barometric pressure, and will be described in a later report.

§ 2. DESCRIPTION OF THE APPARATUS

The counter arrangement used in the present experiment is shown in fig. 1. ABC . . . P represent stations, separated by 54 metres. Each station contains a single G.M. counter of area 200 cm², filled with an ethyl formate–argon mixture, which is found to eliminate the need for temperature control. To obtain the greatest reliability over long periods, each counter fed into a quench unit, which, at each count, reduced the potential on the wire below the Geiger threshold for a period of 0·5 msec. The quench pulse also triggered a blocking oscillator circuit, which generated a 30 v, 1 μsec pulse in a coaxial cable, terminated by a 70 ohm resistor in the central trailer at Q. Delay lines were inserted in the cables from F, G, J and K to make the total delay from all the stations the same.

In the trailer, the pulses from the stations are arranged to cut off the current in one of sixteen triodes, whose anodes, connected together, are supplied from the cathode of another triode whose grid is maintained at +150 v (fig. 2). The current through each of the sixteen triodes is stabilized at 2·5 ma by a large cathode resistor connected to a negative supply. Thus each pulse changes the total current by 2·5 ma, and makes a pulse of 10 v in a 4K resistor. These pulses are fed into three discriminators, with thresholds at 22, 32, and 42 volts. Thus the first is triggered by a 3-fold coincidence, and the second and third by 4- and 5-fold coincidences.

Fig. 1

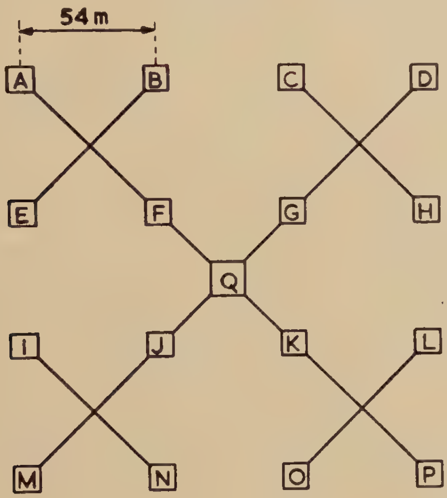

G.M. Counter arrangement.

The events were recorded by five pens on a moving chart. Two pens were used to make a mark each solar and sidereal half hour, and the other three pens recorded 3-, 4- and 5-fold coincidences.

The resolving time of the coincidence circuit was 1 μsec, and the total rate of all sixteen counters was about 100/sec. The calculated random counting rate of 3-fold events was about 0·5% of the true rate and was neglected.

An additional piece of apparatus was a neon hodoscope. This consisted of twenty-four coincidence circuits, eight of which do not concern the present experiments, each connected to a double triode circuit arranged to switch off a small neon lamp when triggered. This hodoscope was more reliable in operation than one in which the neon lamps were switched on when a shower was detected. The coincidence circuits were fed from the sixteen stations, and also from a master pulse produced whenever the 3-fold discriminator was triggered. A photograph was then taken automatically. In this way, a record of which counters were involved in each coincidence was obtained. These records were used to make the analysis of 8-fold coincidences referred to later. A report on the study of the structure of air showers from these records is also in preparation.

Fig. 2

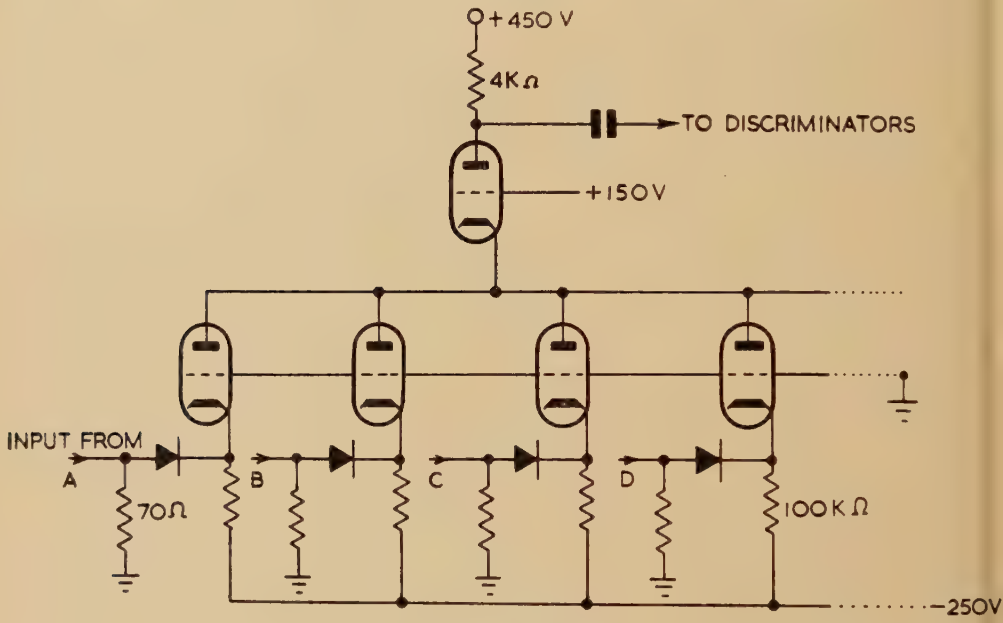

Pulse adding circuit.

A ratemeter and pen recorder was used to provide automatic checking of the operation of the counter stations. The input of the ratemeter was connected to the signal lead from each of the stations in succession for a period of half an hour. Thus each counter was checked three times a day. Faults and breakdowns could easily be detected, and the suspect part of the record was excluded from the analysis.

In order to eliminate spurious pulses from the mains, the apparatus was run from a motor alternator. At intervals, the apparatus was run with the H.T. on the Geiger counters below their threshold. No spurious coincidences were observed during these periods.

§ 3. Analysis of the Results

Calculations based upon different assumptions about the lateral structure of air showers, including the Molière structure function (Molière 1946), were made to estimate the energy of the primary particles producing the showers. All the calculations broadly agree that the most probable number of particles in showers which cause 3-fold coincidences is about 7×10^5, and the mean number about 10^6. This number is then used in conjunction with cascade theory (Rossi and Greisen 1941) to arrive at the energy value quoted in the table, col. 1.

Shower Events		Solar Time						Sidereal Time					
		Fundamental			2nd harmonic			Fundamental			2nd harmonic		
Energy ev	Rate/h	Prob.	Amp. %	Phase	Prob.	Amp. %	Phase	Prob.	Amp. %	Phase	Prob.	Amp. %	Phase
$>10^{16}$	10·1	51	0·61	—	30	0·82	—	49	0·63	200°	12	1·1	117°
$>2\times10^{16}$	3·18	87	0·50	—	10	2·0	—	9·8	2·05	143°	0·7	3·0	111°
$>5\times10^{16}$	1·27	37	2·2	—	35	2·2	—	0·7	4·9	157°	8·1	3·5	135°
$>10^{17}$	0·18	56	6·7	—	65	5·8	—	27	10·1	60°	90	2·8	153°

The other energy values have been derived in the same way. The table, col. 2, shows the rate at which showers were observed. If we could assume that the ‘ sensitive area ’, i.e. the area inside which the cores of the showers must fall in order that a coincidence should be recorded, was independent of energy, we could deduce directly that the energy spectrum in this region was given by $R(>E) \propto E^{-1\cdot7}$, $R(>E)$ being the rate of incoming primaries with energy greater than E. In fact, the sensitive area is likely to be smaller for large showers than for small ones. The value 1·7 for the exponent is thus an upper limit. We therefore conclude that the usual power law spectrum (Hilberry 1941, Barrett *et al.* 1952) continues at least to 10^{17} ev.

The results were also analysed in the following way. The chart from the 5 pen recorder was examined, and the number of events of each type occurring between the half-hour marks in solar and sidereal time counted. Forty-eight columns were then drawn up containing the number of counts obtained between 0000 h and 0030 h, between 0030 and 0100 h and so on through the day. A record of the number of days examined for each half hour interval was also taken so that when all the charts were analysed, the counts in each half hour interval could be normalized to the same number of running days. A similar analysis was undertaken from the hodoscope films for 8-fold events. The results obtained by taking the counts in 24 hourly intervals are shown in fig. 3. The heavy line is the mean rate, and the dotted lines represent the standard deviation. By visual inspection one can see that there are no large variations with either solar or sidereal time. In order to put this result more quantitatively, we have calculated the amplitude of the best sine wave through the points and also the amplitude of the second harmonic. These values are given in the table, columns 4, 7, 10, 13 and in columns 3, 6, 9, 12 are given the probabilities that such an amplitude should arise as a result of random fluctuations (Chapman and Bartels 1940).

It is immediately clear that there are no significant variations in solar time. Out of 8 analyses, only one has a significance level greater than 10%, a result which might easily be obtained if the counts were distributed at random. We conclude that the showers producing 3-fold coincidences in this apparatus are isotropic to better than 1% in solar time, the 5-fold coincidences to about 2%, and the 8-fold coincidences to about 6%.

Fig. 3

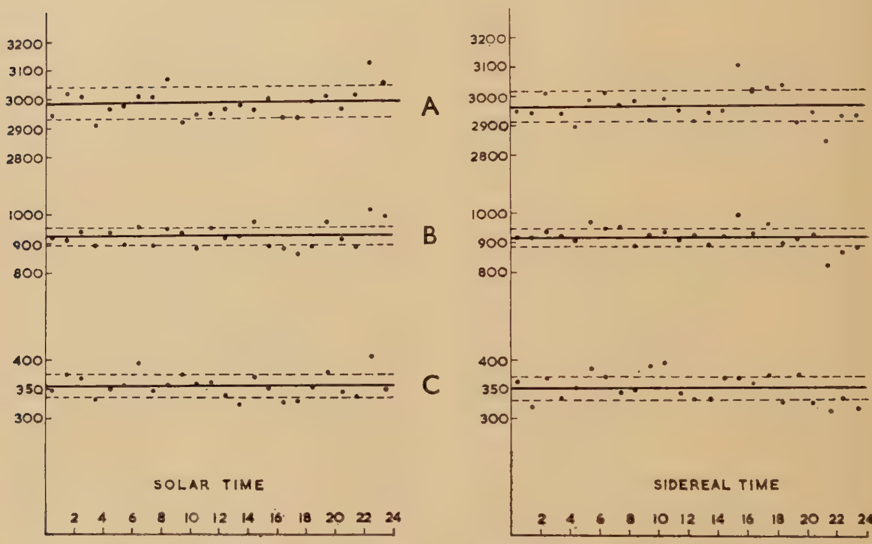

Shower Energies: A$\geqslant 10^{16}$ ev; B$\geqslant 2\times 10^{16}$ ev; C$\geqslant 5\times 10^{16}$ ev.

In the sidereal analysis, we again have no very compelling result. However, two out of the eight analyses reach a significance level of about 1%, and this must be regarded as suggestive. The phases and amplitudes of the sine waves have been plotted on a harmonic dial in fig. 4, where the dotted circles represent the standard deviation, and the solid circles the 10% probability level. On this diagram, the probability of the 'true' point being outside the standard deviation circle is 61%, and therefore the standard deviation circles are quite likely not to intersect, even if the true phase and amplitude are the same in each case. However, it can be seen that a constant phase and amplitude of about 1000 h and 3% would be consistent with the results, but it also seems reasonable to suggest a constant phase and an amplitude which increases with the energy of the showers.

The relatively large value of the second harmonic indicates that the distribution shows some rather rapid change. This appears to be a decrease in the region 20–24 h L.S.T. However, we wish to emphasize, that although the statistical uncertainty looks quite small, experience shows that it is unwise to rely on any single result.

§ 4. Discussion

We wish now to consider these results in the light of some theories of the origin of the cosmic radiation which have been put forward in recent years.

It was suggested (Richtmeyer and Teller 1949, Alfvén 1949) that the origin of all the cosmic radiation was the sun and that the particles emitted were kept circulating about in the neighbourhood of the solar system by the action of an extended magnetic field of strength $\sim 10^{-5}$ gauss. By circulating in this field for period 10^3–10^8 years, the cosmic radiation would become isotropic. The upper limit in energy at which isotropy is observed is that at which the magnetic field is no longer able to retain the particles in orbits through the solar system. On this theory it was expected that no protons in excess of 10^{14} ev and no other particles in excess of 10^{16} ev would be observed.

Fig. 4

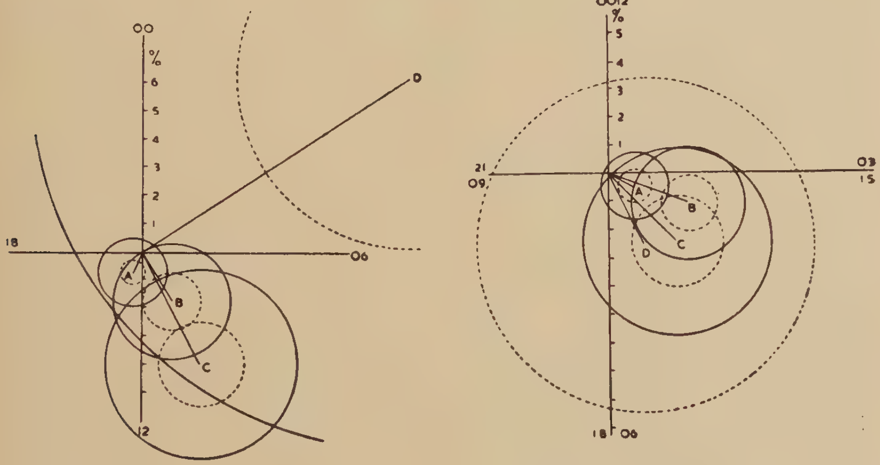

(*a*) Fundamental. (*b*) 2nd Harmonic.

Dotted circles—standard deviation. Full circles— 10% probability.

The result of the present experiment shows that there is a remarkable degree of isotropy in the primary radiation even up to 10^{16}–10^{17} ev and that the power law energy spectrum still holds in this energy region. This contradicts the conclusions of the Richtmeyer–Teller theory and supports the hypothesis that the highest energy primary particles are not solar in origin. The radius of curvature for a particle of 10^{17} ev in a field of 10^{-5} gauss is 30 light years (1 lyr $\cong 10^{18}$ cm) which shows that the orbits of such particles would be in interstellar space and thus the particles would not be retained in the neighbourhood of the sun. In other discussions (Cocconi 1951, Barrett *et al.*, *loc. cit.*) it has also been pointed out that, although a solar origin may be ascribed to the lowest energy primaries, the highest energy particles must come from the interstellar space of the galaxy as a whole.

Another theory developed at the same time as Richtmeyer's and Teller's was that of Fermi (1949). In this, he suggested a mechanism whereby the cosmic ray particles could be accelerated as a result of collisions with the magnetized gas clouds which wander through interstellar space. The particle's energy increases in opposing collisions and decreases in overtaking collisions, but since the former are more probable, a nett gain of energy results. Provided that the nett gain of energy exceeds the energy lost by ionization, the particle energy increases until it is finally lost in some catastrophic collision. The sources of the highest energy particles (i.e. the sites of the last accelerating collision) would be more or less evenly distributed throughout interstellar space. Fermi showed that these assumptions led to a power law energy spectrum of the primary radiation, but with the rate of increase of energy assumed by him, it was not possible to accelerate the heavy ions, owing to their large ionization loss.

The Fermi theory has recently been modified and extended by Morrison, Olbert and Rossi (1954). These authors assume a more rapid energy gain and a loss of particles to intergalactic space. This modification allows the acceleration of heavy nuclei. By applying diffusion theory to the scattering by the gas clouds and determining the age velocity distribution of the particles, it is shown that a power law spectrum is again obtained for both protons and heavy nuclei. To explain the isotropy of the low energy primaries it has to be assumed that the average distance between scattering centres is only 1 light year, and the theory predicts that the power law spectrum should fail above about 10^{15} ev, at which energy, anisotropy should become apparent. This again is contradicted by the results of the present experiment.

More information about the magnetic field in interstellar space has been given in recent papers (Fermi and Chandrasekhar 1953). It is now believed that this field (still of average strength $\sim 10^{-5}$ gauss) is directed along the spiral arms of the galaxy, and it is supposed that magneto-hydrodynamic waves, of wave length $\sim 10^{4}$ light years and amplitude $\sim 10^{-6}$ gauss, travel along these arms with a velocity of the order of 10^{6} cm sec^{-1}. It has been suggested to us by W. B. Thompson that such waves may play an important part in accelerating the cosmic ray particles by means of a rather complicated betatron effect, which occurs during the time when the magnetic field is increasing, and which accelerates the particles between collisions of the type suggested by Fermi. The particles would in general be confined within the spiral arm. If this suggestion proves to be correct, the time variations of the primary radiation will have to be related to our position in the spiral arm, and to the motions of the particles within it. Speculations on this point would lead us to look for anisotropy of the high energy radiation connected with (1) a drift of particles along the arm, (2) a drift outwards along the radii, (3) motion round the arm. Such speculations will have little weight until both the theory and the observations are more definite. Even before this suggestion had been made, it had, however, occurred to us that the minimum indicated at 20–24 h L.S.T. takes place at a time when the apparatus is facing inwards along the spiral arm in which the solar system is situated.

It is evident from this short discussion that the results of the experiment have a considerable bearing on our knowledge of the origin of cosmic rays, since each of the current groups of theories (i.e. those based on a solar origin and those based on acceleration in interstellar space) would have to be modified to explain the apparent isotropy and power law energy spectrum in the region 10^{16}–10^{17} ev.

It is unfortunate that observations of showers at sea level cannot, as far as we know, give any information about the nuclear charge of the primary particle. This can only be studied in nuclear emulsions at great altitude and the area of the apparatus is then so small that statistically valid measurements are virtually impossible for energies above 10^{13} ev. However, further knowledge of the distribution in energy (i.e. the power law) of the highest energy primary particles and of their distribution in direction, independent of the nuclear charge, will be valuable. This can only be obtained by increasing, very greatly, the area in which extensive showers can be observed. We are therefore planning a larger experiment of the type described here, to test the power law and search for time variations in the region 10^{17}–10^{18} ev. In this connection it is interesting to note that the radius of curvature of a proton with an energy of $\sim 10^{18}$ ev in a field of 10^{-5} gauss, is 3×10^{20} cm which is nearly equal to the supposed radius of the spiral arm. We shall therefore be approaching a region of energy in which we might expect some change in the behaviour of the radiation, quite independent of the details of any theory of the acceleration of the particles.

ACKNOWLEDGEMENTS

We are grateful to Mr. W. J. Whitehouse for criticism of this paper and to Dr. W. B. Thompson for some discussion about the origin of the cosmic radiation. We also wish to thank Mr. A. M. McIntyre and his staff who undertook the initial layout of the lattice array. We thank Dr. E. Bretscher for his continued interest in this field of work and for permission to publish these results.

REFERENCES

Alfvén, H., 1949, *Phys. Rev.*, **75**, 1732.
Adams, N., 1950, *Phil. Mag.*, **41**, 503.
Barrett, P. H., and Eisenberg, Y., 1952, *Phys. Rev.*, **85**, 674.
Barrett, P. H., Bollinger, L. M., Cocconi, G., Eisenberg, Y., and Greisen, K., 1952, *Rev. Mod. Phys.*, **24**, 133.
Chapman, S., and Bartels, J., 1940, *Geomagnetism*, 579 *O.U.P.*
Citron, A., 1952, *Z. f r Naturfor.*, **7a**, 712.

Cocconi, G., 1951, *Phys. Rev.*, **83,** 1193.

Daudin, J., and Daudin, M. J., 1953, *Proceedings of the Bagnères-de-Bigorre Conference.*

Elliot, H., 1952, *Progress in Cosmic Ray Physics* (Amsterdam : North Holland Publishing Co.).

Elliot, H., and Dolbear, D. W. N., 1951, *J. Atmos. Terr. Phys.*, **1,** 205.

Farley, F. J. M., and Storey, J. R., 1954, *Nature, Lond.*, **173,** 445.

Fermi, E., 1949, *Phys. Rev.*, **75,** 1169.

Fermi, E., and Chandrasekhar, S., 1953, *Ap. J.*, **118,** 113.

Hilberry, N., 1941, *Phys. Rev.*, **60,** 1.

Hodson, A. L., 1951, *Proc. Phys. Soc.* A, **64,** 106.

Molière, G., 1946, *Cosmic Rays* (Ed. W. Heisenberg, Dover Publications).

Morrison, P., Olbert, S., and Rossi, B., 1954, *Phys. Rev.*, **94,** 440.

Richtmeyer, R. D., and Teller, E., 1949, *Phys. Rev.*, **75,** 1729.

Rossi, B., and Greisen, K., 1941, *Rev. Mod. Phys.*, **13,** 240.

Sherman, N., 1953, *Phys. Rev.*, **89,** 25.

Sekido, Y., Masuda, T., Yoshida, S., and Wada, M., 1951, *Phys. Rev.*, **83,** 658.

Simpson, J. A., Fonger, W., and Treiman, S. B., 1953, *Phys. Rev..* **90,** 934.

CXXIV. *Statistics of the Occupation of Dislocation Acceptor Centres*

By W. T. Read, Jr.
Bell Telephone Laboratories, N.J.*

[Received May 26, 1954]

Abstract

This paper is a sequel to a previous one (Read 1954) dealing with the acceptor centres associated with dislocations in germanium. The previous paper developed two approximations for the statistics of occupation of dislocation acceptors. This paper presents some further approximations that take account of the non-uniform spacing of accepted electrons along the dislocation. It also treats the case where the dislocation acceptors have a range of energy levels (rather than a single level). The several approximations are compared by plotting the fraction of acceptors that are full *vs.* temperature for a particular example.

§ 1. Introduction

This is the second in a series of papers on the electrical effects of dislocations in germanium. The first paper (Read 1954) discussed the observed acceptor-type behaviour of dislocations in germanium in terms of the dangling bonds on the extra plane of a dislocation having some edge component. In the present paper it is sufficient to regard a dislocation in germanium as a row of acceptor centres, or sites, where extra electrons can be added. For dislocations in or near the edge orientation, the spacing between sites is the order of a few Ångstroms. The energy level of these dislocation acceptors appears to be slightly above the middle of the gap—see Pearson, Read and Morin (1954).

In n-type germanium with the Fermi level above the dislocation acceptor level, the dislocation accepts electrons from the conduction band and becomes negatively charged. Surrounding the negatively charged dislocation is a cylindrical region of fixed positive space charge. The first paper derived the electrostatic energy as a function of the fraction f of sites that have accepted electrons and acquired a negative charge. Two statistical approximations were obtained for the temperature variation of f, and f *vs.* T plots were given for a particular example.

The present paper forms a sequel to the first one and is a further study of the statistics of occupation of dislocation acceptors in n-type germanium. The problem is peculiar in that the added electrons on a dislocation are so closely spaced. Because of the strong coulomb forces between neighbouring electrons, the electrons in dislocation energy levels form a one-dimensional lattice.

---

* Communicated by the Author.

In the first paper the statistics of occupation of dislocation acceptors was treated on the basis of two approximations. In one, the minimum energy approximation, the accepted electrons were assumed to be uniformly spaced along the dislocation. In the other, which was based on Fermi statistics, all ways of arranging the electrons in sites along the dislocation were assumed to have the same energy. The present paper gives some further approximations that take account of the effect on energy of the non-uniform spacing of the accepted electrons on the dislocation.

§ 2. Single Energy Level—Non-Uniform Spacing

As in the first paper we consider the case where the line of acceptor states have a single electronic energy level $\mathscr{E}_2$. (Later in this paper we consider the case where the dislocation acceptors have a range of energy.) Let $\mathscr{E}_2$ be measured upward from the top of the valence band at the dislocation. (The energy level $\mathscr{E}_v$ of the top of the valence band will vary in the space charge region around the dislocation.)

At the absolute zero of temperature the accepted electrons, or full sites, are uniformly spaced along the dislocation at intervals of $a=c/f$ where f is the fraction of sites that are full and c is the spacing between sites. As the temperature is raised above $T=0^\circ\mathrm{K}$ some of the electrons on the dislocation acquire enough thermal energy to jump into neighbouring sites; so the spacing between electrons becomes non-uniform. Let $\delta\mathscr{E}_s$ be the added electrostatic energy of non-uniformity and let S be the entropy. As in the first paper we let $\mathscr{E}_s$ be the electrostatic energy for uniformly spaced electrons. Again measure the Fermi level $\mathscr{E}_\mathrm{F}$ upward from the valence band in the normal n-type material. (See fig. 2 of the first paper.) The free energy F per electron measured relative to the free energy of an electron in the normal n-type material is

$$F=\mathscr{E}_2-\mathscr{E}_\mathrm{F}+\mathscr{E}_s+\delta\mathscr{E}_s-TS. \qquad (2.1)$$

We shall define

$$\delta F=\delta\mathscr{E}_s-TS\leqslant 0 \qquad (2.2)$$

as the added free energy of non-uniformity. To find the f *vs.* T relation we minimize the free energy fF per site with respect to f. This gives

$$\mathscr{E}^*(f)=\mathscr{E}_\mathrm{F}(T)-\mathscr{E}_2-\delta F^*(f,T) \qquad (2.3)$$

where $\mathscr{E}^*(f)=(d/df)f\mathscr{E}_s(f)$ was found in the first paper. In this paper we find

$$\delta F^*=\frac{\partial}{\partial f}f\delta F=\delta F+\frac{\partial\delta F}{\partial\ln f}. \qquad (2.4)$$

§ 3. Energy of Non-Uniformity $\delta\mathscr{E}_s$

Let x_i be the displacement of the ith electron from the position it has when the electrons are uniformly spaced. $\delta\mathscr{E}_s$ is a function of all the x_i's. Since the electrons are in acceptor centres x_i must be an integral multiple of the spacing c between sites.

In this section we find $\delta\mathscr{E}_s$ using an Einstein approximation, in which each electron is assumed to move in the average field of the other electrons. Then the energy of each electron is a function only of its own displacement. In § 5 we discuss in some detail the conditions under which this approximation is good.

Since the field of the fixed positive space charge vanishes along the dislocation, the energy of non-uniformity comes entirely from the forces between electrons. An electron that has a displacement x will be acted on by a field $E(x)$ due to the other electrons and will have an added energy

$$q\int_0^x E(x)\,dx$$

where q is the electronic charge and

$$\begin{aligned} qE(x) &= \frac{q^2}{\kappa}\sum_{n=1}^{\infty}\left[\frac{1}{(na-x)^2}-\frac{1}{(na+x)^2}\right] \\ &= \frac{(4q^2)}{(\kappa a^3)}x\left[\Sigma\frac{1}{n^3}+\frac{2x^2}{a^2}\Sigma\frac{1}{n^5}\dots\right] \\ &= Kx\left\{1+1{\cdot}72\frac{x^2}{a^2}\dots\right\} \qquad (3.1) \end{aligned}$$

where κ is the dielectric constant. The linear stiffness coefficient K is a function of f

$$K=\frac{4q^2}{\kappa a^3}\Sigma\frac{1}{n^3}=\frac{4{\cdot}80\,\mathscr{E}_0}{c^2}f^3. \qquad (3.2)$$

$\mathscr{E}_0=q^2/\kappa c$ is the energy of interaction of electrons in neighbouring sites.

We shall deal with the case where the displacement x is small compared to a, so that the linear term is a good approximation.

The added electrostatic energy is $\frac{1}{2}Kx^2$. Thus if the displacement is nc (where n must be an integer), the added electrostatic energy is $\delta\mathscr{E}_n=\frac{1}{2}K\,c^2n^2=(2{\cdot}40\;\mathscr{E}_0f^3)\,n^2$. $\delta\mathscr{E}_s$ is the average of $\delta\mathscr{E}_n$; so

$$\delta\mathscr{E}_s=(2{\cdot}40\;\mathscr{E}_0f^3)\,\overline{n^2} \qquad (3.3)$$

where $\overline{n^2}$ is determined from statistics as will be discussed in the following section.

§ 4. STATISTICS

In this section we consider the statistics of the system of electrons spaced non-uniformly in sites along the dislocation. For a given f the statistics of the system is specified by the distribution of electrons among the values of n; that is, we divide the electrons into groups where all those in the nth group have added energy $\mathscr{E}_n=2{\cdot}40\;\mathscr{E}_0f^3n^2$. Thus the system is one to which Boltzmann statistics applies. The number of electrons having displacement nc is proportional to $\exp(-\mathscr{E}_n/kT)$ where k is Boltzmann's constant. It will be convenient to define a parameter

$$z=\frac{2{\cdot}40\,\mathscr{E}_0f^3}{kT}. \qquad (4.1)$$

The probability of finding an electron with displacement nc is proportional to $\exp(-zn^2)$. We shall express the final results as a function of the parameter exp $(-z)$, which is a measure of the non-uniformity. It is the ratio of the number of electrons having displacement $x=+c$ to the number having displacement $x=0$. For the uniform distribution exp $(-z)=0$ and

Fig. 1

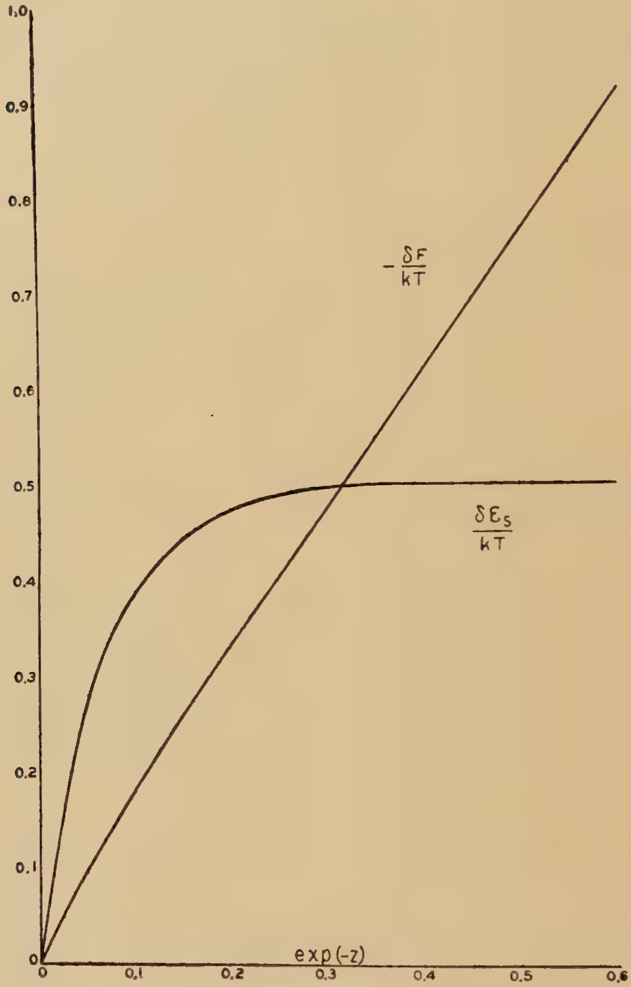

Variation of decrease $-\delta F$ in free energy and increase $\delta\mathscr{E}_S$ in electrostatic energy with non-uniformity, which increases with exp $(-z)$, where $z=2{\cdot}40\ \mathscr{E}_0 f^3/kT$.

for a completely random distribution exp $(-z)=1$. However, the present approximation breaks down before we reach a completely random distribution. (We discuss this in detail in § 5.)

The added free energy δF is

$$\delta F=-kT \ln \Sigma \exp(-zn^2) \quad . \quad . \quad . \quad . \quad . \quad . \quad . \quad (4.2)$$

where the sum is taken from $-\infty$ to ∞. (See J. C. Slater, 1939, *Introduction to Chemical Physics*, p. 50.) Figure 1 shows a plot of $-\delta F/kT$ *vs.* z. For exp $(-z)>0{\cdot}4$, $\delta F=-(kT/2)\ln(\pi/2)$.

From eqns. (3.3) and (4.1)

$$\delta \mathscr{E}_s = kT\, z\, \overline{n^2} \qquad \text{(4.3)}$$

where

$$\overline{n^2} = -\frac{d}{dz} \ln \Sigma \exp(-zn^2). \qquad \text{(4.4)}$$

Thus

$$\delta \mathscr{E}_s = -kT \frac{d \ln \Sigma \exp(-zn^2)}{d \ln z}. \qquad \text{(4.5)}$$

Figure 1 also shows a plot of $\delta \mathscr{E}_s / kT$ *vs.* z. For $\exp(-z) > 0{\cdot}4$, $\delta \mathscr{E}_s = kT/2$.

From eqns. (4.1), (4.2) and (4.5)

$$\frac{\partial\, \delta F}{\partial \ln f} = \frac{\partial\, \delta F}{\partial \ln z} \frac{\partial \ln z}{\partial \ln f} = 3\delta \mathscr{E}_s. \qquad \text{(4.6)}$$

We now have for δF^* in eqn. (2.4)

$$\delta F^* = \delta F + 3\delta \mathscr{E}_s. \qquad \text{(4.7)}$$

So δF^* can be found from fig. 1 for any values of T and f. Thus eqn. (2.3) can be solved for f *vs.* T. The first paper gave $\mathscr{E}^*(f)$ and $\mathscr{E}_{\mathrm{F}}(T)$ for the case of a particular dislocation in 1·7 ohm cm n-type germanium where $c = 4$ Å. The donor and acceptor concentrations were $N_d = 2N_a = 2 \times 10^{15}$ cm^{-3}. The dislocation acceptors were taken as lying 0·225 ev below the conduction band. Figure 2 shows the two approximate f *vs.* T relations derived for this example in the first paper. The approximations are the curves marked M.E. (Minimum Energy) and F. (Fermi). The solid curve marked B. (Boltzmann) in fig. 2 is the f *vs.* T relation as given by eqns. (2.3) and (4.6) of this paper. We shall call this the Boltzmann approximation. As expected this more accurate approximation lies between the other two, which were based on upper and lower limits for the free energy.

§ 5. LIMITATIONS AND REFINEMENTS

This section discusses how the assumptions made in deriving the Boltzmann approximation limit the range of its validity. Some refinements are considered which extend the range of validity and indicate the accuracy.

Correlated Displacements

The Einstein model gives the correct average energy of non-uniformity per electron $\delta \mathscr{E}_s$ when the displacements are completely uncorrelated; that is, when the probability that an electron will have a given displacement is independent of the displacements of the other electrons. At low temperatures and high values of f the energy per electron $\delta \mathscr{E}_s$ is small compared to the energy of interaction of neighbouring electrons; so the strong coulomb forces between electrons cause the displacements to be highly correlated. That is, if the displacements were analyzed into a Fourier series, the long wavelengths would account for a major part of the deviation from uniformity. Thus the Einstein model overestimates the energy $\delta \mathscr{E}_s$ for a given $\overline{n^2}$. However, this error does not seriously affect the f *vs.* T curve as we now show by using another approximation—one that *underestimates* $\delta \mathscr{E}_s$.

Suppose we consider only the interactions between nearest neighbours, which are spaced at intervals a in the uniform distribution. Now define x_i as the change in distance between the ith and $i+1$st electrons.

Fig. 2

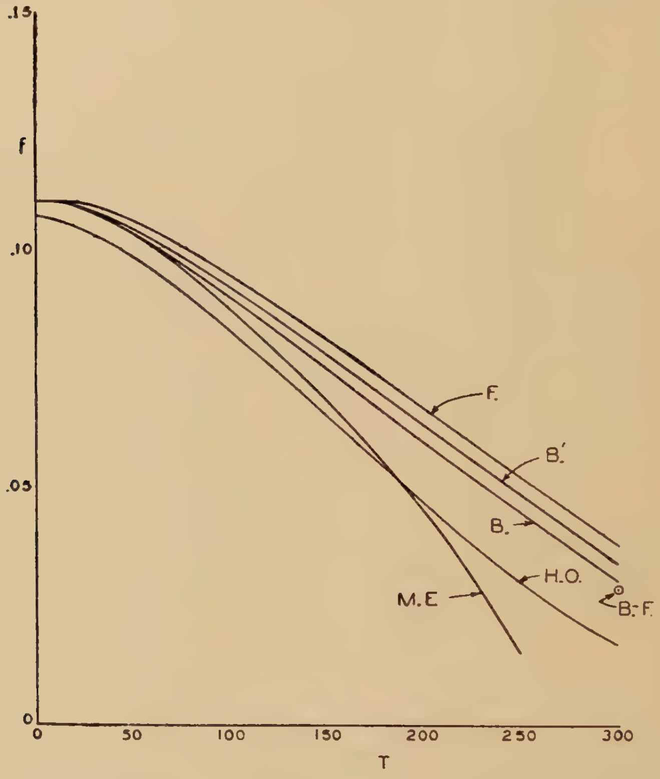

Variation of the fraction f of dislocation acceptors that are full with T=absolute temperature. The approximations are: **B.**=Boltzmann, **F.**=Fermi, **M.E.**=Minimum Energy, and **H.O.**=Harmonic Oscillator.

Again $x_i = nc$ where n is an integer. If we require that x_i be small compared to a and take account of the fact that positive and negative displacements are equally probable, then we find that $\delta \mathscr{E}_s = \mathscr{E}_0 f^3 \overline{n^2}$, which differs from eqn. (3.3) by a factor of 2·4. This gives a lower limit to $\delta \mathscr{E}_s$ because it neglects all interactions except those between nearest neighbours. The curve marked B'. in fig. 2 was obtained in the same way as the one marked B. except that the relation $\delta \mathscr{E}_s = \mathscr{E}_0 f^3 \overline{n^2}$ was used instead of eqn. (3.3). The two curves differ only slightly.

Non-linearity

As the root mean square displacement increases, the non-linear terms in the electric field become important. These are not as serious as might be thought, however. For example, from eqn. (3.1), we see that the cubic term is only about 10% of the linear term even for $x=a/4$. Neglect of the non-linear terms leads to underestimating $\delta\mathscr{E}_s$ and, therefore, tends to compensate for the effect of assuming the displacements are uncorrelated.

Lower Limit for Free Energy

As discussed in the first paper Fermi statistics gives a lower limit for the free energy. This corresponds to taking $\delta\mathscr{E}_s=0$ and giving S its maximum value, which is found from the number of possible ways of filling a fraction f of the acceptors. However, if eqn. (4.2) is extended to sufficiently low f it gives values of δF lower than the lower limit given by Fermi statistics. Physically this means that the x_i become so large that the electrons are no longer confined to discrete intervals on the dislocation; consequently some of the electron distributions that are counted as different in Boltzmann statistics are, in fact, indistinguishable. This error will be most serious at higher temperatures. In the remainder of the section we find f at $T=300°\text{K}$ by a further approximation that combines Boltzmann and Fermi statistics.

Fig. 3

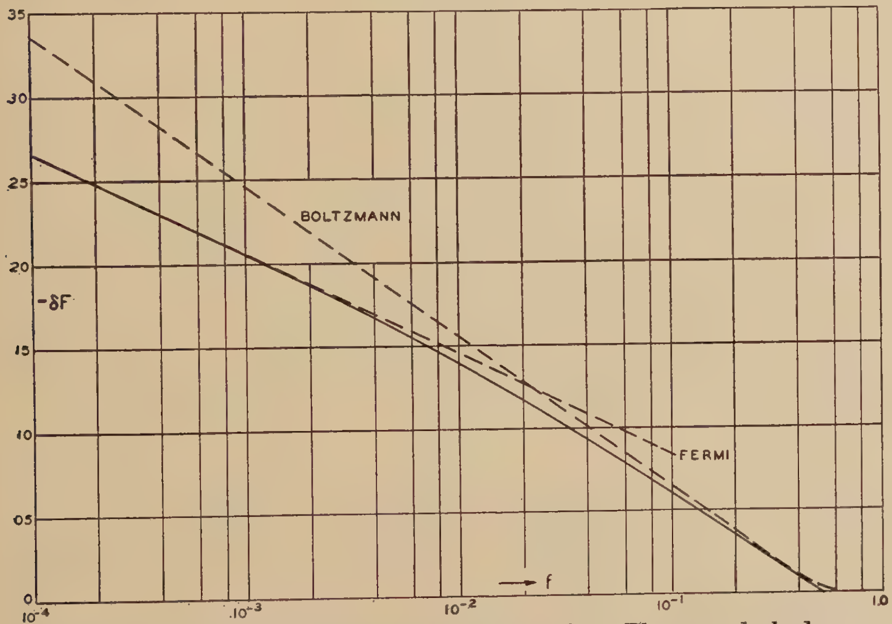

Decrease $-\delta F$ in free energy *vs.* f at $T=300°\text{K}$. The two dashed curves represent Fermi and Boltzmann statistics, respectively, which are limiting forms.

Figure 3 is a plot of $-\delta F$ *vs.* f at $T=300°\text{K}$. The two dashed curves are from Boltzmann and Fermi statistics respectively. In Fermi statistics

$-\delta F = +TS$ where S is uniquely determined by f. The Boltzmann curve depends on the parameter $\mathscr{E}_0$ in eqn. (4.1). For the particular example we have considered (where $c=4$ Å and $k=16$), $\mathscr{E}_0=0{\cdot}225$ ev. At high values of f the root mean square displacement is small compared to a, and the Boltzmann curve becomes an increasingly good approximation. At low f, δF approaches the lower limit given by Fermi statistics. The solid curve in fig. 3 approaches the Boltzmann curve at high f and the Fermi curve at low f and makes a smooth transition between the two limiting forms. The point B.–F. in fig. 2 was found by taking δF^* from the solid curve in fig. 3. This corrected point lies only slightly below the uncorrected Boltzmann curve in fig. 2. The reason for the small change is that errors in δF and $\delta \partial F/\partial \ln f$ tend to compensate. The final result is relatively independent of the exact form of the solid, or transition, curve in fig. 3.

Uncertainty in $\mathscr{E}^*$ at low f

The above uncertainties are peculiar to the Einstein model and resulting Boltzmann statistics. At low values of f all the approximations to the f *vs.* T curve are subject to the uncertainty in $\mathscr{E}^*$ at low f. As explained in § 7 of the first paper, there is no definite space charge unless the spacing a between accepted electrons is smaller than both R and the mean spacing $L=(N_d-N_a)^{-1/3}$ between excess donors. An even more stringent requirement comes from the assumption, made in deriving $\mathscr{E}_s(f)$ and $\mathscr{E}^*(f)$, that the positive space charge is uniformly distributed. This will become exact as the radius R of the space charge cylinder becomes large compared to the mean spacing between excess donors. As shown in the first paper eqn. (7.5),

$$\frac{R}{L}=\sqrt{\frac{fL}{\pi c}}. \quad \ldots \ldots \ldots \quad (5.1)$$

In the example of fig. 2, $L=10^3$ Å. Thus even at the maximum f, R is only about $3L$. At $f=0{\cdot}0126$, $R=L$. This uncertainty in the formula for $\mathscr{E}^*(f)$ may be as serious as any other single source of error in the final f *vs.* T curve.

§ 6. THE HARMONIC OSCILLATOR APPROXIMATION

In the previous sections we have considered the case where the dislocation acceptors have a single energy level $\mathscr{E}_2$. This will certainly be the case when c is large enough, that is, when the dislocation is near enough to the screw orientation. As the angle between the dislocation and its slip vector increases, and the dislocation moves toward the edge orientation, c decreases and approaches a minimum of $0{\cdot}886\,b$ where b is the interatomic spacing in a $\langle 110\rangle$ direction (see § 2 of the first paper). In germanium $b=4$ Å. As c decreases, the wave functions of adjacent dangling bonds overlap more. Thus what, at large c, was a single energy level may become a range of levels, or energy band.

Let $\mathscr{E}_2$ be the minimum energy of an electron in a dislocation acceptor and let $\mathscr{E}_b$ be the band width. Then an accepted electron can be accelerated and can acquire a maximum kinetic energy $\mathscr{E}_b$ while still remaining in the dislocation acceptors. The energy $\mathscr{E}$ of an accepted electron will be a function of its momentum P along the dislocation and will be a minimum $\mathscr{E}_2$ at $P=0$ and a maximum at $P=h/2c$. We shall use the approximation $\mathscr{E}=\mathscr{E}_2+\mathscr{E}_b\,[1-\cos(2\pi cP/h)]$. The equivalent mass m^* for an electron whose kinetic energy is small compared to $\mathscr{E}_b$ is given by

$$\frac{1}{m^*}=\left(\frac{d^2\mathscr{E}}{dP^2}\right)_{P=0}=\frac{4\pi^2c^2\mathscr{E}_b}{h^2} \quad . \; . \; . \; . \; . \; . \quad (6.1)$$

where h is Plank's constant ($=4{\cdot}14\times10^{-15}$ ev sec).

Again we use an Einstein model, where each electron moves in the average field of the other electrons and the maximum displacement is small enough that the restoring force is approximately linear. Then each electron oscillates with frequency ν where $(2\pi\nu)^2=K/m^*$. From eqns. (3.2) and (6.1) we have for the quantum $h\nu$ of vibrational energy

$$h\nu=f^{3/2}\sqrt{(4{\cdot}80\;\mathscr{E}_2\,\mathscr{E}_b)}. \quad . \; . \; . \; . \; . \; . \; . \quad (6.2)$$

Each electron is thus a harmonic oscillator having one degree of freedom. The average number $\bar{n}$ of energy quanta per electron above the zero point energy $\frac{1}{2}\,h\nu$ is

$$\bar{n}=\frac{1}{\exp(h\nu/kT)-1}. \quad . \; . \; . \; . \; . \; . \; . \quad (6.3)$$

(See any treatment of the Einstein theory of specific heat of a solid.)

The average vibrational energy per electron $(\bar{n}+\frac{1}{2})\,h\nu$ is half kinetic and half electrostatic (in contrast to the previous, static, approximations, in which the energy of non-uniformity was assumed to be entirely static). The entropy per electron is $S=k\,[(1+\bar{n})\ln(1+\bar{n})-\bar{n}\ln\bar{n}]$ and the free energy of non-uniformity is

$$\begin{aligned}\delta F&=(\bar{n}+\tfrac{1}{2})\,h\nu-T\,S\,(\bar{n})\\&=\frac{h\nu}{2}+kT\ln\left[1-\exp\left(-\frac{h\nu}{kT}\right)\right].\end{aligned} \quad . \; . \; . \; . \; . \; . \quad (6.4)$$

It is convenient to regard δF as an explicit function of $\bar{n}$ and ν. Equation (6.3) comes from $(\partial/\partial\bar{n})\,\delta F\,(\bar{n},\nu)=0$. If we use this and remember that ν is a function of f, we have from (2.4)

$$\begin{aligned}\delta F^*&=\delta F+f\frac{\partial\,\delta F}{\partial\nu}\frac{\partial\nu}{\partial f}\\&=\delta F+\nu\frac{\partial\,\delta F}{\partial\nu}\frac{\partial\ln\nu}{\partial\ln f}.\end{aligned} \quad . \; . \; . \; . \; . \; . \; . \; . \quad (6.5)$$

From (6.4) $(\partial\,\delta F/\partial\nu)=(\bar{n}+\frac{1}{2})\,h$ and from (6.2), $(\partial\ln\nu/\partial\ln f)=\frac{3}{2}$. Thus

$$\delta F^*=\frac{3h\nu}{2}\left(\bar{n}+\frac{5}{6}\right)+kT\ln(1+\bar{n}) \quad . \; . \; . \; . \quad (6.6)$$

where (6.3) gives $\bar{n}$ *vs.* $(h\nu/kT)$ and (6.2) gives $h\nu$ as a function of f. From (6.6) and (2.3) we can find the f *vs.* T curve.

The harmonic oscillator approximation involves an additional parameter, m^* or $\mathscr{E}_b$, not present in the previous, static, approximations. There is also another limitation on the range of validity: the kinetic energy $\delta\mathscr{E}_2 = \frac{1}{2} h\nu (\bar{n}+\frac{1}{2})$ must be small compared to $\mathscr{E}_b$ otherwise the electron will not stay on the parabolic part of the $\mathscr{E}$ *vs.* P curve and the average kinetic energy will not be equal to the average potential energy. If $\delta\mathscr{E}_2$ comes out larger than the band width, then we can conclude that the oscillator approximation is a poor one and that the energy of non-uniformity is mainly static. When $\delta\mathscr{E}_2 \leqslant \mathscr{E}_b$ is small compared to $\delta\mathscr{E}_s$, then a static approximation will be valid.

We now return to the example which we used to illustrate the f *vs.* T curves (fig. 2) for the static approximations. The curve marked H.O. in fig. 2 is the oscillator approximation for the same example with $\mathscr{E}_b = 0{\cdot}10$ ev The equivalent mass m^* is then 4·75 times the mass of a free electron. Equation (6.2) becomes $h\nu = 0{\cdot}33 f^{3/2}$. The harmonic oscillator curves for f *vs.* T are subject to the same uncertainties discussed in § 5. Again the assumption of uncorrelated displacements introduces errors at low T, which are relatively unimportant since the energy of non-uniformity has a small effect at low T. We could get another limiting approximation by considering only nearest neighbour interactions. We would then have a Debye model rather than an Einstein model. A still more accurate approach would be to treat the electrons as a one-dimensional plasma and investigate the oscillations. At higher temperatures errors due to non-linear restoring force come in and tend to cancel the errors due to correlated displacements. At still higher temperatures the displacements become large enough that violations of the exclusion principle are significant. However, for the H.O. curve of fig. 2, the free energy drop $-\delta F^*$ is well below the limiting value given by Fermi statistics even at $T = 300°$. A construction like fig. 2 had little effect on the 300° point. On the other hand the uncertainty in $\mathscr{E}^*(f)$ is greater than for the Boltzmann approximation because f is lower; this may well be the most important single source of error at the high temperature end of the curve.

The requirement that $\delta\mathscr{E}_2$ be small compared to $\mathscr{E}_b$ is satisfied throughout the temperature range.

ACKNOWLEDGMENT

The author wishes to thank C. Herring for much helpful advice and discussion.

REFERENCES

PEARSON, G. L., READ, W. T. Jr., and MORIN, F. J., 1954, *Phys. Rev.*, **93**, 666.
READ, W. T. Jr., 1954, *Phil. Mag.*, **45**, 775.

CXXV. *A Restricted Quantum Statistical Proof of the Third Law of Thermodynamics*

By P. T. LANDSBERG*
Randal Morgan Laboratory, University of Pennsylvania, Philadelphia†

[Received June 12, 1954]

ABSTRACT

A restricted proof is given of the third law of thermodynamics. The restriction resides in the fact that the proof applies only in the limit of an infinitely large system (the 'limit L'). An additional restriction is that it applies only to non-interacting and structureless quantum mechanical particles whose quantum states satisfy certain requirements (the 'class O' of systems). The essence of the proof depends on showing that the free energy of the system, as averaged over a grand canonical ensemble and expressed per unit volume of the system, is of the form $a-bT^d(b>0, d>1)$ near the absolute zero.

§ 1. INTRODUCTION

AN important task of statistical mechanics is to furnish an explanation of thermodynamics. In particular, the problem of establishing the second law, by proving the so-called H-theorem, has been attacked by several writers. The first important achievement to be based on quantum mechanics was due to Pauli (1928), who utilized the method of transition probabilities. His result is therefore valid only for restricted time intervals. An assumption of random *a priori* phases, to replace the classical assumption of molecular chaos was sufficient to yield the H-theorem in the form $dH/dt \leqslant 0$ for these restricted time intervals, H being a certain quantity characteristic of the ensemble under consideration. An extension to arbitrary time intervals is due to Klein (1931) and Tolman (1938). It was shown later that, subject to the above and certain additional assumptions, the ensemble average of a quantity H at a certain time, and the long time average of a quantity H for the system of interest, are almost always very nearly the same (von Neumann 1929, Pauli and Fierz 1937).

No quantum statistical proof is, however, available of the third law. The problem was recently taken up by Simon (1951). He considered under what conditions it is possible to infer Nernst's theorem from the experimental fact that the specific heat of physical systems vanishes as

---

[*] On leave of absence from the Department of Natural Philosophy, University of Aberdeen, Aberdeen, Scotland.

[†] Communicated by Professor F. E. Simon, F.R.S. An abstract of this paper was given in Section V of the International Congress of Mathematicians, Amsterdam, 1954.

the absolute zero is approached. He points out that a system for which this inference is *not* valid must have rather curious properties, and asks if one needs a supplementary postulate to express the fact that they do not occur in nature. The answer seems to us to be in the affirmative, since even a system whose free energy satisfies the simple relation $F=a(x\ldots)-b(x\ldots)T$ near $T=0$, x_1, $x_2\ldots$ being external parameters of the system, has a specific heat which vanishes near $T=0$, but does not necessarily satisfy Nernst's theorem. Simon pointed out that the condition $pV=sU$ where s is a constant and U the internal energy of the gas, is a sufficient supplementary condition. This supplementary condition has the merit that it follows from the quantum statistics of ideal gases, but it still leaves the vanishing of the specific heat to be explained.

We shall show here that the position is somewhat more favourable. For a careful formulation of the quantum statistics of the ideal gas furnishes in fact an expression for the free energy from which both the third law and the vanishing of the specific heat can be deduced. By restricting attention to non-interacting particles without internal degrees of freedom, we are, of course, dealing only with the theoretically simplest case. A generalization of the present argument to imperfect gases would be desirable.

The most important difficulty which has to be overcome is that one cannot exclude on quantum mechanical grounds the possibility of degeneracy of the lowest energy level of a system (Ludloff 1931, Schottky 1943). This suggests that the third law in Planck's form (for our purposes this may be stated in the form ‘ the entropy of a system tends to zero as the absolute temperature tends to zero ’) may not be rigorously true for finite systems, but that it may be a law which attains validity only in certain limiting cases.

The case with which we shall deal here is that of a system of non-interacting particles in the ‘ limit L ’. The limit L is the limit in which the total number of particles N, as averaged over a grand canonical ensemble, and the volume V of each system of the ensemble, are each allowed to tend to infinity so as to keep the ratio N/V a finite and non-zero constant, which will be denoted by ρ. Under these conditions the distinction between the coarse-grained and the fine-grained probabilities, which plays such an important part in the proofs of the H-theorem, can be neglected, since it cannot affect the results. The following definition will be required. A system of class O is one which consists of structureless non-interacting quantum mechanical particles, such that each satisfies the following requirements : (i) there is an infinity of particle quantum states whose particle energies are E_1, $E_2\ldots$; the labelling of the states is arranged so that $E_j\leqslant E_{j+1}$ for all j ; (ii) E_j is finite if j is finite ; (iii) all energy levels with finite j behave like $E_j=E_0+b_jV^{-\theta}$ for large volumes V, where b_j is independent of the volume, and E_0 is the value to which all those E_j's tend in the limit L for which j is finite ; (iv) for large volumes there exists a finite positive integer M, such that a continuous spectrum approximation is valid for $j>M$, and the jth quantum state is given by $E_j=E_0+cV^{-\theta}j^{\tau}$ for $j>M$. M must exceed the degeneracy ω_1 of the lowest particle energy E_1 of the system of interest when its volume is finite. Under (iv) one might equivalently specify the density of states function

$$N(\epsilon)=\frac{1}{\tau}\left(\frac{V^{\theta}}{c}\right)^{1/\tau}(\epsilon-E_0)^{1/\tau-1}.$$

In all cases of interest $\theta=\tau$ (Landsberg 1954 a), and this will be assumed.

We need some assumption which will enable us to extrapolate physical laws to temperatures which are infinitely close to the absolute zero. The assumption which we shall adopt, and which will be referred to as assumption (A), is "*the relations for ensemble averages near $T=0$ and in the limit L, are assumed to remain valid as T tends to zero*".

All our conclusions concerning conditions at the absolute zero will be deduced from the following result : *For a system of class O the free energy per unit volume* (as averaged over a grand canonical, or a canonical, ensemble) *is, at temperatures near the absolute zero and in the limit L, given by*

$$f=a-bT^{d} \qquad (b>0,\, d>1). \qquad \ldots\ldots \quad (1)$$

A proof of this result is given in § 2. Basically, it depends on certain simple theorems which hold for systems of class O in the limit L (Landsberg 1954 c).

The relation between the third law and Carathéodory's (macroscopic) formulation of thermodynamics is an additional problem. It does not seem to have been discussed so far, and will be the subject of a subsequent communication.

§ 2. PROOF OF (1)

We shall average over a grand canonical ensemble, and define the ensemble average of the entropy per system by

$$\bar{S}\equiv -k\sum_{n_1}\sum_{n_2}\ldots P(n_1, n_2, \ldots)\log P(n_1, n_2, \ldots),$$

where

$$P(n_1, n_2, \ldots)\equiv \exp\{\Omega+\sum_i(\mu-\beta E_i)n_i\}, \qquad \beta\equiv 1/kT.$$

Ω and μ are independent of the suffix i, and n_i is the number of particles in the ith quantum state. The n_i-summation is over all permitted occupation numbers and the i-summation is over all particle quantum states of a system. Let $\bar{U}$ be the mean energy per system. Then the mean free energy per system is given by

$$\bar{F}\equiv \bar{U}-T\bar{S}=\mu kT\bar{N}\mp kT\sum_i \log\left[1\pm\exp(\mu-\eta_i)\right], \qquad \eta_i\equiv E_i/kT, \qquad (2)$$

where the top signs apply to Fermi–Dirac systems, and the bottom signs to Bose-Einstein systems. We must distinguish four cases.

(*a*) *Fermi–Dirac systems.* For any finite integer in

$$\rho \sim \frac{1}{V}\sum_{j=m}^{\infty}\{\exp(\mu-\eta_j)+1\}^{-1} \sim \frac{1}{\tau}\left(\frac{kT}{c}\right)^{1/\tau}\int_0^\infty \frac{x^{1/\tau-1}\,dx}{1+\exp(x-\mu+\eta_0)}, \qquad (3)$$

where $\sim$ denotes equality in the limit L. The first relation is due to the fact that $\bar{n}_j/V \sim 0$ when j is finite, where $\bar{n}_j$ is the mean occupation number of the jth quantum state. The last expression is obtained by taking $m=M$ and using statement (iii) in the definition of a system of class O. The average free energy per unit volume of a system of the ensemble, $f \equiv \bar{F}/V$, satisfies similarly by (2)

$$f \sim \mu kT\rho - \left(\frac{kT}{c}\right)^{1/\tau} kT\int_0^\infty \frac{x^{1/\tau}\,dx}{1+\exp(x-\mu+\eta_0)}. \quad . \quad . \quad (4)$$

In virtue of assumption (A) the integral in (3) must diverge like $T^{-1/\tau}$ as $T \to 0$. It follows that $\mu-\eta_0 \to \infty$ as $T \to 0$, so that the approximation

$$\int_0^\infty \frac{x^s\,dx}{1+\exp(x-a)} = \frac{a^{s+1}}{s+1}\left[1+\frac{\pi^2 s(s+1)}{a^2}+\ldots\right], \qquad s>-1, \qquad (5)$$

can be used near $T=0$. By combining (3) and (5) one can obtain an approximate expression for μ near $T=0$. This expression and eqn. (5) are then used to eliminate both the integral and μ from (4). The result is

$$f \sim \rho E_0 + \frac{c\rho^{\tau+1}}{\tau+1} - \frac{c\rho^{\tau+1}}{\sigma\tau}\left(\frac{\pi kT}{c\rho^\tau}\right)^2. \quad . \quad . \quad . \quad . \quad . \quad . \quad (6)$$

(*b*) *Bose–Einstein system with* $\tau>1$. Our basic equations are now

$$\rho \sim \frac{1}{\tau}\left(\frac{kT}{c}\right)^{1/\tau}\int_0^\infty \frac{x^{1/\tau-1}\,dx}{\exp(x-\mu+\eta_0)-1}, \quad . \quad . \quad . \quad . \quad . \quad . \quad (7)$$

$$f \sim \mu kT\rho - kT\left(\frac{kT}{c}\right)^{1/\tau}\int_0^\infty \frac{x^{1/\tau}\,dx}{\exp(x-\mu+\eta_0)-1}, \quad . \quad . \quad . \quad (8)$$

since such a system does not show the phenomenon of condensation (Landsberg 1954 a). We need the results

$$\int_0^\infty \frac{x^s\,dx}{\exp x-1} = \Gamma(s+1)\,\zeta(s+1), \quad s \geqslant 0, \quad . \quad . \quad . \quad . \quad . \quad . \quad . \quad . \quad . \quad (9)$$

$$\int_0^\infty \frac{x^s\,dx}{\exp(x-a)-1} = \Gamma(s+1)\Gamma(-s)(1-e^a)^s, \quad 0 \leqslant -a \ll 1, \quad -1<s<0. \quad (10)$$

$\Gamma(x)$, $\zeta(x)$ are the usual Gamma and Riemann Zeta functions respectively. (10) is due to de Groot *et al.* (1950). In virtue of assumption (A) the integral in (7) must diverge like $T^{-1/\tau}$ as $T \to 0$, so that, by (10), $\mu \to \eta_0$ as $T \to 0$. By combining (7) and (10) one can obtain an approximate expression for μ near $T=0$. This expression and eqn. (9) are then used to eliminate both the integral and μ from (8). The result is

$$f \sim \rho E_0 - \Gamma(1+1/\tau)\,\zeta(1+1/\tau)c^{-1/\tau}(kT)^{1+1/\tau}. \quad . \quad . \quad . \quad (11)$$

(*c*) *Bose–Einstein systems with* $\tau=1$. The relations (7) and (8) hold again, but the integral in (7) can in this case be evaluated in closed form, and μ is now found to depend exponentially on the temperature. The final result is again given by (11) (with $\tau=1$).

(*d*) *Bose–Einstein systems with* $\tau<1$. Systems of this type are below their condensation temperature near $T=0$, so that eqn. (7), which determines μ, is replaced by

$$\mu=\eta_0 \quad . \quad . \quad . \quad . \quad . \quad . \quad . \quad . \quad . \quad (12)$$

in this case. The equation for f is again given by (8), but is now subject to (12). It therefore reduces immediately to (11).

This establishes the result (1) for the case when one averages over a grand canonical ensemble of systems of class O for which the mean total number of particles per unit volume of the system of interest is $\rho\equiv\bar{N}/V$. By averaging over a canonical ensemble of systems of class O for which the fixed number of particles per unit volume of the system of interest, N/V, is also ρ, one obtains the same result in the limit L, since the distribution functions are then the same (Landsberg 1954 b). This proves assertion (1).

For completeness we give below the values of μ near $T=0$:

$$\mu=\left\{\begin{array}{ll} \dfrac{E_0}{kT}+\dfrac{c\rho^{\tau}}{kT} & \text{(F.D.)} \\ \dfrac{E_0}{kT}-\left[\dfrac{\Gamma(1/\tau)\Gamma(1-1/\tau)}{\tau\rho}\right]^{\tau/(\tau-1)}\left(\dfrac{kT}{c}\right)^{1/(\tau-1)} & (\text{B.E.}, \tau>1) \\ \dfrac{E_0}{kT}-\exp\left(-\dfrac{\rho c}{kT}\right) & (\text{B.E.}, \tau=1) \\ \dfrac{E_0}{kT} & (\text{B.E.}, \tau<1) \end{array}\right\} . \quad (13)$$

§ 3. DISCUSSION

It follows from (1) that for a system of class O in the limit L the mean total energy per unit volume (u), the mean entropy per unit volume (s), and the mean heat capacity at constant volume expressed per unit volume (c_v) are given by

$$u=a+(d-1)bT^d, \qquad s=bdT^{d-1}, \qquad c_v=d(d-1)bT^{d-1}. \quad . \quad (14)$$

Thus both entropy and specific heat tend to zero, and, in this sense, the third law is established for these cases.

The principle of the unattainability of the absolute zero may be formulated as follows. Let $x_1, x_2 \ldots$ be the external parameters of a physical system, and let

$$B(T, x_1, x_2 \ldots)\equiv\frac{[\partial^2F/\partial T\partial x_1]_{x_2,\, x_3,\, \ldots}}{[\partial^2F/\partial T^2]_{x_1,\, x_2,\, \ldots}} . \quad . \quad . \quad . \quad . \quad (15)$$

Then the absolute zero is unattainable if

$$\lim_{T\to 0} B(T, x_1, \ldots)=0 \quad . \quad . \quad . \quad . \quad . \quad . \quad . \quad (16)$$

for all physical systems, and whichever external parameter is chosen to be x_1. It is easy to verify the accuracy of this statement. For instance, Bennewitz (1926)* showed that the quantity $(T/c_v)(\partial p/\partial T)_v$ must tend to zero as the temperature tends to the absolute zero, and our statement (16) is equivalent to a generalization of this. We can infer from (1), as an approximation, that for a large but finite system of class O $F=aV-bVT^d$, where V is the volume of the system. It follows that (one may take x_1 to represent the volume V)

$$B(T, x_1, x_2, \ldots)=\frac{T}{d-1}\left[\frac{\partial \log (bV)}{\partial x_1}\right]_{x_2,\ldots} \quad . \quad . \quad . \quad . \quad (17)$$

If all variables are continuous functions of the external parameters, it follows that the systems of class O satisfy (16), and therefore the unattainability principle. (The general result that Planck's form of the third law implies the unattainability principle could not be used in the present discussion, since the results (14) hold in the limit L, while a finite system is contemplated in (16).)

It might be thought that a possible formulation of the third law is to stipulate the unattainability principle and the condition that $(\partial^2F/\partial T^2)_{x_1}, \ldots$ or c_v/T remain finite as the absolute zero is approached. We see from our results that this form of the third law is violated by those Bose–Einstein systems of class O whose density of states for high quantum numbers is proportional to an inverse power of the energy ($\tau>1$). Such systems, which include the perfect Bose–Einstein gas in a one-dimensional box, are of no practical importance at the present time, but a satisfactory formulation of the third law should presumably apply to them also, particularly so, since they do satisfy the unattainability principle as well as Planck's form of the third law. A satisfactory formulation of the third law should, therefore, not lay down that $\partial^2F/\partial T^2$ or c_v/T be finite at the absolute zero of temperature. To cover the case of the perfect gases it is sufficient to require that (1) hold. Nernst's theorem in Planck's form, the unattainability principle and the vanishing of the specific heat at low temperatures all follow from this result.

APPENDIX

A thorough investigation of the relationships between the various formulations of the third law is due to Bennewitz (1926). We merely wish to put on record here that three results which he states (p. 155) may be disproved by counter examples. The results are :

(i) If $U=F$ at $T=0$, then U and F are finite at $T=0$.

(ii) If $(\partial U/\partial T)_{x_1}\ldots=0$ at $T=0$, then $(\partial F/\partial T)_{x_1}\ldots$ is finite at $T=0$.

(iii) If $(\partial F/\partial T)_{x_1}\ldots=(\partial U/\partial T)_{x_1}\ldots$ at $T=0$, and F is finite at $T=0$, then $(\partial F/\partial T)_{x}\ldots=0$ at $T=0$.

---

* Some remarks on Bennewitz's article are made in the Appendix.

The counter examples (numbered to correspond) are :

(i) If $F=a+b/T$, then $U=F-T(\partial F/\partial T)_{x_1}\ldots=a+2b/T$.

(ii) If $(\partial F/\partial T)_{x_1}\ldots=-a\log(-\log bT)$, then

$$(\partial U/\partial T)_{x_1}\ldots=-a/\log bT(b>0).$$

(iii) If $F=a+bT^p\log T$, then $U=a+bT^p[(1-p)\log T-1]$, $0<p<1$. It follows that $\partial F/\partial T$ and $\partial U/\partial T$ tend to $-\infty$ as the absolute zero is approached.

In these examples a, b are non-zero, finite and continuous functions of the external parameters only, and all equations are supposed to represent conditions near the absolute zero of temperature. Although Bennewitz does not deal with this point explicitly, we believe we follow him in making the convention that if two quantities diverge, both to $+\infty$ or both to $-\infty$, at a certain temperature T, the equation $A=B$ is regarded as applicable at the temperature T.

REFERENCES

Bennewitz, K., 1926, *Handb. d. Phys.* (Berlin : Springer), 9, 172.
de Groot, S. R., Hooyman, G. J., and ten Seldam, C. A., 1950, *Proc. Roy. Soc.* A, **203,** 266.
Klein, O., 1931, *Z. Phys.*, **72,** 767.
Landsberg, P. T., 1954 a, *Proc. Camb. Phil. Soc.*, **50,** 65 ; 1954 b, *Phys. Rev.*, **93,** 1170 ; 1954 c, *Phys. Rev.*, **94,** 469.
Ludloff, H., 1931, *Z. Phys.*, **68,** 433.
Pauli, W., 1928, *Probleme der modernen Physik* (Leipzig : Hirzel, ed. P. Debeye), p. 30. This reference is also known as *Sommerfeld Festschrift.*
Pauli, W., and Fierz, M., 1937, *Z. Phys.*, **106,** 572.
Schottky, W., 1943, *Naturwiss.*, **31,** 400.
Simon, F. E., 1951, *Z. Naturforschg.*, **6a,** 397.
Tolman, R. C., 1938, *Principles of Statistical Mechanics* (Oxford : University Press), p. 461.
von Neumann, J., 1929, *Z. Phys.*, **57,** 30.

CXXVI. *The Isotropic Component of Cosmic Radio-Frequency Radiation*

By J. R. Shakeshaft
Cavendish Laboratory, Cambridge*

[Received June 12, 1954]

Summary

Attempts have been made to interpret the observed galactic radio emission in terms of the integrated radiation from sources having a spatial distribution similar to that of the common optical stars. It is found, however, that such models fail to explain the large intensity observed towards the direction of the galactic poles. The origin of this additional component is discussed and the two most probable explanations seem to be (*a*) the incidence of an isotropic component from extra-galactic sources, and (*b*) the existence of a new class of object having a wide spatial distribution relative to the galactic plane.

The integrated radiation from normal extra-galactic nebulae is shown to be inadequate to account for the observations. An estimate has been made of the intensity likely to be produced by sources of the type associated with the collision of two galaxies, and it is shown that such sources will increase significantly the emission per unit volume. An independent figure can be derived from data on the large scale irregularities in the distribution of galaxies.

The total intensity to be expected from extra-galactic sources is found to depend strongly on the more distant regions of the Universe, and the value obtained, therefore, depends on the Cosmological theory adopted. Accurate measurements of the extra-galactic component might thus be important in distinguishing between different theories.

It is possible to account for the observed polar intensity with extra-galactic sources using Relativistic Cosmology, but not on the Steady-State theory. Recent measurements of the Andromeda nebula have, however, suggested that part of the polar emission may be due to galactic sources and a conclusive distinction cannot therefore yet be made.

§ 1. Introduction

Westerhout and Oort (1951) have shown that the survey of galactic radiation at a frequency of 100 Mc/sec made by Bolton and Westfold (1950) may be explained by assuming that most of the radiation comes from radio stars. In their model these are distributed through the galaxy in the same way as the common Population II stars of types G and K. They pointed out, however, that in order to account for the observed distribution, it was necessary to superimpose on this model an isotropic component of the radiation. At 100 Mc/sec this additional intensity

---

* Communicated by M. Ryle, F.R.S.

corresponds to a brightness temperature T_b of 600°K, where T_b is defined by the Rayleigh–Jeans law :—

$$T_b = \frac{B(\nu)\, c^2}{2k\nu^2},$$

where ν is the frequency, $B(\nu)$ is the brightness in units of flux density per steradian, k is Boltzmann's constant and c is the velocity of light.

In § 2 a number of possible causes of this isotropic component are discussed, one of which is related to the emission from extra-galactic sources ; this possibility is examined in detail in §§ 3 and 4.

In addition to the emission from normal extra-galactic nebulae, recent observations have revealed the existence of a different type of radio source whose emission exceeds by a factor of some 10^5 that of the normal nebulae. Following the accurate determination of the position of the intense radio star in Cygnus by Smith (1951), Baade and Minkowski (1954 a) were able to identify it with a very peculiar galaxy whose spectrum shows the presence of high excitation in the interstellar material ; they concluded that the observations could be explained if the object were in fact two galaxies in collision. Subsequently two similar events have been located at the positions of other radio sources.

From data on the spatial density and size of galaxies an estimate can be made of the spatial density of galaxies in collision at any time. If the relationship between the type of collision and the radio emission were also known, it would then be possible to derive the contribution of such objects to the radio emission per unit volume of space.

In order to deduce the total intensity produced, it is necessary to consider the effect of the red-shift. It is shown in § 4 that owing to the difference between the spectral law of the radio sources and the spectral law of visible stars, the integrated radio intensity will be affected to a much greater degree by the more distant parts of the Universe and the total thus depends critically on the Cosmological theory adopted.

§ 2. POSSIBLE SOURCES OF THE ISOTROPIC COMPONENT

Westerhout and Oort suggested three possible explanations for the radiation not accounted for by their model :—

(*a*) Radiation from the ionosphere.
(*b*) Galactic sources with a very unusual spatial distribution.
(*c*) The integrated radiation from all the normal extra-galactic nebulae.

In addition the following will be considered :—

(*d*) Radiation from ionized hydrogen clouds surrounding the sun.
(*e*) The integrated radiation from colliding galaxies.

These will now be dealt with in turn :—

(*a*) Westerhout and Oort point out that if this mechanism were of importance considerable diurnal variations in the observed intensity would be expected. Apart from this the optical depth of the ionosphere

($\tau = \int \kappa(\nu) ds$ where $\kappa(\nu)$ is the absorption coefficient and *ds* is an element of length) may be calculated. It may be shown that for a reasonable distribution of electron density and temperature with height the radiation at 100 Mc/sec corresponds to an additional temperature of only about 5°K.

(*b*) If the large polar intensity were to be explained in terms of galactic sources, it would be necessary to suppose that they were distributed to large distances from the galactic plane, and also that they extended to radial distances larger than that of the solar system. No such population of optical stars appears to have been observed.

(*c*) The early observations of the nearer extra-galactic nebulae suggested that there would be little hope of accounting for the isotropic component in terms of the emission from normal galaxies. Hanbury Brown and Hazard (1952) however, later suggested, on the basis of observations of the Perseus cluster, that there was a discrepancy between the radio and optical emission from faint galaxies ; on this supposition the integrated radio emission would then be considerably greater than that previously estimated. Recently Baldwin and Elsmore (1954) have made some detailed measurements of the Perseus cluster and have shown that 75% of the radiation is due to NGC 1275, one of the members of the cluster. The remaining emission is in agreement with the value expected if the other members of the cluster have a radio emission comparable with the nearby galaxies which have been observed individually. It is, therefore, concluded that the ratio of optical to radio magnitudes is constant. and in later sections a value of the radio emission from a galaxy of optical magnitude +10 will be taken as $5{\cdot}3 \times 10^{-26}$ w m^{-2} (c/s)$^{-1}$ at 100 Mc/sec (cf. Hanbury Brown and Hazard 1953 a). As will be seen in § 4 this figure is inadequate to account for the brightness temperature of 600°K observed in polar directions.

(*d*) Siedentopf (1953) has shown from measurements of the polarization of the zodiacal light that the electron density in the solar system is much higher than was previously thought to be the case. Strömgren in 1939 gave an expression which relates the diameter of the region within which the interstellar gas is ionized, to the temperature and radius of the exciting star and the density of the gas. Using the values of electron density determined by Siedentopf and assuming an average electron temperature of 10 000°K, it is possible to compute the optical depth of the entire region as viewed from the earth. The results obtained show that the contribution to the brightness temperature at 100 Mc/sec is unlikely to exceed 1°K.

(*e*) The contribution due to colliding galaxies is considered in more detail in the following paragraphs.

§ 3. THE OBSERVATIONAL DATA

In this section an attempt will be made to derive from the very limited observational results enough numerical data to enable an estimate to be made of the emission per unit volume due to colliding galaxies. It is first necessary to find their spatial density and the mean radio emission from such sources.

3.1. *The Spatial Density of Colliding Galaxies*

Suppose that space were filled with a uniform distribution of galaxies, each having a radius a parsecs and a random velocity V parsecs per second, the average spatial density being ρ galaxies per cubic parsec. If it is assumed that an average collision occurs when the centres of two galaxies pass within a distance a of each other, the collisional cross section may be written πa^2 and each galaxy will make $\sqrt{2}\pi a^2 V \rho$ collisions per second. The number of collisions per cubic parsec is then given by $\sqrt{2}\pi a^2 V \rho^2$ and if each collision is assumed to last for a time a/V, the number of collisions occurring at any time in each cubic parsec is $n = \sqrt{2}\pi a^3 \rho^2$.

The greatest uncertainty in deriving n is due to the difficulty of assessing the mean density of galaxies. As has been shown by many workers, galaxies exist in clusters, the density in these being anything up to one thousand times that of the field nebulae. Since the collisional probability is proportional to ρ^2, it might be thought that clusters only need be considered as contributing to collisions. The fraction of space occupied by dense clusters, however, is probably small and also the proportion of elliptical galaxies in clusters is much greater than among the field nebulae. Indeed Spitzer and Baade (1951) have suggested that this characteristic is due to the removal of the interstellar gas by collisions. The development of spiral nebulae is thus prevented and the radio emission, which on present evidence should be related to the gaseous material, may be smaller for collisions involving elliptical nebulae.

Since there are no reliable data on the fractions of space having different galactic densities, the present calculations are based on the mean density, 4×10^{-18} galaxies per cubic parsec (Neyman, Scott and Shane 1953), taking in this and further calculations, the new distance scale to be twice the old. Using this figure and taking a as 10 000 parsecs, the collisional density $n = 7 \times 10^{-23}$ per cubic parsec. Since the effect of clustering will be to increase the number of collisions, this represents a minimum value. There will also be a contribution from peculiar galaxies such as M 87 in Virgo, which has an abnormally intense radio emission, but this cannot at present be estimated.

3.2. *The Known Colliding Galaxies*

3.2.1. *Cygnus–A*, 19·01 (*Ryle, Smith and Elsmore* 1950), 19+4 (*Mills* 1952)

From the photographs obtained by Baade and Minkowski (1954 a), two late-type spiral galaxies appear to be in broadside collision, since emission lines are prominent over the whole disc. Using the observed red-shift, which corresponds to a recessional velocity of 16 830 km/sec the relationship between red-shift and distance (corrected for the new distance scale) gives the distance as 66×10^6 parsecs, and the measured intensity at the earth is :—

$$1350 \times 10^{-25} \text{ w m}^{-2} (\text{c/s})^{-1} \text{ at } 81{\cdot}5 \text{ Mc/sec}$$

and

$$1300 \times 10^{-25} \text{ w m}^{-2} (\text{c/s})^{-1} \text{ at } 100 \text{ Mc/sec.}$$

3.2.2. *NGC* 1275, 03·02 (*Ryle, Smith and Elsmore*), 03+4 (*Mills*)

This object is interpreted (Baade and Minkowski 1954 b) as a tightly-wound spiral penetrating a late-type spiral galaxy. From the red-shift the distance is found to be 20×10^6 parsecs.

The measured intensity at the earth is :—

12×10^{-25} w m^{-2} (c/s)$^{-1}$ at 81·5 Mc/sec (Baldwin and Elsmore 1954).

3.2.3. *NGC* 5128, *Centaurus–A*, 13−4 (*Mills*)

Baade and Minkowski believe this to be a late-type spiral in collision with an elliptical galaxy. De Vaucouleurs (1953), however, is of the opinion that NGC 5128 and several other similar objects he has found in the southern sky near radio sources, resemble the nuclei of peculiar barred spiral galaxies.

The distance is greater than 10^6 parsecs, and the measured intensity is 16×10^{-25} w m^{-2} (c/s)$^{-1}$ at 101 Mc/sec.

3.3. *The Radio Emission Associated with Colliding Galaxies*

Only three examples of colliding galaxies are known at present and these differ in the type of galaxy involved and in the geometry of the collision. They also show marked differences in the intensity of the radio emission, as can be seen from the following table which gives the power radiated per unit bandwidth per unit solid angle ; these figures have been corrected to a frequency of 100 Mc/sec assuming that the spectral law is $I \propto \nu^{-0{\cdot}5}$.

Cygnus–A : $P = 5 \times 10^{26}$ w steradian^{-1} (c/s)$^{-1}$.
NGC 1275 : $P = 4 \times 10^{23}$ w steradian^{-1} (c/s)$^{-1}$.
NGC 5128 : $P > 10^{22}$ w steradian^{-1} (c/s)$^{-1}$.

There is as yet no satisfactory mechanism to account for the emission of radio waves from colliding galaxies, but it seems probable that the radiation is due to the interaction of moving gas clouds, since all the radio sources which have been identified with visible objects show the presence of gaseous material in violent motion. Spiral galaxies such as those in the Cygnus source contain widely distributed interstellar material, whilst elliptical galaxies contain practically none. It has been suggested by Baade and Minkowski that the radio emission from the Centaurus source may be due to the tidal forces causing differential motion of the gas. This might be expected to produce relatively less intensity.

Without a detailed theory for the emission mechanism it is clearly impossible to say how the emission might vary with the density and relative velocity of the gas clouds, or how long the radiation might last after the galaxies have penetrated one another. These questions may be answered if a larger number of identifications can be made, but it is necessary to see what estimate of the total emission can be made from the present limited data.

The observations suggest that a collision between two late-type spirals is very much more effective than other collisions, but the spectroscopic evidence of excitation over the whole disc indicates that the Cygnus source itself may be a rather special example having a rare geometrical configuration ; the emission may therefore exceed that expected from a typical collision. This conclusion may easily be verified from radio data, for if the Cygnus-type sources had a density of 7×10^{-23} per cubic parsec, previously estimated as a minimum value for colliding galaxies, then over the whole sky there would be some 100 000 radio stars with an intensity greater than 10^{24} w m^{-2} (c/s)$^{-1}$. Using preliminary data from the new Cambridge survey of radio stars, it may be estimated that there are some 60 stars with a flux larger than this value. This then fixes a maximum permissible density for Cygnus-type sources ; and their radio emission per unit volume is less than 1/10 of that of normal galaxies.

Having dismissed Cygnus–A as a special case, the consequences of assuming a mean power for collisions of the order of that observed from the Perseus and Centaurus sources must be examined. The loss of energy by radio and optical radiation in the time required for the stars in two galaxies to pass by each other, a/V, is very small compared with the collisional energy of the gas clouds, and since the total emission per unit volume depends on the time during which the radiation persists, it may be that the effective source density is considerably greater than that already estimated. An upper limit may again be placed on this increase by the number of sources actually detected. For example, if 1/3 of the 60 sources with flux larger than 10^{24} w m^{-2} (c/s)$^{-1}$ were colliding galaxies then the density could not be increased by more than a factor of 10 to $n=7\times 10^{-22}$ per cubic parsec. The emission per unit volume due to colliding galaxies would then become $nP=7\times 10^{-22}\times 3\times 10^{23}=210$ w steradian^{-1} (c/s)$^{-1}$ parsec^{-3} which may be compared with the figure due to normal galaxies of 216 w steradian^{-1} (c/s)$^{-1}$ parsec^{-3} ($n=4\times 10^{-18}$ per cubic parsec and $P=5{\cdot}4\times 10^{19}$ w steradian^{-1} (c/s)$^{-1}$).

Thus on this basis we should expect the radio radiation from a large assembly of galaxies to be about twice that calculated for the normal galaxies alone.

Independent evidence for such a conclusion has been provided by the observations of Kraus (1954), and Hanbury Brown and Hazard (1953 b) who have related certain irregularities in the distribution of radio emission to large scale irregularities in the distribution of extra-galactic nebulae. The latter authors conclude that the emission per unit volume exceeds by 1·7 magnitudes (a factor of 4·8) that expected from a consideration of the emission of normal galaxies. More accurate observations of such large-scale structure have recently been made by Baldwin (in preparation) with the new Cambridge radio telescope, and he finds that the factor is probably at least 5. (The optical data on galactic counts are insufficient to get a very precise figure.) It therefore seems likely that the emission per cubic parsec lies in the range 400–1200 w steradian^{-1} (c/s)$^{-1}$. In the next section the integrated intensity associated with such an emission will be derived.

§ 4. THE INTEGRATED RADIATION FROM EXTRA-GALACTIC SOURCES

Before the integrated intensity due to distributed sources of radiation can be derived, it is important to examine the effects caused by the apparent expansion of the Universe. Because of the red-shift, the spectrum and intensity from radiating objects will be dependent on their distances. At optical wavelengths the spectrum from nearby galaxies approximates to that from a black body at a temperature of about 10 000°K, so that galaxies situated at distances where the apparent recession velocity is of the order of half the velocity of light will produce relatively little radiation in the visible spectrum, owing to the rapid fall of intensity on the short wavelength side of the black body curve. It therefore becomes extremely difficult to observe optically at distances greater than this, and the integrated optical radiation is highly convergent.

The radio spectrum both of our own galaxy and of the intense extra-galactic sources, however, shows a comparatively gradual decrease towards the shorter wavelengths. It should, therefore, be feasible to detect individual sources at very much greater distances, whilst the integrated radiation will depend more on the distant regions of the Universe. It is of interest to note that although the Cygnus source is at a distance about 1/10 of that to which optical telescopes have penetrated, its intensity is of the order of 10^3 times that of the weaker radio sources now being detected; it therefore seems probable that a number of the latter are beyond the range of optical instruments.

It is now possible to derive the integrated radiation at a given wavelength in terms of a given Cosmological theory, if the spectrum of the source is known.

Let the total power per unit volume radiated in the frequency range ν to $\nu+\Delta\nu$ be $4\pi nP(\nu)\Delta\nu$ w parsec^{-3} then the total flux observed at the earth is

$$B(\nu)\Delta\nu=\int_0^\infty \frac{nP(\nu')\ \Delta\nu'}{r^2(1+z)^2}\cdot\frac{r^2\,dr}{(1+z)^\alpha}$$

where z is the red-shift, r is the distance, ν' is the frequency at which the radiation was emitted, that has been shifted to the frequency of reception ν, $\Delta\nu'$ is the bandwidth of emission, $\Delta\nu$ is the bandwidth of reception, and α is a constant factor $=0$ for Relativistic Cosmology $\quad$ $=3$ for the Steady-State theory $\Big\}$ Bondi (1952).

The circumstances under which this expression holds are considered later.

The red-shift z is observed to be proportional to distance and $z=r/T$

where $1/T$ is Hubble's constant (corrected for the new scale), also $\nu'/\nu=\Delta\nu'/\Delta\nu=(1+z)=(1+r/T)$. Substituting in the expression above,

$$B(\nu)=\int_0^\infty \frac{nP(\nu')\,dr}{(1+r/T)^{1+\alpha}}.$$

Sciama (personal communication) has shown that it is unnecessary to take into account the optical energy range when this has been shifted to radio frequencies.

Assuming that $P(\nu)\propto\nu^{-0\cdot5}$, then $P(\nu')/P(\nu)=(\nu'/\nu)^{-0\cdot5}=(1+r/T)^{-0\cdot5}$ and

$$B(\nu)=\int_0^\infty \frac{nP(\nu)\,dr}{(1+r/T)^{1\cdot5+\alpha}}=\frac{nP(\nu)T}{(0\cdot5+\alpha)}.$$

Therefore

$$T_b=\frac{B(\nu)c^2}{2k\nu^2}=\frac{nP(\nu)T\lambda^2}{2k(0\cdot5+\alpha)}.$$

It should be noted that this result is correct for the Steady-State theory, but holds for Relativistic Cosmology only if it is possible to neglect

(*a*) Curvature,

(*b*) the variation of $P(\nu)$ with time (since the Universe is evolving and the galaxies observed at greater distances will be at an earlier stage ot development),

(*c*) a possible variation of the red-shift *vs.* distance relationship.

The importance of these corrections will depend on the convergence of the expression for the integrated radiation. To test this convergence it can be integrated to a distance R at which the apparent velocity is half that of light. This distance can be taken as approximately the ' limit ' of the optically observable Universe and the distance beyond which the effects mentioned will play an increasing part. In this case

$$v/c\simeq r/T \quad \therefore\ R\simeq 1/2T$$

and

$$[B(\nu)]_0^R=\tfrac{1}{3}\cdot\frac{nP(\nu)T}{(0\cdot5+\alpha)}.$$

Hence only 1/3 of the total radiation comes from a distance less than $1/2T$, and it is possible that the actual radiation expected using Relativistic Cosmology may be rather different from that calculated here.

However, taking $\lambda=3\text{ m}=10^{-16}$ parsecs,
$k=1\cdot4\times10^{-23}$ joules °K^{-1},
$T=1\cdot1\times10^{9}$ parsecs

and substituting $nP=400$–1200 w steradian^{-1} (c/s)$^{-1}$ parsec^{-3} in the expression for T_b, then T_b lies in the range

314°–942°K when $\alpha=0$, i.e. for Relativistic Cosmology,
45°–135°K when $\alpha=3$, i.e. for Steady-State theory.

§ 5. Conclusions

The observed intensity plot of radio emission shows a greater value towards the galactic poles than can be accounted for by sources distributed like the common optical stars. The integrated emission from extra-galactic sources, and the existence of a population of galactic sources having a wide dispersion have been suggested as possible explanations.

The determination of the total emission from extra-galactic sources depends on a knowledge of the average emission per unit volume of extra-galactic space, and on an investigation of the effects of the red-shift.

Estimates are made of the emission per unit volume due to normal galaxies, as well as that to be expected from the rare but intense colliding galaxies. Other evidence has been obtained of the total emission per unit volume by observations of the enhanced radiation from large scale irregularities in the galactic distribution.

It is found that the integrated intensity depends strongly on the Cosmological theory assumed. Using the data derived here it is seen to be possible to account for the polar intensity with the extra-galactic sources alone on the Relativistic theory but not the Steady-State theory. The present results cannot yet, however, be used to distinguish conclusively between the two theories, both because of the possible errors in the assumptions made in the calculations, and also because recent observations of the Andromeda nebula by Baldwin (1954) have suggested that the radio emission extends over an appreciably larger angle than the optical emission. There is, therefore, some evidence in favour of a population of radio sources in the Andromeda nebula which has a more extended distribution than the optical stars ; if such a population exists in our own galaxy also, it might be sufficient to account for a considerable fraction of the observed polar intensity. More accurate observations may allow the contribution of extra-galactic sources to be derived well enough to enable a definite distinction to be made between the two theories.

This work was carried out at the Cavendish Laboratory as part of a programme of radio research supported by the Department of Scientific and Industrial Research, to whom the author is indebted for a maintenance grant. He also wishes to thank Professor H. Bondi for a useful discussion and Mr. M. Ryle for valuable advice and help.

REFERENCES

BAADE, W., and MINKOWSKI, R., 1954 a, *Ap. J.*, **119,** 206 ; 1954 b, *Ibid.*, **119,** 215.
BALDWIN, J. E., 1954, *Nature, Lond.*, **174,** 320.
BALDWIN, J. E., and ELSMORE, B., 1954, *Nature, Lond.*, **173,** 818.
BOLTON, J. G., and WESTFOLD, K. C., 1950, *Aust. J. Sci. Res.* A, **3,** 19.
BONDI, H., 1952, *Cosmology* (Cambridge : University Press).
HANBURY BROWN, R., and HAZARD, C., 1952, *Phil. Mag.*, **43,** 137 ; 1953 a, *Nature, Lond.*, **172,** 853 ; 1953 b, *Ibid.*, **172,** 997.
KRAUS, G. D., 1954, *Astro. J.*, **59,** 113.
MILLS, B. Y., 1952, *Aust. J. Sci. Res.* A, **5,** 266.
NEYMAN, J., SCOTT, E. L., and SHANE, C. D., 1953, *Ap. J.*, **117,** 92.
RYLE, M., SMITH, F. G., and ELSMORE, B., 1950, *Mon. Not. R. Ast. Soc.*, **110,** 508.
SIEDENTOPF, H., 1953, *Experentia*, **9,** 134.
SMITH, F. G., 1951, *Nature, Lond.*, **168,** 555.
SPITZER, L., and BAADE, W., 1951, *Ap. J.*, **113,** 413.
STRÖMGREN, B., 1939, *Ap. J.*, **89,** 526.
VAUCOULEURS, G. DE, 1953, *Observatory*, **73,** 877.
WESTERHOUT, G., and OORT, J. H., 1951, *B.A.N.*, **11,** 323.

CXXVII. *Double Pion Production and the Nature of Pseudoscalar Coupling*

By P. Bocchieri* and G. Feldman
Department of Mathematical Physics, The University, Birmingham†

[Received May 26, 1954]

Abstract

A perturbation calculation for single and double pion production is carried out for pseudoscalar, symmetric meson theory at energies in the Birmingham range (about 1000 MeV). It is found that the γ_5 nature of the coupling does not favour double over single production and that, in fact, a large coupling constant would be required to explain a large double to single ratio.

§ 1. Introduction

Preliminary experimental results (Fowler, Shutt, Thorndike and Whittemore 1953) indicate that double pion production in nucleon–nucleon collisions is rather large at nucleon energies of about 2·3 BeV in the laboratory system ; and that at these energies double pion production is probably larger than single production. This result would, at first sight, indicate a large coupling constant between nucleons and mesons. However, one might imagine that if the coupling between nucleons and mesons is pseudoscalar (γ_5), this would favour the occurrence of virtual pairs (in terms of perturbation theory). In that case, those reactions containing an even number of vertices (e.g. double pion production) would be favoured compared to those containing an odd number of vertices (e.g. single pion production). This presumed effect of γ_5 should make itself more apparent if the coupling constant were indeed not too large.

It is the purpose of this paper to carry out a perturbation calculation for double and single pion production in order to see whether a large double to single ratio might be explained in terms of γ_5 coupling rather than in terms of a large coupling constant. We find, in fact, that the γ_5 nature of the coupling alone does not explain a large double to single ratio. In spite of the unsatisfactory nature of a perturbation calculation, we feel that it is worth putting such a calculation on record since, like similar calculations for other reactions, it may be useful for orientation.

In § 2 we evaluate the densities of final states arising in single and double production and make a crude estimate of the matrix elements using arguments similar to those of Fermi (1951). In § 3 we show how to write down, simply, the terms occurring in the cross section and we evaluate them. The results are discussed in § 4.

---

* On leave from the Istituto Nazionale di Fisica Nucleare, Sez-di-Milano.
† Communicated by Professor R. E. Peierls, F.R.S.

§ 2

Throughout the paper we shall be considering the following two reactions:

$$N_1+N_2\rightarrow N_3+N_4+\pi, \qquad (2.1)$$

$$N_1+N_2\rightarrow N_3+N_4+\pi_1+\pi_2, \qquad (2.2)$$

where N_i are nucleons and π_i are mesons. In the laboratory system the threshold for (2.1) is 290 MEV and for (2.2) it is 600 MEV. We shall be calculating cross sections for an incoming nucleon of kinetic energy 940 MEV (i.e. equal to M the nucleon rest mass). In the C.M. system of the two initial nucleons the kinetic energy available is 0·45 M. The mass of the π-meson is 0·15 M, and thus in reaction (2.1) the kinetic energy to be shared between the final particles is 0·30 M, whereas in (2.2) it is 0·15 M. In evaluating the integrals from the density of final states below, we shall assume these energies to be non-relativistic. In view of the errors of other approximations to be made, this would seem adequate.

The cross section for either (2.1) or (2.2) is

$$\sigma=\frac{2\pi}{v}\int|H|^2\rho(E)\,dQ, \qquad (2.3)$$

where H is the matrix element, $\rho(E)$ is the density of final states and dQ the suitable differential factors. v is the relative velocity of the incoming nucleons. We use units in which $\hbar=c=1$.

For single production

$$\rho_1(E)\,dQ_1=\delta(\mathbf{p}_3+\mathbf{p}_4+\mathbf{q})\,\delta\left(\frac{\mathbf{p}_3{}^2+\mathbf{p}_4{}^2}{2M}+\frac{\mathbf{q}^2}{2\mu}-T_1\right)d^3p_3\,\frac{d^3p_4\,d^3q}{(2\pi)^6}, \qquad (2.4)$$

where $\mathbf{p}_3$, $\mathbf{p}_4$ and $\mathbf{q}$ are the momenta of the outgoing nucleons and meson respectively, μ is the meson mass and M the nucleon mass and T_1 is the kinetic energy available in the C.M. $T_1=0{\cdot}30\,M$ for an incoming nucleon of 940 MEV kinetic energy.

If we assume the matrix element is energy independent (or varies slowly with energy) we can integrate over the variables dQ_1 in (2.3) easily by making the transformation

$$\mathbf{p}_3+\mathbf{p}_4=\mathbf{a}, \quad \mathbf{p}_3-\mathbf{p}_4=\mathbf{b}.$$

This gives

$$\int\rho_1(E)\,dQ_1=\frac{4}{(4\pi)^3}\frac{M^3}{(2M/\mu+1)^{3/2}}T_1{}^2\approx\frac{\sqrt{2}}{(4\pi)^3}\left(\frac{\mu}{M}\right)^{3/2}\left(\frac{T_1}{\mu}\right)^2M^3\mu^2. \qquad (2.5)$$

For double production

$$\int\rho_2(E)\,dQ_2=\int\delta(\mathbf{p}_3+\mathbf{p}_4+\mathbf{q}_1+\mathbf{q}_2)\delta\left(\frac{\mathbf{p}_3{}^2+\mathbf{p}_4{}^2}{2M}+\frac{\mathbf{q}_1{}^2+\mathbf{q}_2{}^2}{2\mu}-T_2\right)$$

$$\times d^3p_3\,d^3p_4\,\frac{d^3q_1\,d^3q_2}{(2\pi)^9}. \qquad (2.6)$$

We can carry out this integral by making the substitution

$$\left.\begin{aligned}\mathbf{p}_3+\mathbf{p}_4&=\mathbf{a}, \quad \mathbf{p}_3-\mathbf{p}_4=\mathbf{b}\\ \text{and} \quad \mathbf{q}_1+\mathbf{q}_2&=\boldsymbol{\alpha}, \quad \mathbf{q}_3-\mathbf{q}_4=\boldsymbol{\beta}.\end{aligned}\right\} \quad . \quad . \quad . \quad . \quad . \quad . \quad . \quad (2.7)$$

This gives

$$\int \rho_2(E)\, dQ_2=\frac{1}{2\pi}\,\frac{1}{(4\pi)^4}\,\frac{128}{105}\left(\frac{M}{\mu}\right)^{3/2}(1+\mu/M)^{-3}\left(\frac{T_2}{\mu}\right)^{7/2}\mu^8$$

$$\approx\frac{1}{2\pi}\,\frac{1}{(4\pi)^4}\,\frac{128}{105}\left(\frac{\mu}{M}\right)^{3/2}\left(\frac{T_2}{\mu}\right)^{7/2}M^3\,\mu^5. \quad . \quad . \quad (2.8)$$

It is of interest at this stage to make an estimate of the matrix element as carried out by Fermi (1951).

Each meson vertex in fig. 1 contributes $f/\sqrt{2\omega}$ where f is the coupling constant (essentially scalar coupling) and ω is the energy of the meson. This gives for the matrix element near threshold

$$\sqrt{2}\,f^3/\mu^{7/2}. \quad . \quad . \quad . \quad . \quad . \quad . \quad . \quad . \quad . \quad . \quad (2.9)$$

Fig. 1

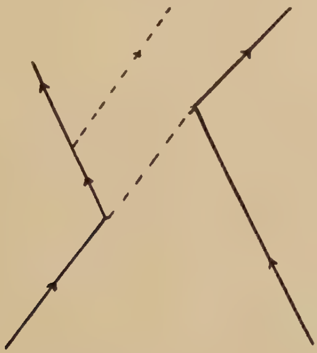

Single meson production.

(The result is slightly different from Fermi since we have allowed for various permutations of the vertices.) For an incoming nucleon of 940 Mev we get for the matrix element

$$\tfrac{3}{4}\,f^3/\mu^{7/2}. \quad . \quad . \quad . \quad . \quad . \quad . \quad . \quad . \quad . \quad . \quad (2.10)$$

We shall crudely fix the coupling constant by fitting the results to near threshold single pion production, that is, at about 340 Mev. A 340 Mev incoming nucleon corresponds to $T_1=\frac{1}{6}\mu$ and we get

$$\sigma_\pi\,(340)=1{\cdot}5\times 125\left(\frac{f^2}{4\pi}\right)^3 \text{mb.} \quad . \quad . \quad . \quad . \quad . \quad . \quad (2.11)$$

Assuming the cross section is 0·6 mb this gives $f^2/4\pi\approx 1/7$. For an energy of 940 Mev $T_1=2\mu$ and we get

$$\sigma_\pi\,(940)\approx 25 \text{ mb.} \quad . \quad . \quad . \quad . \quad . \quad . \quad . \quad . \quad . \quad (2.12)$$

We compare this with the result for total p–p cross section for 1 Bev protons. Brookhaven (Leavitt and Chen 1954) find a total p–p cross section of 49 mb. The elastic cross section at 400 Mev is about 25 mb.

We now estimate the double meson production cross section at 940 MEV and we get

$$H_2 \approx 4 f^4/\mu^5. \qquad \text{(2.13)}$$

At 940 MEV, $T_2 = \mu$ and we are led to the following ratio :

$$\frac{\sigma_{2\pi}(940)}{\sigma_\pi(940)} \approx \frac{1}{8}. \qquad \text{(2.14)}$$

It is of interest to extrapolate these results to Brookhaven energies (2·3 BEV incoming nucleon). The validity of this extrapolation depends on (*a*) the ratio of the matrix elements for double and single production remaining fairly constant with energy and (*b*) the non-relativistic approximation to the density of states (2.5) and (2.8) being valid at this energy. Although we could evaluate the density of states more accurately we feel it is not worth the trouble in view of (*a*). Under these assumptions we obtain

$$\frac{\sigma_{2\pi}(2300)}{\sigma_\pi(2300)} \approx \frac{3 \cdot 5}{1}. \qquad \text{(2.15)}$$

§ 3

In this section we evaluate by means of a graphical technique the squares of the matrix elements for single and double meson production. These have already been calculated for single production by Morette (1949).

First let us consider single production. One can draw the Feynman graphs for this reaction. One of these is shown in fig. 2.

Fig. 2

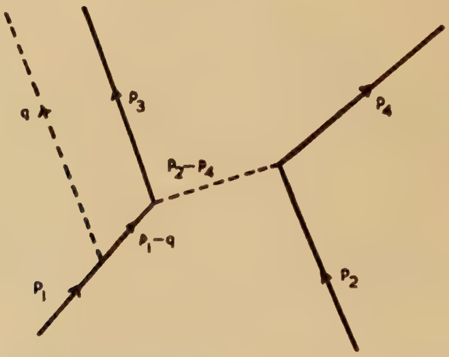

Typical Feynman graph in single pion production.

There are eight such graphs, four arising from the meson '*q*' coming off each leg and the same number when particles 1 and 2 are interchanged. Thus the matrix element H_1 will contain eight terms. Since we are going to sum over final and average over initial spins and isotopic spins it is easier to work with the square of the matrix elements $|H_1|^2$ which contains 64 terms. We can directly draw graphs* for the terms appearing in $|H_1|^2$. They fall into two classes which we call the ordinary terms and the exchange terms. An example of an ordinary term is given in fig. 3 (*a*). This is just a graphical representation of the square of the term given in fig. 2. The prescription used in writing down the terms which arise is as follows.

$$\left.\begin{array}{ll} \text{Each } \longrightarrow & \text{gives } S_{\mathrm{F}}(p)=-\dfrac{\gamma p+iM}{p^2+M^2}. \\[2ex] \text{Each } \rightarrow\!-0-\!\leftarrow & \text{gives } \Lambda_{+}(p)=\dfrac{M}{p_0}\,\dfrac{\gamma p+iM}{2iM}. \\[2ex] \text{Each } -\,-\rightarrow-\,- & \text{gives } \Delta_{\mathrm{F}}(p)=\dfrac{\delta_{ij}}{p^2+\mu^2}. \\[2ex] \text{Each } -\,-\!\rightarrow\!-0-\!\leftarrow\!-\,- & \text{gives } \dfrac{1}{2p_0}\,\delta_{ij}. \end{array}\right\} \quad \ldots \quad (3.1)$$

Each vertex gives $g\gamma_5\,\tau_i$. (p is a four momentum and $\gamma p=\gamma_\mu\,p_\mu$.) One must multiply by 1/16 coming from the averaging over the initial spin and isotopic spin states. All of the 2π factors have been taken care of in the definitions (2.3) and (2.4). We have assumed the interaction Hamiltonian to be

$$\mathscr{H}_i(x)=ig\bar{\psi}(x)\gamma_5\psi(x)\tau_i\phi_i(x). \quad \ldots\ldots \quad (3.2)$$

There are 32 of these ordinary terms. They arise when the meson line q begins on some line in the lower half of the diagram and ends on some line in the upper half. Each closed loop gives rise to a trace over the Dirac matrices and isotropic spin matrices. One can easily see that 16 of these terms are zero. They are those diagrams in which the meson q begins in one loop and ends in the other. This gives rise in γ_5 coupling to three γ_5's in each loop and the trace of three γ_5's with the other γ's is zero. An example of the exchange terms is given in fig. 3 (*b*). This is one continuous loop and so gives rise to one trace which will be more difficult to evaluate. There are 32 such terms.

The expression for $|H_1|^2$ corresponding to fig. 3 (*a*) is

$$(-1)\,\frac{9}{32}\,g^6\,\frac{1}{E_1E_2E_3E_4}\,\frac{1}{q_0}\,\frac{(p_2\cdot p_4+M^2)[2(p_1\cdot q)(p_3\cdot q)+\mu^2(p_1\cdot p_3+M^2)]}{[2(p_1\cdot q)+\mu^2]^2[p_2\cdot p_4+M^2-\mu^2/2]^2} \quad \ldots\ldots\ldots \quad (3.3)$$

At the energy of double pion production threshold $E_1=E_2=M+\mu$, and on the average $E_3=E_4=M+\mu/4$ and $q_0=3/2\mu$. Neglecting powers of μ/M, this term contributes

$$\frac{3}{40}\,\frac{g^6}{\mu^2M^5}. \quad \ldots\ldots\ldots \quad (3.4)$$

And finally the total matrix element is (the exchange terms contributing less than 10% at this energy)

$$\frac{2}{5}\,\frac{g^6}{\mu^2M^5}. \quad \ldots\ldots\ldots \quad (3.5)$$

---

* This suggestion was made by Professor R. E. Peierls.

We now come to the graphs in double production. A typical graph is shown in fig. 4 (*a*). There are altogether 40 such graphs in the matrix element H_2 and thus the square of the matrix element $|H_2|^2$ will contain 1600 terms, 800 of which will be ordinary terms of the form shown in fig. 3 (*a*) (containing an extra meson line, however) and 800 will be of the exchange type (fig. 3 (*b*)). Now, as in single production a certain number of the ordinary terms will be zero whenever there are 3 γ_5's in one loop. There are 384 such terms. The others can be evaluated using the prescription of (3.1).

Fig. 3

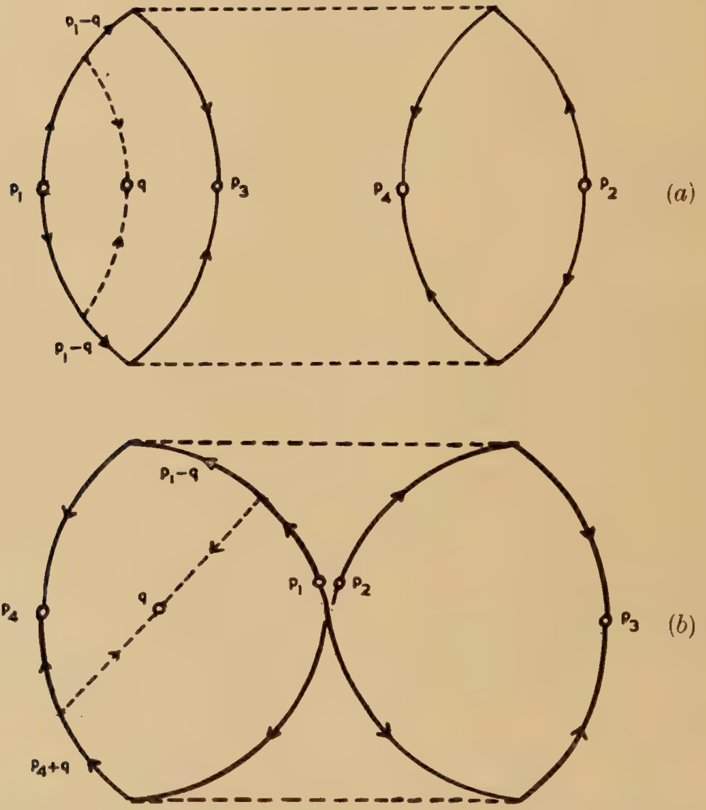

Graphical representation of the square of the matrix element in pion production. (*a*) An ordinary term. (*b*) An exchange term.

In evaluating the various terms we may notice just what effect the γ_5 coupling has. Naively, one might expect that the contribution from fig. 4 (*a*) would be greater than that from fig. 4 (*b*); since if we believe that in a time ordered event γ_5 has large matrix elements only between positive and negative energies, then the largest part of 4 (*a*) is the time ordered graph 4 (*c*) consisting entirely of ‘ large ’ matrix elements, whereas the largest part of 4 (*b*) is 4 (*d*) which contains only two ‘ large ’ matrix elements. However, it turns out that both 4 (*a*) and 4 (*b*) contribute about the same amount to the total matrix element.

Fig. 4

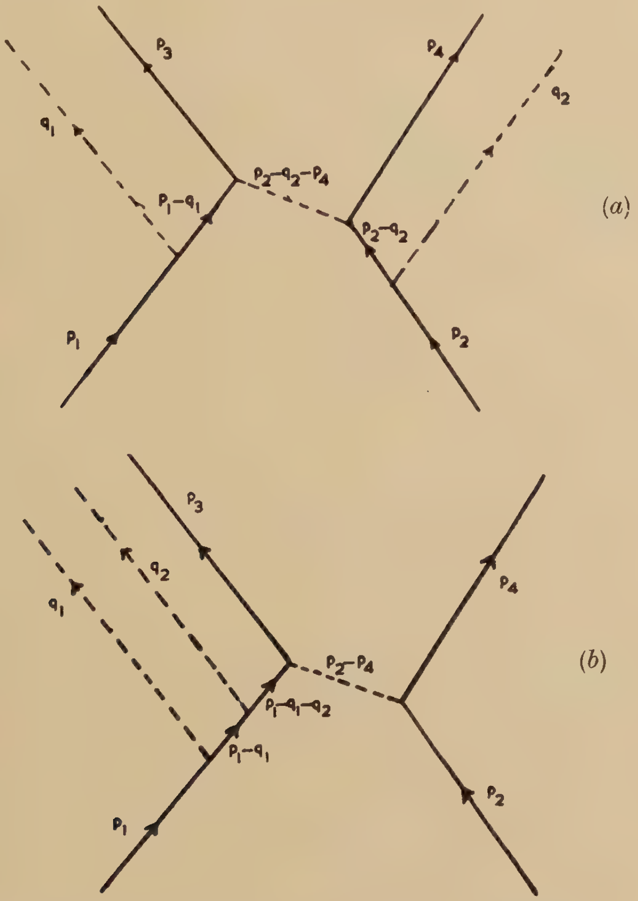

Typical Feynman graphs in double pion production.

One can easily see* why the graphs 4 (*c*) and 4 (*d*) are of the same order of magnitude. In the three-dimensional treatment, the matrix element between a positive and negative energy component is of order 1, whereas between two positive energy components it is of order $|\mathbf{p}|/M$ where $|\mathbf{p}|$ is the momentum of the nucleon. At threshold, each incoming nucleon must have a kinetic energy (in the C.M. system) equal to μ and therefore its momentum is $\sqrt{(2\mu M)}$. Thus the vertices in 4 (*c*) contribute $(1)^4=1$ and those in 4 (*d*) contribute $(1)^2[\sqrt{(2\mu/M)}]^2=2\mu/M$. The energy denominator of 4(c) is $(1/2M)^2 1/\mu$ and for 4(d) it is $1/2M(1/\mu)^2$. Thus both 4(c) and 4(d) are of the same order of magnitude.

---

* This very simple argument is due to Dr. G. E. Brown.

Fig. 4

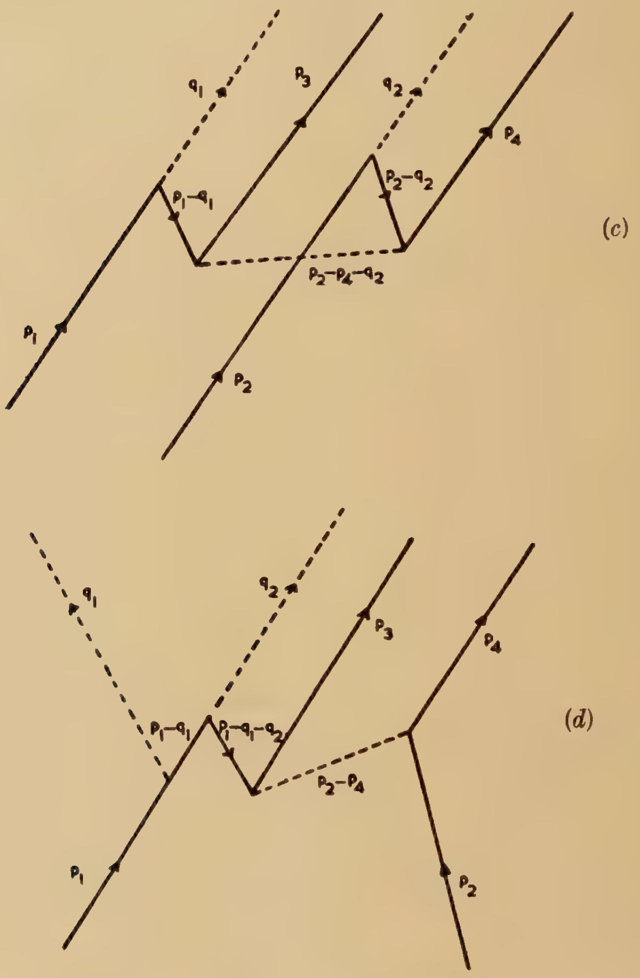

The corresponding time-ordered graphs.

The square of the term in fig. 4 (a) gives (at threshold)

$$\frac{g^8}{2^6}\frac{1}{\mu^4 M^6}, \quad \ldots \ldots \quad (3.6)$$

neglecting higher powers of μ/M; and the square of term 4 (b) gives one-quarter of this result.

After a good deal of algebra we arrive at the final answer for $|H_2|^2$ (which includes the sum and average over final and initial isotopic spins respectively)

$$\frac{21}{16}g^8\frac{1}{\mu^4 M^6}. \quad \ldots \ldots \quad (3.7)$$

The results for the cross sections are

$$\sigma_\pi = \left(\frac{g^2}{4\pi}\right)^3 \left(\frac{\mu}{M}\right)^{3/2} \frac{4}{5}\sqrt{2\pi}\left(\frac{T_1}{\mu}\right)^2 \left(\frac{1}{M}\right)^2 \approx 0{\cdot}08 \left(\frac{T_1}{\mu}\right)^2 \left(\frac{g^2}{4\pi}\right)^3 \text{mb}, \qquad (3.8)$$

$$\sigma_{2\pi} = \left(\frac{g^2}{4\pi}\right)^4 \left(\frac{\mu}{M}\right)^{5/2} \frac{8}{5}\left(\frac{T_2}{\mu}\right)^{7/2} \left(\frac{1}{M}\right)^2 \approx 0{\cdot}006 \left(\frac{T_2}{\mu}\right)^{7/2} \left(\frac{g}{4\pi}\right)^4 \text{mb}, \qquad (3.9)$$

where $T_1 = 2\mu$ and $T_2 = \mu$ for a 940 Mev incident proton.

This gives

$$\frac{\sigma_{2\pi}(940)}{\sigma_\pi(940)} \approx \frac{1}{50}\left(\frac{g^2}{4\pi}\right). \qquad (3.10)$$

If we fit the coupling constant to $\sigma_\pi(940) \approx 25$ mb, we find $g^2/4\pi \approx 4{\cdot}5$ giving a result of the order of 1 to 10, for the ratio of double to single production at this energy. If we extrapolate the results to Brookhaven energies (where $T_1 \approx 6\mu$, $T_2 \approx 5\mu$) under the same crude assumptions as stated in § 1 we find

$$\frac{\sigma_{2\pi}(2300)}{\sigma_\pi(2300)} \approx \frac{7}{12}\frac{g^2}{4\pi} \approx \frac{2{\cdot}6}{1}. \qquad (3.11)$$

We may compare these results with the still cruder ones (2.14) and (2.15).

§ 4. Conclusions

The results of the above calculation indicate that one must be careful when using arguments about γ_5 coupling. One cannot say that a reaction with an even number of vertices will be favoured over one with an odd number. Nor can one say that a graph with the maximum number of pairs produced will be larger than another graph. It is important to examine the momenta involved. A reaction at threshold need not necessarily involve small momenta. Double pion production requires each incoming nucleon to have a kinetic energy of at least μ. This is essentially why the matrix elements shown in figs. 4 (*a*) and 4 (*b*) are of the same order of magnitude.

If the ratio of the cross sections for double to single pion production is indeed large at Birmingham and Brookhaven energies this would indicate a large coupling constant for pseudoscalar theory but would give little indication as to whether the coupling is pseudoscalar or not (cf. eqns. (3.10), (3.11) and (2.14), (2.15)).

We should like to thank Professor R. E. Peierls and Dr. P. T. Matthews for many interesting and valuable discussions.

References

Fermi, E., 1951, *Elementary Particles* (Yale University Press).

Fowler, W. B., Shutt, R. P., Thorndike, A. M., and Whittemore, W. L., 1953, *Phys. Rev.*, **91,** 758.

Leavitt, C. P., and Chen, F. F., 1954, *Bull. Amer. Phys. Soc.*, **29,** No. 4, 75.

Morette, C., 1949, *Phys. Rev.*, **76,** 1432.

CXXVIII. *An Elementary Reasoned Account of the General Circulation of the Atmosphere*

By M. J. Lighthill
Department of Mathematics, University of Manchester*

[Received June 29, 1954]

Summary

The paper (which makes no claim to originality) gives an elementary survey of the physical causes believed to underly the more energetic features of the general circulation.

The geographical distribution of temperature implies hydrostatically a strong fall of the pressure from the tropics to the poles at any fixed altitude in the upper troposphere. This produces geostrophically (in the main) the strong westerly winds found at all latitudes in that region. Simple estimates indicate why a typical wind speed is 20 m/sec.

The wind distribution near the ground, a secondary effect, is intelligible only if there is everywhere a poleward flow of west-east angular momentum (taken about the earth's axis). The required flow reaches a maximum of around 3×10^{26} dyn cm, at latitude 30°. In the tropics and sub-tropics the angular momentum must flow against its own gradient. It can do so to the necessary extent, however, as a result of the poleward motions down pressure gradients in the upper troposphere which are needed to maintain the energy of the general circulation, which is dissipated at a rate of around 5×10^3 ergs/cm^2/sec. In the cyclone belt, the assumption behind this statement (that isobars in the upper troposphere lie east-west, on the whole) is constantly violated, but there the flow of angular momentum (down its own gradient) presents no difficulty, and is doubtless achieved by the cyclones themselves.

§ 1. Introduction

This paper is intended as a contribution to the relations between meteorologists and general physicists. It concerns the 'explanation of the general circulation'.

A physicist, wishing to arrive at some understanding of the basic physical causes underlying the general circulation of the atmosphere, cannot easily do so from a survey of the best known accounts of meteorology. He discovers early that the schoolbook descriptions of hot air rising at the equator and flowing towards the poles and being deflected into a westerly direction by Coriolis force are quite inadequate

---

* Communicated by the Author.

to explain the strength of the Westerlies in the temperature zones. Apart from this, he is told, for example, by Brunt (1939), in his invaluable *Physical and Dynamical Meteorology*, that " it is not possible at present to put forward any satisfactory theory of the general circulation " (p. 413), " nor at this stage can we say that the cyclone, anticyclone and general circulation are not merely three aspects of one problem " (p. 403), and that " the latest writings on the frontal analysis of depressions, on the anticyclones, and on the general circulation, all indicate a recognition of the complexity of the phenomena, and less readiness to attempt general theories " (p. 418).

All this is very damping, as the general circulation is the most energetic and permanent feature of the atmosphere, and a physicist is inclined to believe that the general laws of mechanics and thermodynamics should be sufficient to give an order-of-magnitude explanation of such a predominant feature of a relatively accessible part of the universe. The details of the instability of fronts, and of the production of periodic quasi-regular disturbances of the general circulation, are problems of prime importance to the meteorologist, but secondary from the point of view of the physicist, who would not expect a simple description of these elaborate perturbation effects in terms of basic laws.

In fact, however, putting aside the finer details (with which the meteorological experts are naturally deeply concerned), enough information exists already to quieten the physicist's fears lest the rules of physical reasoning are inadequate to illuminate even the broadest general features of the situation. The following remarks are not intended to be in any way original, and their content will mostly be familiar to meteorologists. They are put forward, principally, as a sample of what can most appropriately be said about the subject to physicists in general—for example, when the topic is mentioned in sixth-form or university physics teaching.

The primary phenomenon is the tendency to strong westerly mean circulation, at all latitudes, in the upper part of the troposphere. This is treated first, in § 2. The distribution of mean winds near the ground is a kind of by-product, whose discussion is postponed to §§ 3 and 4.

§ 2. THE CIRCULATION IN THE UPPER PARTS OF THE TROPOSPHERE

In terms of energy content, the mean wind distribution at the earth's surface is a secondary effect compared with the much stronger mean circulation at greater heights. In the upper half of the troposphere the prevailing wind is westerly at all latitudes, with mean velocities of the order of 20 m/sec. It is natural to try to explain this, the most energetic feature of the situation, first.

The circulation is associated with a mean pressure distribution in the upper parts of the troposphere which falls fairly steadily (at any fixed height above sea level) from the tropics to the poles. The mean isobars have a clear tendency to lie in east–west directions, and they encircle the earth without a break except for certain ' highs ' over the continents in summer. The mean pressure excess at the equator over that at the same altitude at the poles is of the order of 50 mb and is considerably more than the difference at sea level.

One needs to explain only this mean pressure distribution, for this appears quite sufficient to maintain the observed mean circulation as, in the main, a ' geostrophic ' wind. In other words, the wind is approximately along the isobars and provides, on the average, as much Coriolis force per unit volume as will balance the poleward force due to pressure gradient. In symbols, it satisfies

$$(2\omega \sin \phi)\rho u = \frac{\partial p}{\partial y}, \quad . \quad . \quad . \quad . \quad . \quad . \quad . \quad . \quad (1)$$

where ω is the earth's angular velocity ($7{\cdot}3 \times 10^5\ \mathrm{s}^{-1}$), ϕ is the latitude, ρ the density, u the velocity along the isobars, and $\partial p/\partial y$ the pressure gradient normal to them.

Now the pressure distribution seems clearly explicable as a direct result of the temperature distribution, which in turn is maintained by the distribution with latitude of incoming solar heat. The mean temperature decreases, of course, from the tropics to the poles, and the pressure gradient in the upper part of the troposphere is an inevitable hydrostatic consequence. For the pressure must fall off with altitude more gradually in the tropics, where the density is reduced. Hence the pressure at higher altitudes must be much greater in the tropics than at the poles—unless there is a large difference the other way at the ground. The latter is impossible, however, because of the frictional resistance of the ground to really strong mean geostrophic winds (this will be considered further in § 3).

A simple numerical estimate of the effect is obtainable from the well-known distribution of pressure in an atmosphere in which the temperature is independent of altitude. This is

$$p = p_0 \exp\left(-gz/RT_0\right), \quad . \quad . \quad . \quad . \quad . \quad (2)$$

where p_0 and T_0 are the pressure and temperature at sea level, z is height above sea level, and R is the gas constant for air. If p_0 and T_0 vary with y, which we may take as signifying distance from the nearest pole (to fix the ideas), then at fixed altitude

$$\frac{\partial p}{\partial y} = \left(\frac{dp_0}{dy} + \frac{p_0 gz}{RT_0^2}\frac{dT_0}{dy}\right)\exp\left(-gz/RT_0\right). \quad . \quad . \quad . \quad . \quad (3)$$

This pressure gradient takes its maximum value at the altitude

$$z = \frac{RT_0}{g}\left(1 - \frac{p_0^{-1}\,dp_0/dy}{T_0^{-1}\,dT_0/dy}\right), \quad . \quad . \quad . \quad . \quad . \quad (4)$$

where its value is

$$\left(\frac{\partial p}{\partial y}\right)_{\max} = 0{\cdot}4\,\frac{p_0}{T_0}\frac{dT_0}{dy}. \quad . \quad . \quad . \quad . \quad . \quad . \quad . \quad . \quad (5)$$

This result is interesting as showing that, whatever the pressure gradient on the ground,* the largest pressure gradient will be at altitude, and proportional to the sea-level temperature gradient. The altitude (4) at which this maximum pressure gradient is achieved varies little if one is dealing with annual mean pressures; the bracketed factor remains near 1,† because at sea level the mean temperature varies with latitude by a greater fraction of its absolute value than does the mean pressure. Under these circumstances, the altitude (4) corresponds to a pressure of around 300 to 400 mb, such as is found in the upper parts of the troposphere.

The mean geostrophic wind velocity u corresponding to the mean pressure gradient (3) is given by (1) as

$$\frac{1}{2\omega \sin \phi} \frac{1}{\rho} \frac{\partial p}{\partial y} = \frac{1}{2\omega \sin \phi} \left(\frac{1}{\rho_0} \frac{dp_0}{dy} + \frac{gz}{T_0} \frac{dT_0}{dy} \right). \quad . \quad . \quad . \quad (6)$$

This gives a linear increase of geostrophic wind with height, at a rate

$$\frac{g}{2\omega \sin \phi} \frac{1}{T_0} \frac{dT_0}{dy} \quad . \quad . \quad . \quad . \quad . \quad . \quad . \quad . \quad . \quad (7)$$

per unit of altitude.

The above results are especially valuable because, when the calculations are repeated with a realistic value of the lapse-rate (rate of decrease of temperature with height), the conclusions are negligibly changed, the 0·4 (which in (5) represented e^{-1}) being retained to one significant figure. The change in (7) is even smaller. These results are hardly surprising since the temperature at 300–400 mb is less than 20% below its sea-level value.

As order-of-magnitude explanations of what is observed, the results (5) and (7) seem quite satisfactory. Equation (5) suggests that the change of mean pressure between tropics and poles in the upper part of the troposphere (where the pressure is around 300 to 400 mb) should be about 40% of the relative change of sea-level temperature, multiplied by the sea-level pressure (1000 mb). Taking the relative difference in absolute temperature as one-fifth, we obtain 80 mb for the pressure change, a slight overestimate. The 'sea-level temperatures' used should really be chosen as somewhat less extreme values, however, since they ought to represent typical atmospheric temperatures outside the thermal boundary layer near the ground.

An average value of (7), 'weighted' by a factor sin ϕ (which is reasonable since the mean temperature gradient is smaller in lower latitudes‡), is

$$\frac{g}{2\omega r} \frac{\Delta T_0}{T_0}, \quad . \quad . \quad . \quad . \quad . \quad . \quad . \quad . \quad (8)$$

---

* Subject to the limitation that the altitude (4) is positive.

† This has been used also in (5), the exponential of minus the bracketed factor being replaced by 0·4 to one significant figure.

‡ Actually, the theory given ('thermal wind' theory) is less accurate in the tropics than elsewhere, since Coriolis force is smaller for small ϕ, and so dominates the situation far less.

where $r = 6{\cdot}4 \times 10^8$ cm is the mean radius of the earth (so that

$$g/2\omega r = 10^{-2}\mathrm{s}^{-1}),$$

and $\Delta T_0/T_0$ is the relative temperature difference between tropics and poles. If the latter is again taken as one-fifth, this estimate of average velocity gradient upwards represents an increase of 20 m/sec in 10 km, which is of the right order of magnitude.

As a final remark, it is worth noting that the analysis suggests that the kinetic energy of the thermal wind per unit altitude will not reach its maximum until a very great height—very roughly, twice that indicated in (4). Note that the momentum density ρu is greatest at the height (4), but that the energy density $\frac{1}{2}\rho u^2$ is still increasing there, since u is increasing.

§ 3. THE MEAN WINDS NEAR THE GROUND

It was suggested in § 2 that the mean winds near the ground are largely prevented from attaining speeds as high as those found at greater altitudes, because a high wind near the ground is resisted by such a great frictional force. We must now consider how it is that the air near the ground at a particular latitude, in the temperate zones for example, can possess any mean westerly component of velocity, in spite of the resulting frictional couple which must be tending (on the average) to reduce the west-east angular momentum about the earth's axis of the air at that latitude. The gravitational and pressure forces on the belt of air at the latitude in question cannot alter its angular momentum about the earth's axis, since they all act through that axis. Hence the angular momentum loss can be made up only by a steady mean inflow of angular momentum from the lower latitudes, where the mean winds at the ground have an easterly component, so that in those latitudes the frictional couple constantly creates west–east angular momentum rather than destroying it.

There is no conjecture in this part of the theory. We can be certain that in the temperate zones, where the mean geostrophic winds near the ground are westerly (veering towards S.W.* in the frictional layer, since therein the Coriolis force is reduced but the pressure gradient is unaltered), the inflow of west–east angular momentum from lower latitudes must exceed the outflow towards higher latitudes. Conversely, in the trade-wind zones, where the mean geostrophic winds near the ground are easterly (veering towards N.E.† in the frictional layer, for the same reason as before), the outflow of west–east angular momentum towards higher latitudes must exceed the inflow from lower latitudes. This is because the friction of the ground is in such a direction as to reduce easterly winds, and so increase west–east angular momentum.

Thus, to explain the mean winds near the ground, it is necessary to suppose a continual mean flow of west–east angular momentum from the tropics to the poles, a flow which reaches its maximum at around 30° latitude. Then the air at latitudes higher than this is continually gaining west–east angular momentum, and so can afford to have a certain mean velocity in this direction even at the ground, with the resisting couple which this entails. The air at latitudes less than 30° is continually losing west–east angular momentum. Hence the westerly velocity component of this air is reduced, and takes such a negative value at the ground that the resulting frictional couple just makes up, on the average, for the angular momentum lost.

---

* N.W. in the southern hemisphere.

† S.E. in the southern hemisphere.

To put it more graphically—if friction were far stronger than it is, there would be little mean circulation at the ground, and the general increase with height described in § 2 would be an increase from zero. In reality, however, the flow of angular momentum polewards causes a general reduction of this circulation in the trade-wind zones, and a general increase in the temperate zones, both changes being limited by the frictional resistance of the ground.

§ 4. THEORIES OF THE POLEWARD FLOW OF WEST–EAST ANGULAR MOMENTUM

The considerations of §3 have made clear what is the last main feature needing explanation, if an ‘ elementary reasoned account ’ of the general circulation is to be achieved. It is a poleward mean flow of angular momentum, reaching a maximum at around 30° latitude, and falling to zero at the poles as well as somewhere near the equator. Knowing as we do the sea-level mean wind distribution, and a rough approximation to the law which relates the frictional resistance of the ground to the wind speeds near it, we can calculate (Priestley 1951) the order of magnitude of angular momentum flow which is required. The maximum to which it rises is about 3×10^{26} dyn cm. This corresponds to a mean flow of westerly momentum, crossing each centimetre of the thirtieth parallel of latitude, of around $1{\cdot}6 \times 10^{8}$ dynes. Such a flow has been observed directly by Starr and White (1951, 1952) by analysing records at a large number of meteorological stations situated at around 30°N.

It is this poleward flow of angular momentum concerning which the greatest uncertainty and controversy among meteorologists exists. It appears from their discussions that several mechanisms for it exist.

One mechanism, which is certainly among those present, and has high suggestive value, was put forward in 1936 by the great aerodynamicist Ludwig Prandtl, who reproduces it (1952) in his book *The Essentials of Fluid Dynamics*. The small attention which it has received among meteorologists may perhaps be due to Prandtl's undoubtedly too rigid ignoration of other mechanisms.

This mechanism must be mentioned, however, because it is concerned with the process by which the general circulation in the upper troposphere, considered in § 2, is maintained against any energy losses that may occur. The mean circulation loses kinetic energy by a variety of causes, most of which can be summed up in the phrase 'the tendency of disturbances to the mean circulation (such as turbulence, cyclones, and even annual changes like the great continental anticyclones) to equalize the momentum of different parts of it, and hence reduce the energy'.* How does the mean circulation regain this energy? Evidently, it can do so only if the poleward forces (namely, pressure gradients) which produce it are allowed to *push* the air a bit.† Thus, if dissipation is taken into account, the mean winds in the upper troposphere can no longer be taken simply along the isobars, but must be imagined to have, at least sometimes, a component down the pressure gradient.

Now, these velocity components down the pressure gradient must tend to generate a poleward flow of west–east angular momentum. For the work done by pressure gradient is $(\partial p/\partial y)v$ per unit volume, where v is the velocity down it.‡ The flow of angular momentum is proportional to $(\rho u)v$ per unit volume, provided that the isobars in the upper troposphere lie roughly in the east–west direction. Since by eqn. (1) for the geostrophic wind, ρu is proportional to $\partial p/\partial y$, any north–south movements that put energy into the general circulation must also give a poleward flow of angular momentum. In the trade-wind zone, for example, the upper air moves polewards and the lower air moves equatorwards, and this transfers angular momentum because the upper air has the stronger westerly circulation.

This is the only place in the theory where any secondary north–south circulation ('due to hot air rising at the equator', a circulation which played such an important part in the older accounts of the subject) is mentioned. Note however its completely secondary function, which is merely to maintain a slight preponderance of west–east angular momentum in higher latitudes, so that the prevailing winds near the ground may have westerly components in higher latitudes and easterly components in lower latitudes. Near the equator, the process can reasonably be described as 'hot air rising', for there Coriolis forces are at their weakest, so that the tendency for air to move down a pressure gradient must be at its strongest. The reason why even equatorial air, at the great heights to which it rises (expanding up a saturated adiabatic), is deflected into a westerly direction, even though no Coriolis force is available for the purpose, must be that exchange of westerly momentum with neighbouring latitudes is continually occurring in the upper troposphere.

---

* Jeffreys (1926) made calculations which led to the rejection of a mechanism similar to that of Prandtl. The reason, however, why the Jeffreys mechanism gave insufficient flow of angular momentum, was that only the direct action of turbulence (in the frictional layer) on the mean circulation was taken into account as a means of reducing its energy. Now, although turbulence is the final translator of kinetic energy into heat, the large-scale disturbances form a most important intermediate stage in the degradation process. This was recognized by Jeffreys in a later paper (1933), which gives a theory more closely similar to that put forward here.

† They are enabled to do so, of course, by the fact that, if the geostrophic wind is weakened from any cause, the air can flow down the pressure gradient, which then exceeds the opposing Coriolis force.

‡ i.e. in the negative y-direction.

However, the secondary circulation certainly does not penetrate to 30°N, where Starr and White (1951, 1952) found negligible mean north–south wind components. There, it is the upper tropospheric air with strongest westerly components which moves North, while the upper tropospheric air with weakest westerly components moves South; however, this process equally transfers angular momentum polewards and puts energy into the general circulation.

It is possible to compute the mean rate of kinetic energy loss by the general circulation which would be required, according to Prandtl's theory, to produce the angular momentum flow which Priestley (1951) inferred from the east–west components of wind velocity observed near the ground. The average loss required is 5×10^3 ergs/sec per square centimetre of the earth's surface. This agrees with a direct estimate of atmospheric energy dissipation due to Brunt (1926). Both estimates have only order-of-magnitude significance. They imply that the kinetic energy of the atmosphere would decay by a factor e^{-1} in around one day if the temperature distribution which maintains the motion ceased to be maintained (in turn) by the difference in geographical distribution between the incoming solar radiation and the outgoing terrestrial radiation. The estimates give an efficiency of around 2% for the atmosphere as a heat engine, taking the heat supply to be that portion of solar radiation which is not instantly reflected. An engine describing a Carnot cycle with a temperature difference of one-fifth of the absolute temperature would have an efficiency of about 20%. The atmosphere can be congratulated if it has really achieved an efficiency of one-tenth of ideal efficiency, under distinctly unfavourable conditions.

The Prandtl mechanism undoubtedly pays too little attention to angular momentum transport by the disturbances to the mean flow—whereas the importance of all kinds of disturbances in reducing the kinetic energy of the mean circulation is explicitly emphasized in the theory. This omission is particularly important in the cyclone belt—both because the disturbances there are particularly large, and because, in a region where the angular momentum per unit mass is decreasing polewards, any disturbances are likely, in smoothing the distribution, to cause further transport polewards. Again, the hypothesis of the Prandtl theory that on the whole the isobars in the upper troposphere lie in an east–west direction is violated more constantly in the cyclone belt than anywhere else.

In the lower latitudes, however, including those around 30° (where the greatest flow of angular momentum is required), disturbances are probably less important. For any irregular system of disturbances would make angular momentum flow towards the region of least angular momentum—i.e. towards the tropics. On the other hand, specially regular systems of disturbances, which have been postulated by some authors, do not seem very likely.

One kind of disturbance that is doubtless present is a *fluctuation* in the northerly components of both wind and pressure gradient. The Prandtl theory is sufficiently elastic, however, to admit fluctuations of this kind. At any instant the work being done by pressure gradient on unit volume of fluid is its product with the velocity component down it. Provided that the isobars in the upper troposphere remain approximately in the east–west direction, this product is proportional to the poleward flow of angular momentum at that instant. The annual means of both energy input and flow of angular momentum at the latitude in question would then be approximately in this fixed, known, proportion to one another—as was assumed above in obtaining the figure of 5×10^3 for the mean dissipation rate.

Starr and White (1951, 1952) found that in fact there are no significant mean north–south motions in the upper troposphere at 30°N. But the strong northerly components in that region occur on the average where strong westerly components are also present, while strong southerly components coincide with weak westerly components. Evidently, the mean effect of this is both to replenish the energy of the general circulation and to produce poleward flow of angular momentum.

To sum up, the required flow of angular momentum in the tropics and sub-tropics can largely be achieved by means of such northerly winds down the pressure gradients in the upper troposphere as are required to maintain the energy of the westerly circulation in that region. It is probable, however, that in the cyclone belt an important amount of transport is achieved by the cyclones themselves.

Acknowledgments

I have pleasure in thanking Mr. F. B. Smith for valuable discussions, and for help in the reduction of data. The comments of Sir Harold Jeffreys, Mr. T. H. Ellison and Dr. G. B. Whitham, on reading an early draft of the paper, were most useful to the author.

References

Brunt, D., 1939, *Physical and Dynamical Meteorology* (Cambridge : University Press).

Jeffreys, H., 1926, *Quart. J. Roy. Met. Soc.*, **52,** 85 ; 1933, *The Function of Cyclones in the General Circulation* (Lecture to the Int. Met. Assn., Lisbon).

Prandtl, L., 1952, *The Essentials of Fluid Dynamics* (London : Blackie).

Priestley, C. H. B., 1951, *Austral. J. Sci. Res.* A, **4,** 317.

Starr, V. P., and White, R. M., 1951, *Quart. J. Roy. Met. Soc.*, **77,** 215 ; 1952, *Ibid.*, **78,** 62.

CXXIX. *The Specific Heat of Liquid Helium II as a Function of Pressure*

By G. R. Hercus* and J. Wilks
Clarendon Laboratory, Oxford†

[Received June 22, 1954]

Abstract

The specific heat of liquid helium has been measured at several densities over the temperature range 1° to 2°K. The values obtained under the saturated vapour pressure are about 10% higher than those observed by earlier workers; the results are briefly discussed.

§ 1. Introduction

Previous workers have shown that the application of pressure to liquid helium produces large changes in the position of the λ-point, the thermal conductivity, the viscosity and the velocities of first and second sound. Apart from some measurements in the immediate region of the λ-point there are, however, hardly any values for the specific heat under pressure. The present measurements were therefore undertaken to obtain more detailed information, particularly in the range 1° to 2°K where most of the other experiments have been performed. Besides the measurements at higher pressures, we have also obtained values along the liquid–vapour equilibrium curve; these are about 10% higher than those given recently by Kramers, Wasscher and Gorter (1952). Although we cannot suggest any reason for this discrepancy, we are publishing the present results as a first step in clarifying the position.

§ 2. The Experiment

A schematic diagram of the apparatus is shown in fig. 1. The vessel A held liquid helium under atmospheric pressure and served as a thermal shield which allowed the cryostat B to be cooled to about 1·0°K without undue loss of liquid helium. This cryostat was so constructed that liquid helium totally surrounded the thick walled calorimeter C which contained the mole or so of liquid helium on which the measurements were made. The calorimeter also contained a long resistance heater which was non-inductively wound, and a carbon film thermometer deposited on a perspex former. The necessary electrical leads were brought out of the calorimeter through seals and were then brought into good thermal contact with the cryostat before passing up to higher temperatures.

---

[*] Now at the Division of Industrial Chemistry, Commonwealth Scientific and Research Organisation, Melbourne, Australia.

[†] Communicated by Sir Francis Simon, F.R.S.

Although standard methods of low temperature calorimetry were employed, the column of liquid helium, through which the pressure was applied to the calorimeter, necessitated some precautions in the design of the apparatus. This capillary, D, was made as narrow as was convenient, in order to reduce the heat flow along it ; the sections between the hydrogen bath E and vessel A and between vessels A and B were each about 20 cm long and of 0·3 mm I.D., while that between the cryostat and the calorimeter was 10 cm long and of 0·15 mm I.D. Within the two baths A and B, the german silver capillary was replaced by copper tubing of greater diameter (2 mm I.D.) which passed right through the liquid helium in the baths. This arrangement was designed to reduce the temperature difference between the liquid helium in the tubes and that in the surrounding baths. A calculation, based on the results of Keesom, Saris and Meyer (1940) for the heat flow along a capillary of liquid helium and on the results of Kapitza (1941) for the thermal resistance of a helium–copper interface, shows that in the case of the bath B the temperature difference should be negligible ; this conclusion was confirmed by a subsidiary experiment with and without helium in the capillary. Were it not so, the temperature of the specimen and the thermometer

Fig. 1

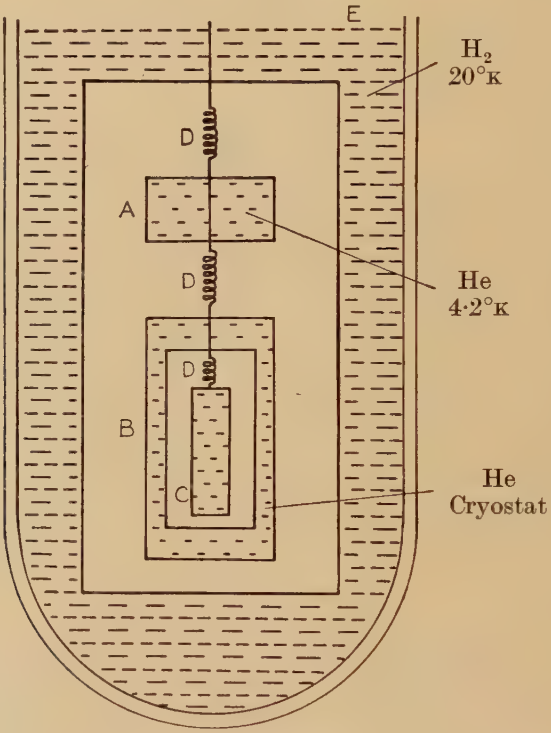

Schematic diagram of the calorimeter and cryostat.

would not have been the same as that of the bath, and the thermometer calibration would have been inaccurate. Good thermal contact between the helium in the capillary and the bath B also ensured that the liquid in the capillary above B was thermally isolated from that in the calorimeter.

Particular attention was paid to obtaining as steady temperature conditions as possible, and the following experimental procedure was adopted. The temperature of the cryostat was maintained at some convenient value for about 30 minutes to allow the calorimeter to attain thermal equilibrium. The resistance of the carbon thermometer was then measured and the vapour pressure of the helium in the cryostat noted so as to obtain a calibration point for the thermometer. (Below 1·4°, the temperature of the cryostat was measured more accurately by a magnetic susceptibility thermometer calibrated against the vapour pressure at the higher temperatures.) Heat was then supplied for a period of about 20 seconds by a stop-watch controlled circuit and observations made of the new temperature of the calorimeter. As the capillary of liquid helium acted as a comparatively large thermal link, the calorimeter drifted back towards the cryostat temperature and this drift rate was observed in order to make the usual extrapolation. In all cases save for one or two points near 1·0° the extrapolation was linear and introduced only a very small error.

§ 3. THE SPECIFIC HEAT

While making a measurement of the specific heat the helium in the calorimeter was isolated by closing off the top of the capillary; thus, after a small correction for the dead volume of this capillary, our results gave the specific heat at constant volume, C_v. As a matter of convenience we chose to maintain the pressure over the helium at some constant value during each run, only isolating the calorimeter during an actual measurement; hence each set of experimental points consists of values of C_v at densities corresponding to a given pressure. Our results obtained under the saturated vapour pressure and under one atmosphere pressure are shown in fig. 2; as is to be expected the difference between the two sets of values of C_v is less than the experimental error. The earlier results of Keesom and Clusius (1932) and Keesom and Keesom (1932 and 1935) for the specific heat under the saturated vapour pressure are also shown, corrected to the 1949 temperature scale; in the region with which we are concerned their points are rather scattered. The measurements of Hull, Wilkinson and Wilks (1951) were primarily concerned with the temperature region below 1°K and were carried out using a closed capsule technique not very suitable for measurements at higher temperatures; the experiments of Keesom and Westmijze (1941) have never been reported in any detail. Thus the most reliable of the earlier measurements in this region would appear to be those of Kramers, Wasscher and Gorter (1952), and it is a matter of concern that our values are about 10% higher than theirs. We became aware of this discrepancy at an early stage in the measurements and checked over our work in some detail but could find no reason to modify our values. We estimate our accuracy at ±2%; Kramers, Wasscher and Gorter do not estimate theirs but the scatter on their results suggests that it is about the same or a little less. Thus, 5% discrepancy between the results would not call for special comment, but 10% is more difficult to account for. Figure 3 shows the only relevant results obtained previously under higher pressures —a few scattered points due to Keesom and Clusius (1932) at 'about 19 atm'; two of these are actually higher than our values for 19·8 atm. which are also shown.

Fig. 2

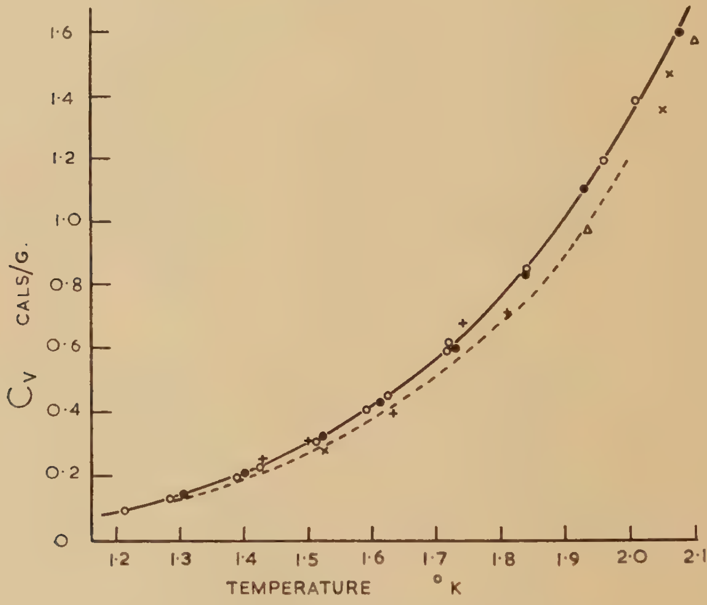

The specific heat of liquid helium (C_v).

○	Under 1 atm pressure	Hercus and Wilks
●	Under the sat. vap. pressure	Hercus and Wilks
△	,,	Keesom and Keesom 1932
+	,,	Keesom and Clusius 1932
×	,,	Keesom and Keesom 1935
----	,,	Kramers *et al.* 1952

Values of C_v may also be obtained, far less directly, from the velocity of second sound together with observations of either the torque on a Rayleigh Disc due to waves of second sound (Pellam and Hanson 1952) or the motion of a pile of plates oscillating in the liquid (Andronikashvili 1946). Here again the evidence is inconclusive quite apart from any questions concerning the validity of the two fluid model which is used in the calculations. Figure 4 shows values of the specific heat under the vapour pressure deduced by Pellam and Hanson (1952) from Rayleigh Disc experiments. These points agree better with our results than with the Leyden ones, but the scatter on them indicates that the experiment

Fig. 3

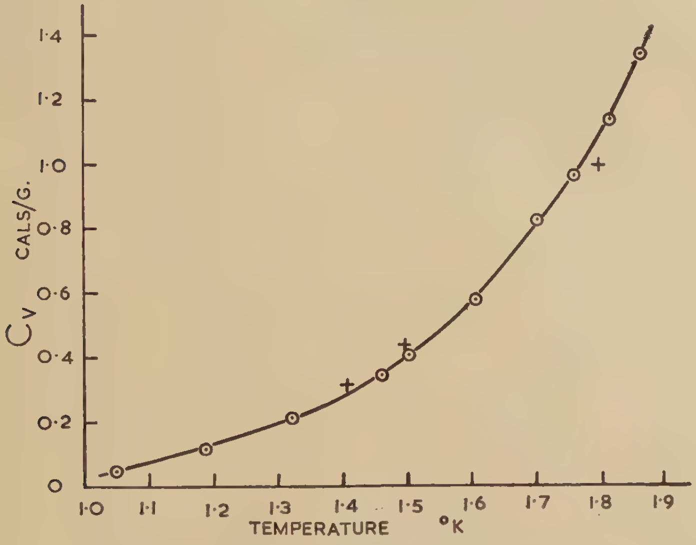

The specific heat of liquid helium (C_v).

⊙ Under 19·8 atm pressure Hercus and Wilks
+ Under ~ 19 atm pressure Keesom and Clusius 1932

Fig. 4

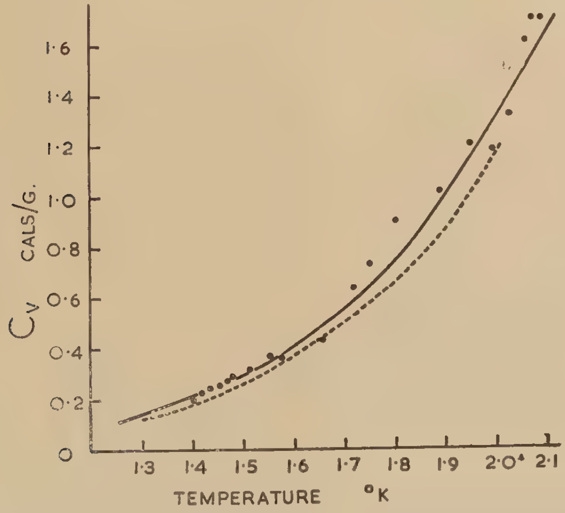

The specific heat of liquid helium under the saturated vapour pressure.

— Hercus and Wilks
- - - Kramers, Wasscher and Gorter
● Pellam and Hanson (Rayleigh Disc)

is a delicate and difficult one. The oscillating disc experiment is also difficult (Andronikashvili 1946, 1948, Hollis-Hallet 1952), and the absolute values of the density of the normal fluid, ρ_n, obtained from it are accurate to only about 10% because of uncertain geometrical corrections.

Using our results, together with the isopycnal data of Keesom and Keesom (1933), we have constructed table 1 which gives smoothed interpolated values of C_v for five different densities. (These densities correspond roughly with the pressures at which sets of measurements were made.) The increase of specific heat with density may of course be deduced from Keesom and Keesom's isopycnal data. This is not a very satisfactory procedure as it involves taking the second differential of a smoothed curve, but to within the possible accuracy the calculated pressure dependence is the same as we observe. This isopycnal data has also been used to obtain approximate values of the difference between C_p and C_v for the five densities mentioned in table 1; as may be seen in table 2, the difference is small except in the region near the λ-point.

Table 1. The Specific Heat of Liquid Helium. C_v

	C_v (cals g^{-1} deg.$^{-1}$)				
ρ (g cm^{-3})	0·1465	0·1525	0·1630	0·1675	0·1715
T°K					
1·10	0·052			0·070	
1·15	0·068			0·090	
1·20	0·089		0·099	$0{\cdot}11_4$	$0{\cdot}13_7$
1·25	$0{\cdot}11_0$		$0{\cdot}12_5$	$0{\cdot}14_6$	$0{\cdot}17_6$
1·30	$0{\cdot}13_9$		$0{\cdot}15_7$	$0{\cdot}18_5$	$0{\cdot}21_7$
1·35	$0{\cdot}17_0$		$0{\cdot}18_9$	$0{\cdot}22_6$	$0{\cdot}26_6$
1·40	$0{\cdot}20_7$	$0{\cdot}21_0$	$0{\cdot}23_0$	$0{\cdot}27_4$	$0{\cdot}32_0$
1·45	$0{\cdot}25_0$	$0{\cdot}25_4$	$0{\cdot}27_7$	$0{\cdot}32_9$	$0{\cdot}38_4$
1·50	$0{\cdot}29_7$	$0{\cdot}30_5$	$0{\cdot}34_0$	$0{\cdot}39_0$	$0{\cdot}47_0$
1·55	$0{\cdot}35_0$	$0{\cdot}36_0$	$0{\cdot}40_6$	$0{\cdot}46_1$	$0{\cdot}54_0$
1·60	$0{\cdot}41_0$	$0{\cdot}46_6$	$0{\cdot}48_1$	$0{\cdot}54_3$	$0{\cdot}65_3$
1·65	$0{\cdot}48_0$	$0{\cdot}50_0$	$0{\cdot}57_9$	$0{\cdot}63_5$	$0{\cdot}50_0$
1·70	$0{\cdot}56_0$	$0{\cdot}58_2$	$0{\cdot}68_0$	$0{\cdot}75_6$	$0{\cdot}87_5$
1·75	$0{\cdot}64_2$	$0{\cdot}67_8$	$0{\cdot}79_7$	$0{\cdot}88_0$	1·03
1·80	$0{\cdot}74_3$	$0{\cdot}78_3$	$0{\cdot}93_5$	1·04	
1·85	$0{\cdot}86_0$	$0{\cdot}90_5$	1·08		
1·90	$0{\cdot}99_1$	1·04	1·21		
1·95	1·14	1·19			
2·00	1·30				
2·05	1·48				

Table 2. $C_p - C_v$ expressed as a percentage of C_v

	Pressure of Helium				
T°K	1 Atm	5 Atm	15 Atm	20 Atm	25 Atm
1·5	0·01	0·2	1·0	2·1	3·3
1·6	0·03	0·3	1·8	3·0	5·9
1·7	0·05	0·5	2·9	4·2	9·3
1·8	0·09	0·7	4·4	8·0	
1·9	0·14	1·0	10·1		
2·0	0·17				

§ 4. THE ENTROPY

It is, of course, not possible to obtain absolute values of the entropy from our measurements because they do not extend to the lowest temperatures. In the case of helium under its saturated vapour pressure one could take the entropy at about 1·2°K to be that given by Kramers, Wasscher and Gorter (1952) but in view of the discrepancy between the specific heat results this hardly seems justifiable. However, by plotting our values of the specific heat logarithmically it may be seen that below 1·3° the temperature dependence follows a T^6 law, as do the Leyden values. We have therefore assumed that this relation may be extrapolated down to 0·6° where the entropy has become very small (Hull, Wilkinson and Wilks 1951). In this way we obtain values of the entropy which are about 10% higher than those of Kramers, Wasscher and Gorter over the entire temperature range. A similar extrapolation has been made at the higher pressures and table 3 shows values of the entropy at five different densities obtained by a numerical integration of C_v.

These new values of the entropy would explain two sets of experimental observations which have not hitherto agreed with theory. Kapitza (1941) measured the fountain effect in liquid helium and observed greater pressure differences than those predicted by the relation given by H. London (1939) $\Delta p/\Delta T = \rho S$; that is, the values for the entropy which he deduced from his experiments were greater than those calculated from the specific heat measurements. Kapitza also measured the heat of transport by observing the rate of flow through a superleak into a vessel to which heat was supplied. Assuming the relation from the London theory that this quantity of heat Q should be equal to TS, he deduced further values for the entropy in agreement with his previous ones. Recently Chandrasekhar (1952) has repeated the latter experiment replacing the superleak by a link of helium film; his results are in agreement with Kapitza's. Although there has been much discussion of the validity of the London relations, the fact that both types of experiment (on fountain pressure and heat of transport) lead to the same value for the entropy suggests that we are dealing with reversible processes for which they should apply. In any case it is not at all clear how *both* experiments could give rise to too great a value for the entropy. The discrepancies are however removed by taking our new values for the entropy as is shown in fig. 5. It has however to be noted that the results of Meyer and Mellink (1947) and van den Meijdenberg, Taconis, Beenakker and Wansink (1954) for the fountain pressure lead to somewhat lower values for the entropy; unfortunately the scatter on some of their points is of the order of 10% and it is hard to draw any firm conclusions.

Table 3. The Entropy of Liquid Helium

	S (cal g^{-1} deg.$^{-1}$)				
ρ (g cm^{-3})	0·1465	0·1525	0·1630	0·1675	0·1715
T °K					
1·20	0·014		0·016	0·019	0·022
1·25	0·018		0·020	0·025	0·028
1·30	0·023		0·026	0·031	0·036
1·35	0·029		0·033	0·039	0·045
1·40	0·036	0·036	0·040	0·048	0·056
1·45	0·044	0·044	0·049	0·058	0·068
1·50	0·053	0·054	0·059	0·071	0·083
1·55	0·064	0·064	0·072	0·084	0·099
1·60	0·075	0·077	0·086	$0{\cdot}10_0$	$0{\cdot}11_8$
1·65	0·088	0·091	$0{\cdot}10_2$	$0{\cdot}11_9$	$0{\cdot}14_0$
1·70	$0{\cdot}10_4$	$0{\cdot}10_7$	$0{\cdot}12_1$	$0{\cdot}13_8$	$0{\cdot}16_4$
1·75	$0{\cdot}12_1$	$0{\cdot}12_6$	$0{\cdot}14_2$	$0{\cdot}16_3$	$0{\cdot}19_1$
1·80	$0{\cdot}14_1$	$0{\cdot}14_6$	$0{\cdot}16_6$	$0{\cdot}19_0$	
1·85	$0{\cdot}16_3$	$0{\cdot}16_9$	$0{\cdot}19_4$		
1·90	$0{\cdot}18_7$	$0{\cdot}19_5$	$0{\cdot}22_5$		
1·95	$0{\cdot}21_5$	$0{\cdot}22_4$			
2·00	$0{\cdot}24_6$				
2·05	$0{\cdot}28_0$				

One further consequence of accepting higher values for the entropy would be that some recalculation of the absolute temperature scale would be called for but as the changes will be very small we see no point in discussing this in detail until there is a generally accepted value for the specific heat.

§ 5. LANDAU'S THEORY

Finally we may note that these results offer, at least in principle, an interesting check on Landau's theory of liquid helium (Landau 1941, 1947). Such confirmation as this theory has so far received has come from observations on the liquid under its saturated vapour pressure, whereas the theory should presumably apply equally well to liquid helium

II of any density. As many properties of the liquid are very sensitive to pressure, it would therefore be instructive to see how far the theory can account for their behaviour at higher densities.* However, the only relevant results previously obtained under pressure have been the velocities of second sound (Maurer and Herlin 1950) and these by themselves were insufficient to check the theory. At first sight it appears that by combining these results with our specific heat measurements one could both check the theory and evaluate, for each density, the three parameters (Δ μ p_0) in Landau's equation for the roton energy spectrum.

Landau considers helium at some fixed density and gives expressions for the specific heat and the density of the normal component, ρ_n, in terms of the three parameters Δ, μ and p_0. It so happens that the temperature dependence of both the specific heat and ρ_n are determined only by the parameter Δ. We may thus determine Δ by two independent methods, either directly from the temperature dependence of the specific heat or by deriving ρ_n from the observed values of the specific

Fig. 5

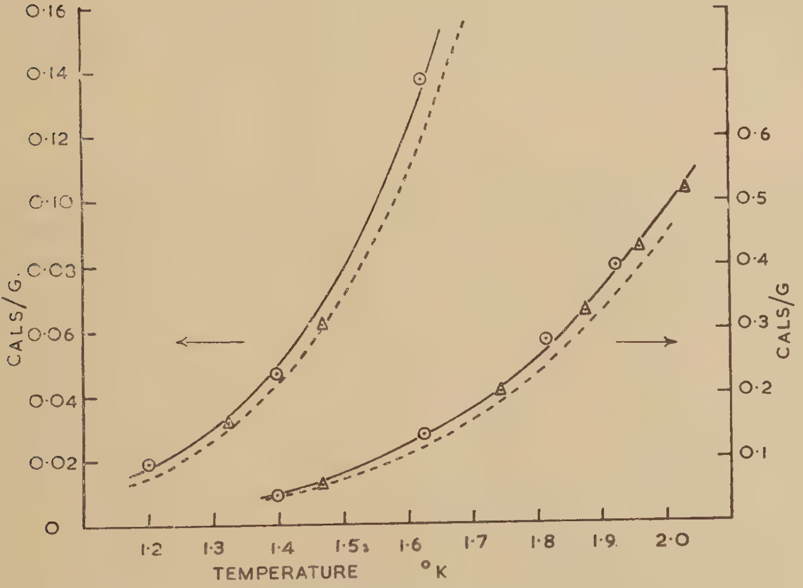

Values of the product TS.

—	Specific heat measurements	Hercus and Wilks
- - -	” ” ”	Kramers *et al.*
⊙	Heat of transport	Chandrasekhar
△	Fountain effect	Kapitza

---

* In this connection it should be noted that as the difference between C_p and C_v is not negligible at the higher densities, it is important to specify carefully the conditions under which measurements are made.

heat and the velocity of second sound and then determining its temperature dependence. The other two parameters, μ and p_0, may then be found from the absolute magnitudes of the specific heat and of ρ_n. However, if we attempt to determine Δ, μ and p_0 for helium at a given density we find that the values of Δ deduced from the temperature dependence of the specific heat and from ρ_n are not in complete agreement. It is true that this discrepancy is only about 5% but as Δ enters into the expression for the specific heat as a high exponential power, a 5% variation corresponds to about a 50% variation in specific heat. Thus, to decide how good an approximation to the truth Landau's roton formula is, we require values for the specific heat, entropy and velocity of second sound, which are accurate to about 0·1%. Any further investigation of this point—and also of the previously discussed question as to whether the London relations for the fountain pressure and allied phenomena are really exact—would require much more accurate measurements of all the quantities concerned than are yet available.

ACKNOWLEDGEMENTS

We wish to thank Sir Francis Simon for his interest in the experiment, and Mr. J. A. Newell for his assistance in making the measurements. We also wish to thank the University of Oxford for the award of an I.C.I. Fellowship (J.W.) and the Australian National University for the award of a research scholarship (G.R.H.).

REFERENCES

ANDRONIKASHVILI, E. L., 1946, *J. of Phys. U.S.S.R.*, **10,** 201 ; 1948, *Zu. Eksper. Theor. Fiz.*, **18,** 424.
CHANDRASEKHAR, B. S., 1952, *Dissertation* (Oxford).
HOLLIS-HALLET, A. C., 1952, *Proc. Roy. Soc.* A, **210,** 404.
HULL, R. A., WILKINSON, K. R., and WILKS, J., 1951, *Proc. Phys. Soc.* A, **64,** 379.
KAPITZA, P. L., 1941, *J. of Phys. U.S.S.R.*, **4,** 181.
KEESOM, W. H., and CLUSIUS, K., 1932, *Commun. Leiden*, 219 e.
KEESOM, W. H., and KEESOM, A. P., 1932, *Commun. Leiden*, 221 d ; 1933, *Ibid.*, 224 d and 224 e ; 1935, *Physica*, **2,** 557.
KEESOM, W. H., SARIS, B. F., and MEYER, L., 1940, *Physica*, **7,** 817.
KEESOM, W. H., and WESTMIJZE, W. K., 1941, *Physica*, **8,** 1044.
KRAMERS, H. C., WASSCHER, J. D., and GORTER, C. J., 1952, *Physica*, **18,** 329.
LANDAU, L., 1941, *J. of Phys. U.S.S.R.*, **5,** 71 ; 1947, *Ibid.*, **11,** 91.
LONDON, H., 1939, *Proc. Roy. Soc.* A, **171,** 484.
MAURER, R. D., and HERLIN, M. A., 1951, *Phys. Rev.*, **81,** 444.
MEYER, L., and MELLINK, J. H., 1947, *Physica*, **13,** 197.
PELLAM, J. R., and HANSON, W. B., 1952, *Phys. Rev.*, **85,** 216.
VAN DEN MEIJDENBERG, C. J. N., TACONIS, K. W., BEENAKKER, J. J. M., and WANSINK, D. H. N., 1954, *Physica*, **20,** 157.

CXXX. *The Surface Energy of Sodium*

By Allen B. Scott*
H. H. Wills Physical Laboratory, University of Bristol †

[Received July 28, 1954]

Abstract

The surface energy of sodium, calculated by the use of the free-electron model, is modified by considering the increased electrostatic energy in the surface if the positive charge is assumed to be localized in the planes of the atomic nuclei instead of distributed uniformly. While the theoretical surface energy is increased significantly, the theory does not yet account for the energy observed experimentally.

Several attempts to calculate the surface energy of metals by the use of the free-electron model have been made (Brager and Schuchowitzky 1946, Huang and Wyllie 1949, Huntington 1951). Such calculated energies should most nearly agree with experimental observation for the alkali metals, for which the Fermi energy corresponds closely to that calculated for free electrons. However, the most recent of the surface energy treatments, that of Huntington, yields a value of surface energy for sodium treated as a free-electron metal which is only about one-fourth of the observed value.

Huntington used the surface barrier computed by Bardeen (1936), and evaluated the phase shifts for electrons of various energies up to the Fermi limit which occur upon cutting a new surface in the metal. He found the surface enthalpy to be 88 erg/cm^2; at the melting point the surface free energy was found, by the use of the surface entropy calculated by Huang and Wyllie (1949), to be 54 erg/cm^2. The charge distribution in the surface was that calculated by Bardeen (1936), and is shown in fig. 1 (*a*). The positive charge is assumed to be distributed uniformly right up to the geometrical surface, beyond which its density is zero, while the electronic charge distribution, calculated from the free-electron theory, decreases more gradually and extends well beyond the surface. Charge is conserved, that is the areas under the positive and negative distribution curves are equal. The density of electronic charge in the interior is $-\rho_0$.

It may be seen that a part of the surface energy is electrostatic and arises from the charge distribution in the surface as compared to the interior. Let this part be E_e. The remainder, E_k, is the result of phase shifts and changes in exchange and correlation potentials for the electrons caused by the introduction of the surface.

---

* Communicated by the Author.

† Now at Department of Chemistry, Oregon State College, Corvallis, Oregon, U.S.A.

Even though the positive charge is not distributed uniformly in an actual metal, we may, owing to the insensitivity of the electronic wave functions to the periodic field of the ions, take Bardeen's negative charge distribution and E_k, calculated from Huntington's result, as essentially correct ; we are then free to adopt a model of the surface more nearly representative of an actual metal to compute the electrostatic part of the surface energy. The model used in the calculation is illustrated in fig. 1 (*b*).

Fig. 1

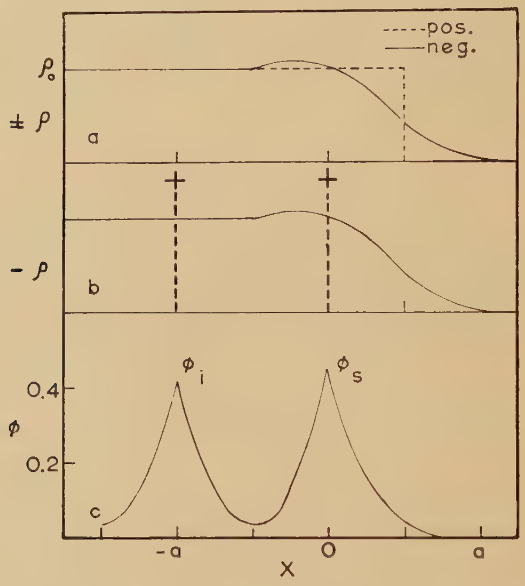

Charge density and potential near the metal surface.

We suppose the charge density to be a function only of x, the direction perpendicular to the surface. The negative charge is distributed according to Bardeen's calculation. Instead of taking the positive charge to be uniform, as in Bardeen's model, we consider it to be uniformly distributed in the planes passing through the nuclei of the metal atoms. For the charge to be conserved, the density of positive charge per unit area in the plane must be $a\rho_0$, where a is the interplanar spacing. For the (110) surface in sodium, a is 5·73 atomic units ; ρ_0 is $3{\cdot}80\times10^{-3}$ atomic units.

The negative charge density curve from Bardeen's figure was tested by determining the moment of the double layer, when the positive charge was distributed as in fig. 1 (*a*). This was done by integrating Poisson's equation numerically from a point outside the metal into the interior. Minor adjustments were made in the curve until the moment was the same as that obtained by Bardeen (0·4 v). The negative density was brought to $-\rho_0$ at $x=-\frac{1}{2}a$. To maintain the same moment, the first plane of positive charge in the non-uniform distribution used here must be located $\frac{1}{2}a$ units from the geometrical surface of Bardeen.

We need first E_e for the case of uniform positive charge distribution so that E_k can be found from Huntington's result. Then we need E_e for the case in which the positive charge is distributed in planes. This, plus E_k, will give the total surface energy for the second case.

The potential, ϕ, was found in each case by numerical integration of Poisson's equation. Since the negative and positive charges are equal, ϕ and $d\phi/dx$ may be taken as zero at large values of x, and the integration carried toward the interior.

In the case of the uniform positive charge distribution the electrostatic energy per unit area of the surface layer is

$$E_e=\tfrac{1}{2}\int_{-\frac{1}{2}a}^{\infty}\rho_c\,\phi\,dx,$$

where ρ_c is the actual charge density, that is, the algebraic sum of the positive and negative densities. The factor $\frac{1}{2}$ enters to avoid counting interactions twice. Since $\rho_c=0$ for $x<-\frac{1}{2}a$, the electrostatic energy in the interior is zero and the integral above gives simply the electrostatic part of the surface energy. E_e for this case was found to $4{\cdot}7\times10^{-5}$ atomic units, or 37 erg/cm². E_k is the difference between this value and 88 erg/cm², or 51 erg/cm².

For the second case we expect that there will be a large electrostatic energy in the interior as well as in the surface ; E_e is the difference between that in the surface and that in the interior. Figure 1 (*c*) shows the variation with x of the potential obtained from the integration of Poisson's equation. The potential at the plane of positive charge nearest the surface is ϕ_s ; at a plane of positive charge in the interior the potential is ϕ_i. The energies per unit area of positive charge in the surface layer and in an interior layer are $a\rho_0\,\phi_s$ and $a\rho_0\,\phi_i$ respectively.

The energy of the negative charge, per unit cross section, in an interior atom is

$$-\int_{-\frac{3}{2}a}^{-\frac{1}{2}a}\rho_0\,\phi\,dx,$$

and in a surface atom is

$$-\int_{-\frac{1}{2}a}^{\infty}\rho\,\phi\,dx,$$

where $-\rho$ is the variable electronic charge density in the surface atom. The excess energy per unit area of surface is then

$$E_e=\tfrac{1}{2}\left[a\rho_0\,(\phi_s-\phi_i)-\int_{-\frac{1}{2}a}^{\infty}\rho\,\phi\,dx+\int_{-\frac{3}{2}a}^{-\frac{1}{2}a}\rho_0\,\phi\,dx\right]$$

where again the factor $\frac{1}{2}$ enters so that interactions are counted only once. ϕ_s was found to be 0·444 and ϕ_i to be 0·424. The energy of the negative charge was found to be $-3{\cdot}76\times10^{-3}$ per unit cross section for a surface atom and $-3{\cdot}53\times10^{-3}$ for an interior atom. All values are given in atomic units. E_e for this case is $1{\cdot}0\times10^{-4}$ atomic units, or 77 erg/cm².

This quantity, added to E_k, gives a total surface energy of 128 erg/cm². The product of the absolute temperature at the melting point times the surface entropy calculated by Huang and Wyllie is 34 erg/cm², so that the surface free energy at the melting point is the difference, or 94 erg/cm².

While this value is larger by 70% than that calculated by Huntington, it is still well below the experimental value given by Poindexter and Kernaghan (1929), who found the surface energy to be 206 erg/cm² near the melting point and to be almost independent of temperature. The small temperature coefficient may mean that the calculated surface entropy is too large.

It is evident that even when we consider the effect of the non-uniformity of positive charge on the electrostatic energy at the surface, the free-electron theory does not yet quantitatively account for the observed surface energy of sodium. It is illustrated here, however, that the electrostatic energy arising from the interaction of the surface ions with the non-uniform electronic charge distribution is a very important part of the surface energy.

ACKNOWLEDGMENTS

The author acknowledges with thanks the encouragement and assistance given him by Professor N. F. Mott, under whose supervision this study was carried out, and valuable aid in the form of a Fulbright Award and a fellowship of the Guggenheim Memorial Foundation.

REFERENCES

BARDEEN, J., 1936, *Phys. Rev.*, **49,** 653.
BRAGER, A., and SCHUCHOWITZKY, A., 1946, *Acta Physiochimica*, **21,** 13.
HUANG, K., and WYLLIE, G., 1949, *Proc. Phys. Soc.*, **62,** 180.
HUNTINGTON, H. B., 1951, *Phys. Rev.*, **81,** 1035.
POINDEXTER, F. E., and KERNAGHAN, M., 1929, *Phys. Rev.*, **33,** 837.

CXXXI. *On the Inhibition of Convection by a Magnetic Field : II*

By S. Chandrasekhar, F.R.S.
Yerkes Observatory, University of Chicago*

[Received July 12, 1954]

Summary

The analysis contained in an earlier paper on the inhibition of thermal convection by a magnetic field is extended to include the case when the impressed magnetic field ($\mathbf{H}$) acts in a direction different from that of gravity ($\mathbf{g}$). A variational method is described for determining the critical Rayleigh number for the onset of convection of any preassigned pattern ; and the result is established that when $\mathbf{H}$ and $\mathbf{g}$ act in different directions the convection which appears at marginal stability is in the form of rolls extended in directions parallel to the plane containing $\mathbf{H}$ and $\mathbf{g}$.

§ 1. Introduction

In an earlier paper (Chandrasekhar 1952 : this paper will be referred to hereafter as I ; see also Thompson 1951) the instability of a horizontal layer of fluid heated below has been examined in the case when the fluid considered is an electrical conductor and a uniform external magnetic field is impressed on the fluid. In developing the general theory in I no restriction was made regarding the direction of the impressed magnetic field ($\mathbf{H}$) relative to that of gravity ($\mathbf{g}$). But in deriving the principal results on the critical Rayleigh numbers for the onset of instability, the assumption was made that the directions of $\mathbf{H}$ and $\mathbf{g}$ coincide. The case when these directions do not coincide was considered only very briefly : it was, in fact, dismissed with the remark that if one restricted oneself to the onset of convection in the form of infinitely extended rolls (in directions parallel to the plane containing $\mathbf{H}$ and $\mathbf{g}$) then the critical Rayleigh numbers derived for the case when $\mathbf{H}$ and $\mathbf{g}$ are parallel can be applied to the more general case (when $\mathbf{H}$ and $\mathbf{g}$ are not parallel) if in the relevant formulae we interpret H $(=|\mathbf{H}|$ in the cases to which the analysis strictly applies) to mean the component of $\mathbf{H}$ in the direction of $\mathbf{g}$. The question whether lower Rayleigh numbers can be reached by considering more complicated patterns of motion than rolls was left open with the conjecture that this is unlikely. In this paper we return to the question which was left open and prove what was conjectured by developing a method which enables one to determine the critical Rayleigh number for the onset of convection of any preassigned pattern.

---

* Communicated by the Author.

§ 2. THE REDUCTION TO A CHARACTERISTIC VALUE PROBLEM

In the notation of I, § 7 (eqns. (117) and (118)) the basic equations are

$$\nabla^4 w = -\frac{\gamma}{\nu}\left(\frac{\partial^2\theta}{\partial x^2}+\frac{\partial^2\theta}{\partial y^2}\right)+\frac{\mu^2 H^2\sigma}{\rho_0\nu}\left(\cos\vartheta\frac{\partial}{\partial z}+\sin\vartheta\frac{\partial}{\partial x}\right)^2 w \quad . \quad . \quad (1)$$

and

$$\nabla^6 w = \frac{|\beta|\gamma}{\kappa\nu}\left(\frac{\partial^2 w}{\partial x^2}+\frac{\partial^2 w}{\partial y^2}\right)+\frac{\mu^2 H^2\sigma}{\rho_0\nu}\left(\cos\vartheta\frac{\partial}{\partial z}+\sin\vartheta\frac{\partial}{\partial x}\right)^2 \nabla^2 w, \quad . \quad (2)$$

where it may be recalled that the orientation of the co-ordinate axes has been so chosen that **H** lies in the *xz*-plane and ϑ denotes the inclination of **H** to the vertical.

If we measure all linear distances in units of the depth of the layer, *d*, and let

$$R=\frac{|\beta|\gamma}{\kappa\nu}d^4 \quad \text{and} \quad Q=\frac{\mu H^2\cos^2\vartheta}{\rho_0\nu}\sigma d^2, \quad . \quad . \quad . \quad (3)$$

eqns. (1) and (2) take the forms

$$\nabla^4 w = -\frac{\gamma}{\nu}d^2\left(\frac{\partial^2\theta}{\partial x^2}+\frac{\partial^2\theta}{\partial y^2}\right)+Q\left(\frac{\partial}{\partial z}+\tan\vartheta\frac{\partial}{\partial x}\right)^2 w \quad . \quad . \quad (4)$$

and

$$\nabla^6 w = R\left(\frac{\partial^2 w}{\partial x^2}+\frac{\partial^2 w}{\partial y^2}\right)+Q\left(\frac{\partial}{\partial z}+\tan\vartheta\frac{\partial}{\partial x}\right)^2\nabla^2 w. \quad . \quad . \quad . \quad (5)$$

Corresponding to an analysis of the disturbance in the horizontal plane in a double Fourier integral, we seek solutions of eqns. (4) and (5) which are of the forms

$$\left.\begin{aligned} w&=W(z)\exp\left[i(a_1x+a_2y)\right]\\ \text{and}\qquad \theta&=\Theta(z)\exp\left[i(a_1x+a_2y)\right],\end{aligned}\right\} \quad . \quad . \quad . \quad . \quad . \quad . \quad . \quad . \quad (6)$$

where a_1 and a_2 are the wave numbers (in the unit $1/d$) of the disturbance in the *x*- and the *y*-directions and W and Θ are functions of the vertical co-ordinate, *z*, only. It should be particularly noted that $W(z)$ and $\Theta(z)$ will in general be complex.

With w and θ given by (6), eqns. (4) and (5) reduce to

$$\left[(D^2-|\mathbf{a}|^2)^2-Q(D+i\varpi)^2\right]W=\frac{\gamma}{\nu}d^2|\mathbf{a}|^2\Theta \quad . \quad . \quad . \quad (7)$$

and

$$(D^2-|\mathbf{a}|^2)\left[(D^2-|\mathbf{a}|^2)^2-Q(D+i\varpi)^2\right]W=-R|\mathbf{a}|^2W, \quad . \quad (8)$$

where

$$D=\frac{d}{dz}, \qquad |\mathbf{a}|^2=a_1^{\,2}+a_2^{\,2} \quad \text{and} \quad \varpi=a_1\tan\vartheta. \quad . \quad . \quad (9)$$

The boundary conditions with respect to which eqns. (7) and (8) must be solved are (cf. I, eqns. (53) and (54)):

$$|W|=|\Theta|=0 \qquad \text{for } z=0 \text{ and } 1 \quad . \quad . \quad . \quad . \quad . \quad (10)$$

and

$$\left.\begin{aligned} |DW|&=0 \qquad \text{on a rigid surface,}\\ |D^2W|&=0 \qquad \text{on a free surface.}\end{aligned}\right\} \quad . \quad . \quad . \quad . \quad . \quad (11)$$

In view of eqn. (7) the boundary conditions (10) are equivalent to

$$|\, W\,| = |\, \{(D^2 - |\,\mathbf{a}\,|^2)^2 - Q(D+i\varpi)^2\} W\,| = 0 \qquad \text{for } z=0 \quad \text{and} \quad 1. \qquad (12)$$

Since W is complex, eqn. (8) together with the boundary conditions (11) and (12) constitute a characteristic value problem in an equation, genuinely, of order twelve. However, eqn. (8) being linear and one with constant coefficients, the problem presents no difficulty of principle. But as the solution of the physical problem requires the determination of the minimum value of R as a function of the two variables $|\,\mathbf{a}\,|$ and ϖ ($\leqslant |\,\mathbf{a}\,| \tan\vartheta$) for various assigned values of Q, it is clear that the practical problem is a very formidable one if the characteristic value problem has to be solved in any direct manner. Fortunately, it will appear that this is not necessary, since, as in I, a more convenient method which is practicable can be devised. This method which is based on a variational principle is described in the following section.

§ 3. The Variational Method

Letting

$$F = [(D^2 - |\,\mathbf{a}\,|^2)^2 - Q(D+i\varpi)^2] W, \qquad . \quad . \quad . \quad . \quad (13)$$

we first rewrite the equation governing W as

$$(D^2 - |\,\mathbf{a}\,|^2) F = -R\,|\,\mathbf{a}\,|^2 W. \qquad . \quad . \quad . \quad . \quad . \quad (14)$$

The boundary conditions (12) now require that

$$|\, F\,| = |\, W\,| = 0 \qquad \text{for } z=0 \quad \text{and} \quad 1. \qquad . \quad . \quad . \quad . \quad . \quad (15)$$

Now multiply eqn. (14) by F^*, the complex conjugate of F, and integrate over the range of z (i.e. from 0 to 1). The left-hand side of the equation gives

$$\int_0^1 F^*(D^2 - |\,\mathbf{a}\,|^2) F\, dz = [F^* DF]_0^1 - \int_0^1 (|\, DF\,|^2 + |\,\mathbf{a}\,|^2 |\, F\,|^2)\, dz. \qquad (16)$$

The integrated part vanishes on account of (15) and we are left with

$$\int_0^1 F^*(D^2 - |\,\mathbf{a}\,|^2) F\, dz = -\int_0^1 (|\, DF\,|^2 + |\,\mathbf{a}\,|^2 |\, F\,|^2)\, dz. \qquad . \quad (17)$$

Considering next the right-hand side of eqn. (14) we have (cf. eqn. (13))

$$\int_0^1 W F^*\, dz = \int_0^1 W[(D^2 - |\,\mathbf{a}\,|^2)^2 - Q(D-i\varpi)^2] W^*\, dz. \qquad . \quad (18)$$

After two successive integrations by parts, the first of the two integrals on the right-hand side of the foregoing equation becomes (cf. I, eqns. (65) and (66))

$$\int_0^1 W(D^2 - |\,\mathbf{a}\,|^2)^2 W^*\, dz = \int_0^1 |\, (D^2 - |\,\mathbf{a}\,|^2) W\,|^2\, dz, \qquad . \quad . \quad (19)$$

while the second of the two integrals can be transformed in the manner

$$\begin{aligned}
\int_0^1 & W(D-i\varpi)^2W^*\,dz \\
&= \int_0^1 W(D^2W^*-\varpi^2W^*-2i\varpi DW^*)\,dz \\
&= -\int_0^1 (|DW|^2+\varpi^2|W|^2)\,dz-2i\varpi\int_0^1 WDW^*\,dz \\
&= -\int_0^1 (|DW|^2+\varpi^2|W|^2-i\varpi WDW^*+i\varpi W^*DW)\,dz \\
&= -\int_0^1 |DW+i\varpi W|^2\,dz. \qquad (20)
\end{aligned}$$

Thus, we have

$$\int_0^1 WF^*\,dz=\int_0^1 [|(D^2-|\mathbf{a}|^2)W|^2+Q|DW+i\varpi W|^2]\,dz. \qquad (21)$$

The result of multiplying eqn. (14) by F^* and integrating over the range of z is therefore

$$R=\frac{\int_0^1 (|DF|^2+|\mathbf{a}|^2|F|^2)\,dz}{|\mathbf{a}|^2\int_0^1 [|(D^2-|\mathbf{a}|^2)W|^2+Q|DW+i\varpi W|^2]\,dz}. \qquad (22)$$

This formula expresses R as the ratio of two positive definite integrals; and as in I, eqns. (70)–(76), it can be shown that eqn. (22) similarly provides the basis for a variational method of solving the underlying characteristic value problem. And the method as applied to eqns. (8), (11) and (12) is the following:

Assume for F an expression involving one or more parameters A_k and which vanishes at $z=0$ and 1. With the chosen form for F determine W as the solution of the equation

$$[(D^2-|\mathbf{a}|^2)^2-Q(D+i\varpi)^2]W=F, \qquad (23)$$

which satisfies the remaining four boundary conditions on W. Then evaluate R according to formula (22) and minimize it with respect to the parameters A_k.

§ 4. The Determination of R when **H** and **g** act in Different Directions and for the Cases (i) when Both Bounding Surfaces are Rigid, (ii) when Both Bounding Surfaces are Free and (iii) when One Bounding Surface is Rigid and the Other is Free

(i) *Both bounding surfaces rigid.* In this case it is convenient to translate the z-axis so that the bounding surfaces are at $z=\pm\frac{1}{2}$.

As the simplest trial function for F which vanishes at $z=\pm\frac{1}{2}$ we shall assume

$$F=\cos\pi z. \qquad (24)$$

This is a trial function with no variational parameters. Nevertheless, from our earlier experience with problems of this kind (cf. I, for example) we may be confident that already this trial function will lead to values of R which are accurate to within 1%.

With F given by (24) the equation to be solved for W is

$$[(D^2-|\mathbf{a}|^2)^2-Q(D+i\varpi)^2]W=\cos\pi z, \quad . \quad . \quad . \quad . \quad . \quad (25)$$

and the general solution of this equation is

$$W=\Gamma_1\exp(i\pi z)+\Gamma_2\exp(-i\pi z)+\sum_{j=1}^{4}A_j\exp(q_jz), \quad . \quad (26)$$

where

$$\left.\begin{aligned}\Gamma_1&=\tfrac{1}{2}[(\pi^2+|\mathbf{a}|^2)^2+Q(\pi+\varpi)^2]^{-1},\\ \Gamma_2&=\tfrac{1}{2}[(\pi^2+|\mathbf{a}|^2)^2+Q(\pi-\varpi)^2]^{-1},\end{aligned}\right\} \quad . \quad . \quad . \quad . \quad . \quad (27)$$

the q_j's ($j=1, \ldots, 4$) are the roots of the quartic equation

$$(q^2-|\mathbf{a}|^2)^2=Q(q+i\varpi)^2, \quad . \quad . \quad . \quad . \quad . \quad . \quad . \quad (28)$$

and the A_j's ($j=1, \ldots, 4$) are constants of integration to be determined by the boundary conditions on W.

It can be readily verified that the roots of eqn. (28) are given by

$$q_1=a+ic, \qquad q_2=-a+ic, \qquad q_3=b-ic, \qquad q_4=-b-ic, \quad . \quad (29)$$

where

$$a=\tfrac{1}{2}(\sqrt{Q}+\alpha_1), \qquad b=\tfrac{1}{2}(\sqrt{Q}-\alpha_1), \qquad c=\tfrac{1}{2}\alpha_2, \quad . \quad . \quad (30)$$

$$\left.\begin{aligned}\alpha_1&=[\tfrac{1}{2}\{(Q+4|\mathbf{a}|^2)^2+16\varpi^2Q\}^{1/2}+\tfrac{1}{2}(Q+4|\mathbf{a}|^2)]^{1/2}\\ \text{and}\quad \alpha_2&=[\tfrac{1}{2}\{(Q+4|\mathbf{a}|^2)^2+16\varpi^2Q\}^{1/2}-\tfrac{1}{2}(Q+4|\mathbf{a}|^2)]^{1/2}.\end{aligned}\right\} \quad . \quad . \quad (31)$$

The boundary conditions to be satisfied by W are

$$W=0 \qquad \text{and} \qquad DW=0 \qquad \text{for } z=\pm\tfrac{1}{2}\,; \quad . \quad . \quad . \quad (32)$$

and these conditions require :

$$\left.\begin{aligned}&\sum_{j=1}^{4}A_j\exp(+\tfrac{1}{2}q_j)=-\sum_{j=1}^{4}A_j\exp(-\tfrac{1}{2}q_j)=-i(\Gamma_1-\Gamma_2)\\ \text{and}\quad &\sum_{j=1}^{4}A_jq_j\exp(+\tfrac{1}{2}q_j)=-\sum_{j=1}^{4}A_jq_j\exp(-\tfrac{1}{2}q_j)=\pi(\Gamma_1+\Gamma_2).\end{aligned}\right\} \quad . \quad (33)$$

It is found that the solution of these equations can be expressed in the forms

$$A_1=A_2^*=\frac{\exp(\tfrac{1}{2}q_1)}{\Delta}\{-i(\Gamma_1-\Gamma_2)X_1+\pi(\Gamma_1+\Gamma_2)Y_1\} \quad . \quad (34)$$

and

$$A_3=A_4^*=\frac{\exp(\tfrac{1}{2}q_3)}{\Delta}\{-i(\Gamma_1-\Gamma_2)X_2+\pi(\Gamma_1+\Gamma_2)Y_2\}, \quad . \quad (35)$$

where

$$\Delta=2[(\alpha_2^2+Q)\cosh\alpha_1+(\alpha_1^2-Q)\cos\alpha_2-(\alpha_1^2+\alpha_2^2)\cosh\sqrt{Q}], \quad . \quad (36)$$

$$\begin{aligned}X_1=q_4(q_3-q_2)&[\exp(q_3+q_2)-\exp(q_4)]+q_2(q_4-q_3)\\ &\times[\exp(q_4+q_3)-\exp(q_2)]+q_3(q_2-q_4)[\exp(q_2+q_4)-\exp(q_3)], \quad (37)\end{aligned}$$

$$\begin{aligned}Y_1=(q_2-q_3)&[\exp(q_2+q_3)-\exp(q_4)]+(q_3-q_4)[\exp(q_3+q_4)-\exp(q_2)]\\ &+(q_4-q_2)[\exp(q_4+q_2)-\exp(q_3)]\,; \quad . \quad . \quad . \quad . \quad . \quad . \quad . \quad . \quad . \quad . \quad (38)\end{aligned}$$

and X_2 and Y_2 are given by expressions which can be obtained by replacing q_2 and q_3 in eqns. (37) and (38) by q_1 and q_2, respectively.

With F and W given by eqns. (24) and (26) we readily find that

$$\int_0^1(|DF|^2+|\mathbf{a}|^2|F|^2)\,dz=\tfrac{1}{2}(\pi^2+|\mathbf{a}|^2), \quad . \quad . \quad . \quad . \quad . \quad (39)$$

and $$\int_0^1 WF^*\,dz=\tfrac{1}{2}(\Gamma_1+\Gamma_2)+\pi\sum_{j=1}^{4}A_j\,\frac{\exp\left(+\tfrac{1}{2}q_j\right)+\exp\left(-\tfrac{1}{2}q_j\right)}{q_j^2+\pi^2}. \qquad (40)$$

Substituting for the q_j's and the A_j's in accordance with eqns. (29), (34) and (35) we find after some very lengthy but straightforward reductions that the integral on the left-hand side of eqn. (40) can be reduced to the form

$$\begin{aligned}\int_0^1 WF^*\,dz=&\tfrac{1}{2}(\Gamma_1+\Gamma_2)\\ &+\frac{2\pi}{\Delta}(\Gamma_1-\Gamma_2)(g_1\,\mathfrak{F}_1+f_1\,\mathfrak{G}_1-g_2\,\mathfrak{F}_2-f_2\,\mathfrak{G}_2)\\ &+\frac{2\pi^2}{\Delta}(\Gamma_1+\Gamma_2)(f_1\,\mathfrak{H}_1-g_1\,\mathfrak{J}_1+f_2\,\mathfrak{H}_2-g_2\,\mathfrak{J}_2), \quad .\ .\ .\quad (41)\end{aligned}$$

where

$$\left.\begin{aligned}f_1=&\,\delta_1[(\pi^2+a^2-c^2)(1+e^a\cos c)+2\,e^a\,ac\sin c],\\ g_1=&\,\delta_1[(\pi^2+a^2-c^2)\,e^a\sin c-2ac(1+e^a\cos c)],\\ \mathfrak{F}_1=&\,2ab(\cos c-e^{-a})\cosh b-2(b^2+2c^2)(\cos c+e^{-a})\sinh b\\ &+2ab(\cos 2c-e^{-a}\cos c)-2bc(\sin 2c+e^{-a}\sin c)\\ &-2c(a\sinh b+b\cosh b)\sin c,\\ \mathfrak{G}_1=&-2ac(\cos c+e^{-a})\sinh b-2bc(\cos c-e^{-a})\cosh b\\ &-2ab\cosh b\sin c+2(b^2+2c^2)\sinh b\sin c\\ &-2ab(\sin 2c+e^{-a}\sin c)-2bc(\cos 2c-e^{-a}\cos c),\\ \mathfrak{H}_1=&-2a(\cos c+e^{-a})\sinh b+2b(\cos c-e^{-a})\cosh b\\ &+4c\sinh b\sin c+2b(\cos 2c-e^{-a}\cos c),\\ \mathfrak{J}_1=&\,4c(\cos c+e^{-a})\sinh b+2(a\sinh b-b\cosh b)\sin c\\ &-2b(\sin 2c+e^{-a}\sin c),\\ \delta_1=&\,[(\pi^2+a^2-c^2)^2+4a^2c^2]^{-1}.\end{aligned}\right\}\quad .\ .\ \ (42)$$

$$\left.\begin{aligned}f_2=&\,\delta_2[(\pi^2+b^2-c^2)(1+e^b\cos c)+2\,e^b\,bc\sin c],\\ g_2=&\,\delta_2[(\pi^2+b^2-c^2)\,e^b\sin c-2bc(1+e^b\cos c)],\\ \mathfrak{F}_2=&\,2ab(\cos c-e^{-b})\cosh a-2(a^2+2c^2)(\cos c+e^{-b})\sinh a\\ &+2ab(\cos 2c-e^{-b}\cos c)-2ac(\sin 2c+e^{-b}\sin c)\\ &-2c(a\cosh a+b\sinh a)\sin c,\\ \mathfrak{G}_2=&-2bc(\cos c+e^{-b})\sinh a-2ac(\cos c-e^{-b})\cosh a\\ &-2ab\cosh a\sin c+2(a^2+2c^2)\sinh a\sin c\\ &-2ab(\sin 2c+e^{-b}\sin c)-2ac(\cos 2c-e^{-b}\cos c),\\ \mathfrak{H}_2=&-2b(\cos c+e^{-b})\sinh a+2a(\cos c-e^{-b})\cosh a\\ &+4c\sinh a\sin c+2a(\cos 2c-e^{-b}\cos c),\\ \mathfrak{J}_2=&\,4c(\cos c+e^{-b})\sinh a+2(b\sinh a-a\cosh a)\sin c\\ &-2a(\sin 2c+e^{-b}\sin c),\\ \delta_2=&\,[(\pi^2+b^2-c^2)^2+4b^2c^2]^{-1}.\end{aligned}\right\}\quad .\ .\ \ (43)$$

Finally, the required value of R (in the chosen approximation) is given (apart from the factor $|\,\mathbf{a}\,|^2$) by the ratio of the expressions on the right-hand sides of eqns. (39) and (41).

Values of R obtained with the aid of the foregoing formulae for various values of Q, $|\,\mathbf{a}\,|$ and ϖ are listed in table 1. We return to a discussion of these values in § 5.

(ii) *Both bounding surfaces free.* With the same trial function for F as before (eqn. (24)) the solution for W will again be given by (26). But the boundary conditions which determine the constants A_j are now different ; they are

$$W=0 \quad \text{and} \quad D^2W=0 \quad \text{for } z=\pm\tfrac{1}{2}. \quad . \quad . \quad . \quad (44)$$

These conditions require :

$$\left.\begin{aligned} &\sum_{j=1}^{4} A_j \exp\left(+\tfrac{1}{2}q_j\right)=-\sum_{j=1}^{4} A_j \exp\left(-\tfrac{1}{2}q_j\right)=-i(\Gamma_1-\Gamma_2)\\ \text{and}\quad &\sum_{j=1}^{4} A_j q_j^2 \exp\left(+\tfrac{1}{2}q_j\right)=-\sum_{j=1}^{4} A_j q_j^2 \exp\left(-\tfrac{1}{2}q_j\right)=i\pi^2(\Gamma_1-\Gamma_2).\end{aligned}\right\} . \quad (45)$$

And the solutions of these equations are found to be expressible in the forms

$$A_1=A_2^*=i(\Gamma_1-\Gamma_2)\frac{\exp\left(+\tfrac{1}{2}q_1\right)}{\Delta}(-X_1+\pi^2 Y_1) \quad . \quad . \quad (46)$$

and

$$A_3=A_4^*=i(\Gamma_1-\Gamma_2)\frac{\exp\left(+\tfrac{1}{2}q_3\right)}{\Delta}(-X_2+\pi^2 Y_2), \quad . \quad . \quad (47)$$

where

$$\Delta=2[(\alpha_1^2+\alpha_2^2)Q \cosh \sqrt{Q}-\alpha_1^2(\alpha_2^2+Q)\cosh \alpha_1+\alpha_2^2(\alpha_1^2-Q)\cos \alpha_2], \quad . \quad . \quad . \quad . \quad (48)$$

$$X_1=q_4^2(q_3^2-q_2^2)[\exp(q_3+q_2)-\exp(q_4)]+q_2^2(q_4^2-q_3^2) \\ \times[\exp(q_4+q_3)-\exp(q_2)]+q_3^2(q_2^2-q_4^2)[\exp(q_2+q_4)-\exp(q_3)], \quad . \quad . \quad . \quad . \quad (49)$$

$$Y_1=(q_2^2-q_3^2)[\exp(q_2+q_3)-\exp(q_4)]+(q_3^2-q_4^2)[\exp(q_3+q_4)-\exp(q_2)] \\ +(q_4^2-q_2^2)[\exp(q_4+q_2)-\exp(q_3)] ; \quad . \quad . \quad . \quad . \quad . \quad . \quad . \quad . \quad . \quad (50)$$

and X_2 and Y_2 are given by expressions which can be obtained by replacing q_2 and q_3 in eqns. (49) and (50) by q_1 and q_2, respectively.

The result of substituting the foregoing expressions for the A_j's in eqn. (40) (which continues to be valid) is to give

$$\int_0^1 WF^*\,dz=\tfrac{1}{2}(\Gamma_1+\Gamma_2) \\ +\frac{2\pi}{\Delta}(\Gamma_1-\Gamma_2)\{g_1(\mathfrak{F}_1-\pi^2\mathfrak{H}_1)+f_1(\mathfrak{G}_1-\pi^2\mathfrak{I}_1) \\ -g_2(\mathfrak{F}_2-\pi^2\mathfrak{H}_2)-f_2(\mathfrak{G}_2-\pi^2\mathfrak{I}_2)\}, \quad . \quad . \quad . \quad . \quad . \quad . \quad . \quad (51)$$

Table 1. Rayleigh Numbers for Various Assigned Values of Q, $|\mathbf{a}|$ and ϖ for the Case when both Bounding Surfaces are Rigid. (In all cases the entry for $\varpi=0$ is for a value of $|\mathbf{a}|$ for which it is known (cf. I, table 2) that the Rayleigh Number attains its Minimum Value for Convection setting in as Rolls)

Q	ϖ	$\|\mathbf{a}\|$	R
100	0·0	4·0	3768
	0·5	3·9	3797
		4·0	3793
		4·1	3795
	1·0	3·9	3875
		4·0	3878
		4·1	3871
	2·0	3·9	4190
		4·0	4181
		4·1	4178
	4·0	3·9	5523
		4·0	5494
		4·1	5474

Q	ϖ	$\|\mathbf{a}\|$	R
10	0	3·25	1954
	0·5		1958
	1·0		1972
	2·0		2026
	4·0		2707
50	0	3·68	2811
	1·0		2876
	2·0		3072
	4·0		3876
500	0	5·16	10120
	2·0		11280
	4·0		15240
1000	0	5·80	17120
	3·0		21580
	6·0		39880
4000	0	7·40	54710
	2·0		60440
10000	0	8·66	124500
	4·0		182700

where, now

$$\left.\begin{aligned}
f_1&=\delta_1[(\pi^2+a^2-c^2)(1+e^a\cos c)+2e^a ac\sin c],\\
g_1&=\delta_1[(\pi^2+a^2-c^2)\,e^a\sin c-2ac(1+e^a\cos c)],\\
\mathfrak{F}_1&=2BD\{(\cos 2c-e^{-a}\cos c)+(\cos c-e^{-a})\cosh b\}\\
&\quad+2AD\{(\sin 2c+e^{-a}\sin c)+\cosh b\sin c\}\\
&\quad+2BC\sinh b\sin c+2(C^2+D^2-AC)(\cos c+e^{-a})\sinh b,\\
\mathfrak{G}_1&=2AD\{(\cos 2c-e^{-a}\cos c)+(\cos c-e^{-a})\cosh b\}\\
&\quad-2BD\{(\sin 2c+e^{-a}\sin c)+\cosh b\sin c\}\\
&\quad+2BC(\cos c+e^{-a})\sinh b-2(C^2+D^2-AC)\sinh b\sin c,\\
\mathfrak{H}_1&=-2D\{(\sin 2c+e^{-a}\sin c)+\cosh b\sin c\}-2B\sinh b\sin c\\
&\quad+2(A-C)\,(\cos c+e^{-a})\sinh b,\\
\mathfrak{J}_1&=-2D\{(\cos 2c-e^{-a}\cos c)+(\cos c-e^{-a})\cosh b\}\\
&\quad-2B(\cos c+e^{-a})\sinh b-2(A-C)\sinh b\sin c,\\
\delta_1&=[(\pi^2+a^2-c^2)^2+4a^2c^2]^{-1},
\end{aligned}\right\}\quad .\ .\ (52)$$

$$\left.\begin{aligned}
f_2&=\delta_2[(\pi^2+b^2-c^2)(1+e^b\cos c)+2e^b bc\sin c],\\
g_2&=\delta_2[(\pi^2+b^2-c^2)\,e^b\sin c-2bc(1+e^b\cos c)],\\
\mathfrak{F}_2&=2BD\{(\cos 2c-e^{-b}\cos c)+(\cos c-e^{-b})\cosh a\}\\
&\quad+2BC\{(\sin 2c+e^{-b}\sin c)+\cosh a\sin c\}\\
&\quad+2AD\sinh a\sin c+2(A^2+B^2-AC)(\cos c+e^{-b})\sinh a,\\
\mathfrak{G}_2&=2BC\{(\cos 2c-e^{-b}\cos c)+(\cos c-e^{-b})\cosh a\}\\
&\quad-2BD\{(\sin 2c+e^{-b}\sin c)+\cosh a\sin c\}\\
&\quad+2AD(\cos c+e^{-b})\sinh a-2(A^2+B^2-AC)\sinh a\sin c,\\
\mathfrak{H}_2&=-2B\{(\sin 2c+e^{-b}\sin c)+\cosh a\sin c\}-2D\sinh a\sin c\\
&\quad-2(A-C)(\cos c+e^{-b})\sinh a,\\
\mathfrak{J}_2&=-2B\{(\cos 2c-e^{-b}\cos c)+(\cos c-e^{-b})\cosh a\}\\
&\quad-2D(\cos c+e^{-b})\sinh a+2(A-C)\sinh a\sin c,\\
\delta_2&=[(\pi^2+b^2-c^2)^2+4b^2c^2]^{-1}.
\end{aligned}\right\}\quad .\ .\ (53)$$

In eqns. (52) and (53) a, b and c have the same meanings as in eqns. (42) and (43) ; in addition we have let

$$A=a^2-c^2,\qquad C=b^2-c^2,\qquad B=2ac\quad\text{and}\quad D=2bc.\quad .\ (54)$$

And again the required value of R (in the chosen approximation) is given (apart from the factor $|\,\mathbf{a}\,|^2$) by the ratio of the expressions on the right-hand sides of eqns. (39) and (51).

Values of R obtained with the aid of the foregoing formulae for various values of Q, $|\,\mathbf{a}\,|$ and ϖ are listed in table 2.

Table 2. Rayleigh Numbers for Various Assigned Values of Q, $|\mathbf{a}|$ and ϖ for the Case when both Bounding Surfaces are Free. (In all cases the Entry for $\varpi=0$ is for a Value of $|\mathbf{a}|$ for which it is known (cf. I, table 1) that the Rayleigh Number attains its Minimum Value for Convection Setting in as Rolls)

Q	ϖ	$\|\mathbf{a}\|$	R
100	0	3·7	2654
	0·5	3·6	2682
		3·7	2678
		3·8	2681
	1·0	3·6	2757
		3·7	2752
		3·8	2754
	2·0	3·6	3064
		3·7	3055
		3·8	3052
	4·0	3·6	4492
		3·7	4366
		3·8	4342
	6·0	3·6	6925
		3·7	6843
		3·8	6773
5	0	2·43	658
	1·0		809
10	0	2·59	923
	0·5		929
	1·0		945
	2·0		1011
	4·0		1276
50	0	3·27	1762
	1·0		1827
	2·0		2026
	4·0		2828
500	0	5·00	8579
	2·0		9687
	4·0		13570
1000	0	5·68	15210
	3·0		19550
	6·0		37820
4000	0	7·31	51520
	2·0		56330
10000	0	8·59	119800
	4·0		177200

(iii) *One bounding surface free and the other rigid.*† In this case it is convenient to have the bounding surfaces at $z=0$ and 1 and choose for F the trial function

$$F=\sin \pi z. \qquad (55)$$

The corresponding solution for W is

$$W=-i\Gamma_1 \exp(i\pi z)+i\Gamma_2 \exp(-i\pi z)+\sum_{j=1}^{4} A_j \exp(q_j z) \qquad (56)$$

where Γ_1, Γ_2 and the q_j's have the same meanings as hitherto. The present boundary conditions on W are

$$W=DW=0 \quad \text{for } z=0, \qquad W=D^2W=0 \quad \text{for } z=1. \qquad (57)$$

These boundary conditions require that

$$\left.\begin{aligned} &\sum_{j=1}^{4} A_j=-\sum_{j=1}^{4} A_j \exp(q_j)=i(\Gamma_1-\Gamma_2), \\ &\sum_{j=1}^{4} A_j q_j=-\pi(\Gamma_1+\Gamma_2) \quad \text{and} \quad \sum_{j=1}^{4} A_j q_j^2 \exp(q_j)=i\pi^2(\Gamma_1-\Gamma_2). \end{aligned}\right\} \qquad (58)$$

The solution of these equations are found to be expressible in the forms

$$A_j=\frac{i}{\Delta}(\Gamma_1-\Gamma_2)X_j+\frac{\pi}{\Delta}(\Gamma_1+\Gamma_2)Y_j \qquad (j=1, \ldots, 4), \qquad (59)$$

where

$$\Delta=2[(\alpha_1^2+\alpha_2^2)\sqrt{Q} \sinh \sqrt{Q}-(Q+\alpha_2^2)\alpha_1 \sinh \alpha_1-(Q-\alpha_1^2)\alpha_2 \sin \alpha_2], \qquad (60)$$

$$\begin{aligned} X_1=\,&q_2(q_4^2-q_3^2) \exp(q_3+q_4)-q_3(q_4^2-q_2^2) \exp(q_2+q_4) \\ &+q_4(q_3^2-q_2^2) \exp(q_2+q_3)-(q_2^2+\pi^2)(q_4-q_3) \exp(q_2) \\ &+(q_3^2+\pi^2)(q_4-q_2) \exp(q_3)-(q_4^2+\pi^2)(q_3-q_2) \exp(q_4), \end{aligned} \qquad (61)$$

$$\begin{aligned} Y_1=\,&(q_4^2-q_3^2) \exp(q_3+q_4)-(q_4^2-q_2^2) \exp(q_2+q_4) \\ &+(q_3^2-q_2^2) \exp(q_2+q_3), \end{aligned} \qquad (62)$$

and the expressions for the remaining X's and Y's can be obtained by suitable permutations of the subscripts of the q's in eqns. (61) and (62).

With F and W given by eqns. (55) and (56) we now find that

$$\int_0^1 (|DF|^2+|\mathbf{a}|^2|F|^2)\,dz=\tfrac{1}{2}(\pi^2+|\mathbf{a}|^2) \qquad (63)$$

and

$$\int_0^1 WF^*\,dz=\tfrac{1}{2}(\Gamma_1+\Gamma_2)+\pi \sum_{j=1}^{4} A_j \frac{1+\exp(q_j)}{q_j^2+\pi^2}. \qquad (64)$$

---

† In obtaining the solution for this case (when **H** and **g** are parallel) in I, it was pointed out that on account of symmetry the 'odd solutions' for the case when both bounding surfaces are rigid provide solutions for the case when one bounding surface is rigid and the other is free ; but that these latter solutions are applicable to a cell depth $d'=\frac{1}{2}d$ and a Rayleigh number which is sixteen times smaller. But it should also have been pointed out that the corresponding value of the parameter Q is four times smaller. Hence, the values of Q given in the first column in table 3 should be divided by 4 to make this table comparable to tables 1 and 2 ; similarly the values of a given in the second column should be divided by 2.

The reduction of the right-hand side of eqn. (64) with the A_j's given by eqns. (59)–(62) is particularly troublesome : it is very long and very complicated, and requires among other 'tricks' the repeated use of the identities

$$\frac{1}{\Gamma_1}=2\prod_{j=1}^{4}(i\pi-q_j) \qquad \text{and} \qquad \frac{1}{\Gamma_2}=2\prod_{j=1}^{4}(i\pi+q_j). \qquad (65)$$

But eventually one finds that

$$\begin{aligned}\int_0^1 WF^*\,dz=\tfrac{1}{2}(\Gamma_1+\Gamma_2)+\frac{8\pi}{\Delta}\Gamma_1\Gamma_2 & \\ \times[[\{2(\Gamma_1-\Gamma_2)[B(\mathfrak{C}^2+D^2)+D(\mathfrak{A}^2+B^2)]+\pi\alpha_1\}(Q+\alpha_2{}^2)\alpha_1\cosh\alpha_1 & \\ -\{2(\Gamma_1-\Gamma_2)[B(\mathfrak{C}^2+D^2)-D(\mathfrak{A}^2+B^2)]+\pi\sqrt{Q}\}(\alpha_1{}^2+\alpha_2{}^2)\sqrt{Q}\cosh\sqrt{Q} & \\ -\{2(\Gamma_1-\Gamma_2)[\mathfrak{A}(\mathfrak{C}^2+D^2)-\mathfrak{C}(\mathfrak{A}^2+B^2)]+\pi\alpha_2\}(\alpha_1{}^2-Q)\alpha_2\cos\alpha_2 & \\ -8(\Gamma_1-\Gamma_2)\{a[\mathfrak{H}\sin c\sinh b+\mathfrak{I}\cos c\cosh b] & \\ +b[\mathfrak{F}\sin c\sinh a+\mathfrak{G}\cos c\cosh a]\}]], & \qquad (66)\end{aligned}$$

where

$$\left.\begin{aligned}\mathfrak{F}&=(\mathfrak{A}^2-B^2)(\Sigma_1\mathfrak{C}-B^2)+2B^2\mathfrak{A}(\mathfrak{C}+\Sigma_1),\\ \mathfrak{G}&=B\{2\mathfrak{A}(\Sigma_1\mathfrak{C}-B^2)-(\mathfrak{A}^2-B^2)(\mathfrak{C}+\Sigma_1)\},\\ \mathfrak{H}&=(\mathfrak{C}^2-D^2)(\Sigma_2\mathfrak{A}+D^2)-2D^2\mathfrak{C}(\mathfrak{A}-\Sigma_2),\\ \mathfrak{I}&=D\{2\mathfrak{C}(\Sigma_2\mathfrak{A}+D^2)+(\mathfrak{C}^2-D^2)(\mathfrak{A}-\Sigma_2)\},\end{aligned}\right\} \qquad (67)$$

$$\left.\begin{aligned}\mathfrak{A}&=\pi^2+A=\pi^2+a^2-c^2\,; \quad \Sigma_1=\tfrac{1}{2}(\alpha_1\sqrt{Q}-\alpha_2{}^2),\\ \mathfrak{C}&=\pi^2+C=\pi^2+b^2-c^2\,; \quad \Sigma_2=\tfrac{1}{2}(\alpha_1\sqrt{Q}+\alpha_2{}^2),\end{aligned}\right\} \qquad (68)$$

and a, b, c, A, B, C and D have the same meanings as in cases (i) and (ii) above (eqns. (29)–(31) and (54)).

Finally, the required value of R (in the chosen approximation) is given (again, apart from a factor $|\mathbf{a}|^2$) by the ratio of the expressions on the right-hand sides of eqns. (63) and (66).

Values of R obtained with the aid of the foregoing formulae for various values of Q, $|\mathbf{a}|$ and ϖ are listed in table 3.

§ 5. THE ONSET OF CONVECTION AS LONGITUDINAL ROLLS WHEN **H** AND **g** ACT IN DIFFERENT DIRECTIONS

We now return to an examination of the results summarized in tables 1, 2 and 3.

First, it should be noted that in all cases the entry for $\varpi=0$ is for a value of $|\mathbf{a}|$ for which it is known from the results in I that the minimum Rayleigh number occurs when the pattern of convection which appears at marginal instability is in the form of longitudinal rolls (i.e. rolls extended in directions parallel to the plane containing **H** and **g**). Thus for a layer of liquid confined between two rigid planes, the lowest Rayleigh number is

Table 3. Rayleigh Numbers for Various Assigned Values of Q, $|\mathbf{a}|$ and ϖ for the Case when One Bounding Surface is Free and the Other Bounding Surface is Rigid. (In all cases the Entry for $\varpi=0$ is for a Value of $|\mathbf{a}|$ for which it is known (cf. I, table 3) that the Rayleigh Number attains its Minimum Value for Convection Setting in as Rolls)

Q	ϖ	$\|\mathbf{a}\|$	R
500	0	5·1	9319
	0·5	5·0	9389
		5·1	9387
		5·2	9393
	1·0	5·0	9596
		5·1	9593
		5·2	9599
	2·0	5·0	10456
		5·1	10450
		5·2	10453
	4·0	5·0	14396
		5·1	14371
		5·2	14358
	6·0	5·0	22684
		5·1	22598
		5·2	22528
25	0	3·17	1713
	1·0		1754
	2·0		1877
	4·0		2378
50	0	3·45	2231
	1·0		2297
	2·0		2496
	4·0		3250
250	0	4·50	5628
	0·5		5671
	1·0		5803
1000	0	5·75	16130
	0·5		16240
	1·0		16580
	4·0		24540
2500	0	6·75	35060
	0·5		35290
	1·0		35980
	4·0		52490
10000	0	8·65	122200
	1·0		125200

obtained for $|\mathbf{a}|=4{\cdot}00$ when $Q=100$ and convection sets in as longitudinal rolls. From the results for $Q=100$ given in table 1 it follows that for ϖ slightly different from zero the minimum Rayleigh number still occurs for $|\mathbf{a}|=4{\cdot}00$; also, that the new minimum slightly exceeds that for $\varpi=0$. For example, for $\varpi=0{\cdot}5$ and $Q=100$ the minimum Rayleigh number is 3793; this should be contrasted with $R_c=3768$ for $\varpi=0$. For larger values of ϖ the minimum appears to shift to somewhat higher values of $|\mathbf{a}|$; but the Rayleigh numbers now exceed R_c at $\varpi=0$ by a substantial margin. Thus in the illustrative example considered the minimum Rayleigh number for $\varpi=1{\cdot}0$ is 3871 and this occurs for $|\mathbf{a}|=4{\cdot}1$. The results for other values of Q and other boundary conditions exhibit the same general behaviour and confirm the conjecture made in I that when **H** and **g** act in different directions convection when it first sets in appears as longitudinal rolls.

In some ways the conclusion arrived at in the last paragraph is a paradoxical one. For, when **H** and **g** are parallel the Rayleigh number depends only on $|\mathbf{a}|^2=a_1^2+a_2^2$ (cf. eqn. (9)) and we expect convection at marginal instability to have a cellular—and, indeed, a hexagonal—pattern. How then, one may ask, does this situation change discontinuously when **H** is inclined only very slightly to the vertical and when, it is asserted, convection at marginal instability must appear as longitudinal rolls? The resolution of this paradox is as follows:

When **H** and **g** act in different directions, differing Rayleigh numbers are required for the marginal appearance of convection with a preassigned pattern. In particular, the most ‘ difficult ’ pattern to excite (other things being equal) is the system of the *transverse* rolls. Once the Rayleigh number is high enough to excite these transverse rolls, we may expect a proper cellular pattern of convection to emerge. The *difference* in the minimum Rayleigh numbers required to excite the longitudinal and the transverse rolls is, therefore, a measure of the extent to which a proper cellular pattern of convection is suppressed at marginal instability. But, and this is the main point of the argument, this difference in the two Rayleigh numbers tends to zero as ϖ $(=a_1 \tan \vartheta \leqslant |\mathbf{a}| \tan \vartheta)$ tends to zero. In other words, when **H** is only very slightly inclined to the direction of gravity, the extent to which *transverse* rolls are suppressed at marginal instability (when *longitudinal* rolls appear) is also only very slight. Finally, when **H** is exactly parallel to **g** this suppression of the cellular pattern ceases and longitudinal and transverse rolls appear simultaneously at marginal instability.

The picture which we have thus arrived at as to what really ‘ happens ’ when **H** and **g** act in different directions constitutes an essential simplification for the general theory of thermal instability. For, it effectively ensures that conclusions reached after an examination of special geometrical situations (such as **H** and **g** are parallel) are of wider scope and generality than the geometrical restrictions under which they were arrived at would appear to warrant. Thus in the problem of the inhibition of thermal convection by rotation (Chandrasekhar 1953) the principal results were derived on the assumption that the direction of the angular velocity, $\mathbf{\Omega}$, is parallel to that of gravity, $\mathbf{g}$. One may now feel confident that the conjecture made in that context namely that if $\mathbf{\Omega}$ and $\mathbf{g}$ are not parallel, convection at marginal instability will be in the form of longitudinal rolls is a correct one. Similarly, in the discussion of the condition for overstability when $\mathbf{H}$ and $\mathbf{g}$ are acting (I, § 8) or when $\mathbf{\Omega}$ and $\mathbf{g}$ are acting (Chandrasekhar 1953, § 8) or when $\mathbf{H}$, $\mathbf{\Omega}$ and $\mathbf{g}$ are all acting (Chandrasekhar 1954) the assumption that all these vectors are parallel is not likely to be a restrictive one.

In concluding this paper I should like to acknowledge my indebtedness to Miss Donna Elbert who carried out all the very laborious numerical calculations involved in the preparation of this paper.

The research reported in this paper has in part been supported by the Geophysics Research Directorate of the Air Force Cambridge Research Center, Air Research and Development Command, under Contract AF 19(604)–299 with the University of Chicago.

References

Chandrasekhar, S., 1952, *Phil. Mag.*, **43,** 501 ; 1953, *Proc. Roy. Soc.* A, **217,** 306 ; 1954, *Ibid.*, **225,** 173.

Thompson, W. B., 1951, *Phil. Mag.*, **42,** 1417.

CXXXII. *Nuclear Orientation of* ^{54}Mn

By M. A. Grace, C. E. Johnson, N. Kurti, H. R. Lemmer
and F. N. H. Robinson
Clarendon Laboratory, Oxford*

[Received July 3, 1954]

Abstract

Orientation of ^{54}Mn at very low temperatures has been attained. The anisotropy of the 0·835 mev γ-radiation emitted in its decay shows that the first excited state of ^{54}Cr has spin 2. Detailed interpretation of the results is discussed.

Continuing our experiments on nuclear orientation in paramagnetic ions (Bleaney, Daniels, Grace, Halban, Kurti, Robinson and Simon 1954, Ambler, Grace, Halban, Kurti, Durand, Johnson and Lemmer 1953) we have investigated the 310 day isotope ^{54}Mn which decays by K-capture followed by a single γ-ray. This particular nucleus was chosen because the magnetic properties of the Mn^{++} ion in various paramagnetic crystals had been established by paramagnetic resonance experiments and, also, because orientation experiments were expected to yield further information on the spin assignments and parity changes in the decay of ^{54}Mn.

Fig. 1

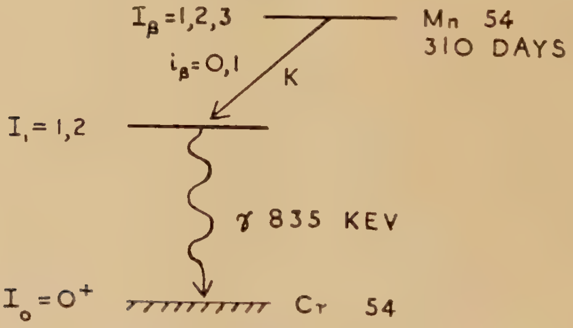

The decay scheme of ^{54}Mn.

The decay scheme for ^{54}Mn has been determined by Deutsch and Elliott (1944) and is shown in fig. 1. The energy available for the K electron capture 0·54±0·02 mev has been deduced from the Q value of $-2·162 \pm 0·005$ mev for the ^{54}Cr(p, n)^{54}Mn reaction measured by Lovington, McCue and Preston (quoted by Collins, Nier and Johnson 1952).

---

* Communicated by the Authors.

From the half-life of 310 days and using the nomogram of Moszkowski (1951) a value for $\log ft$ of 6·2 is obtained. Comparison of this figure with those tabulated by Nordheim (1951) suggests that the transition is allowed or first forbidden, involving a spin change ΔI of 0 or 1. From the existence of coincidences between K X-rays and γ-rays observed by Deutsch and Elliott (1944) the lifetime of the 0·835 MEV state of ^{54}Cr can be assumed to be 10^{-6} sec or less. Since the empirical lifetime given by Goldhaber and Sunyar (1951) for octupole transitions is of the order 10^{-3} sec and for quadrupole transitions of the order 10^{-8} sec or less it can be concluded that the transition is quadrupole or dipole.

Since ^{54}Cr is an even–even nucleus I_0 must be 0 with even parity: I_1 must, therefore, be 1 or 2 and this restricts I_β to 3, 2 or 1. Parity assignments cannot be made to either of these levels.

The three Mn^{++} salts that had been investigated by paramagnetic resonance are manganese fluosilicate, manganese ammonium sulphate and manganese bismuth nitrate (Bleaney and Ingram 1951, Trenam 1953). The resonance spectrum could be interpreted in all cases by a spin Hamiltonian

$$\mathscr{H}=g\beta\mathbf{H}\,.\,\mathbf{S}+DS_z^2+A\mathbf{S}\,.\,\mathbf{I}$$

with $S=5/2$ and $I=5/2$ (for the stable ^{55}Mn). Here DS_z^2 represents the effect of the crystalline electric field which splits the 6-fold degenerate electronic ground state into 3 doublets while $A\mathbf{S}\,.\,\mathbf{I}$ describes the magnetic hyperfine structure coupling. It so happens that in all three crystals the overall Stark splitting is of the order of 0·3°K. This means that below about 0·05°K, even in the absence of an external magnetic field, only the lowest electronic level will be appreciably populated. This lowest state is $S_z=\pm 5/2$ for the fluosilicate and the double nitrate ($D<0$) and predominantly $S_z=\pm 1/2$ for the Tutton salt ($D>0$). The magnetic hyperfine coupling is isotropic and since it is of the same order as the Stark splitting, alignment of the electron spins is accompanied by alignment of the nuclear spins.

Of these three possible salts we chose the double nitrate because it was known from previous work (Daniels and Robinson 1953), that, by incorporating cerium ions as cooling agent, temperatures of the order of 0·003°K could easily be reached by demagnetization from comparatively small fields (10 kilo gauss) at 1°. Our specimen consisted of a single crystal of $Ce_2(NO_3)_6\,.\,Mg_3(NO_3)_6\,.\,24H_2O$, with some of the Mg replaced by 20 micro Curie of ^{54}Mn which had been prepared through the ^{56}Fe(d α)^{54}Mn reaction. After demagnetization the anisotropy ϵ of the γ-radiation was observed as the sample warmed up ($\epsilon=1-I(0)/I(\pi/2)$ where $I(\theta)$ is the counting rate at an angle θ to the crystal axis).

Figure 2 shows the observed variation of ϵ with $1/T^*$. The temperature T^* calculated from Curie's law is known to be identical with the absolute temperature down to 0·006°K and deviates little down to 0·003°K. The results differ both qualitatively and quantitatively from what one would expect. The anisotropy, instead of reaching a temperature independent saturation value at low temperatures, passes through a maximum of 28% at $1/T^*=100$ and then decreases to 21% at $1/T^*=320$. The dotted line shows the anisotropy calculated theoretically using the method of Simon, Rose and Jauch (1951) assuming a nuclear gyromagnetic ratio equal to that of the stable isotope. The calculation has been carried to terms in $1/T^4$. At $1/T=20$ the last term contributes nearly 25% of the anisotropy. The agreement is poor, and by no choice of the gyromagnetic ratio is it possible to fit the experimental and theoretical curves between $1/T^*=1$ and 20. In view of the behaviour of the anisotropy at even lower temperatures we have not thought it worth while to pursue this calculation further.

Fig. 2

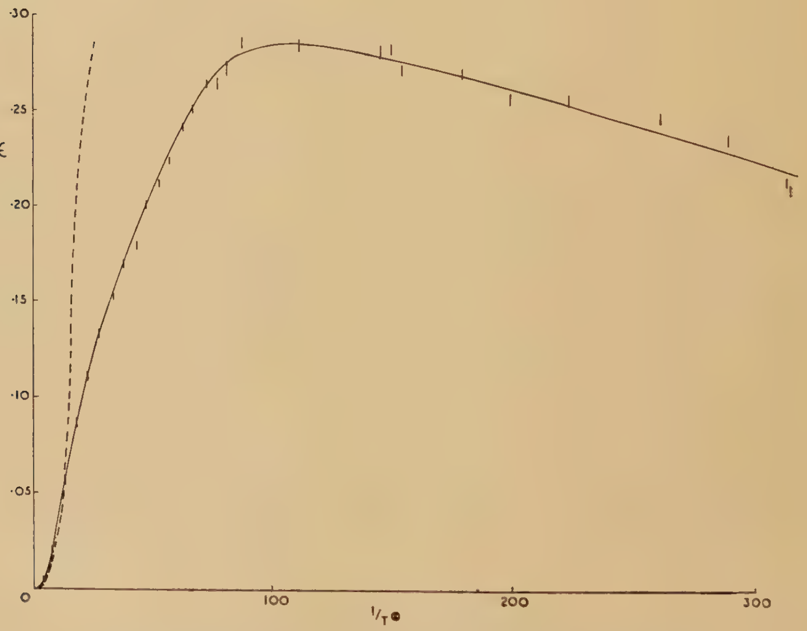

Variation of anisotropy ϵ with $1/T^*$ in zero external field.
The theoretical curve is shown as a dashed line.

The general behaviour, especially the existence of a maximum in the anisotropy, is similar to that found previously in our experiments on ^{60}Co in cobalt cerium nitrate (Ambler *et al.* 1954). It is thought to be caused by the internal field due to the cerium ions which in these crystals are very close to the divalent ions.

We decided therefore to carry out experiments using an external magnetic field of 1000 gauss parallel to the crystal axis. Such a field does not cause a prohibitively large temperature rise since the g value of the cerium ion is very anisotropic ($g_{\parallel}=0{\cdot}25$, $g_{\perp}=1{\cdot}84$) (Cooke, Duffus and

Wolf 1953). If H_i, T_i are the starting field and temperature respectively, H_f the field applied parallel to the crystal axis after demagnetization and T_f the corresponding temperature, we have approximately

$$g_{\perp}H_i/T_i = g_{\parallel}H_f/T_f,$$

e.g., with $H_i = 30$ kgauss, $T_i = 1°\mathrm{K}$, $H_f = 1$ kgauss, we have $T_f = 0{\cdot}0045°\mathrm{K}$. At the same time a field of 1000 gauss is large enough to swamp the effects of both the internal field and the crystalline field.

Fig. 3

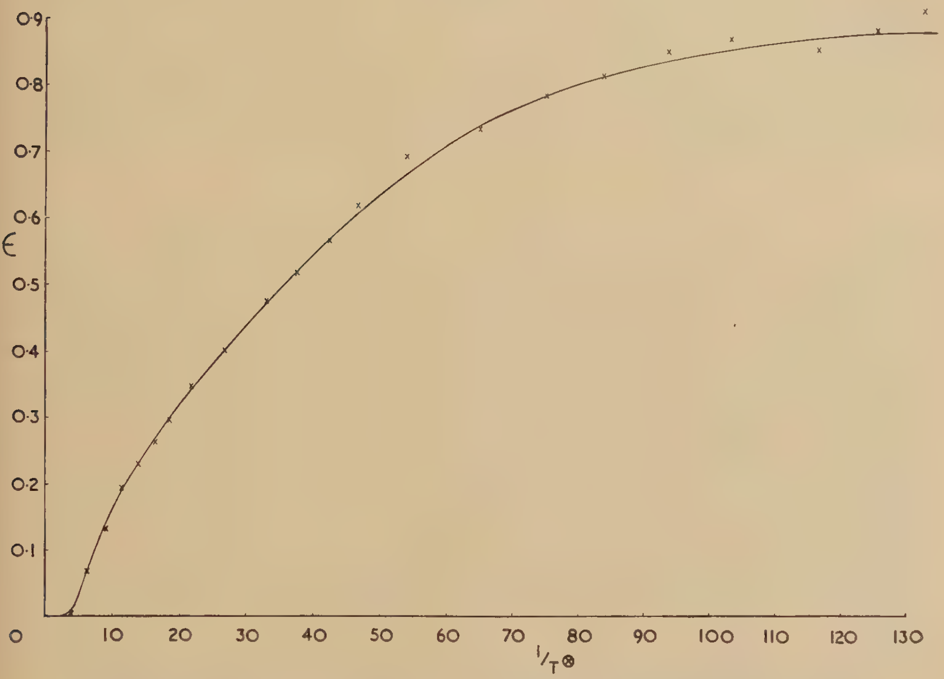

Variation of anisotropy ε with $1/T^*$ in an external field of 1000 gauss. A correction for the finite aperture of the counters has been made.

The general form of the dependence of ε on $1/T^*$ found in these magnetic h.f.s. polarization experiments is shown in fig. 3 where it is seen that anisotropies up to +90% were recorded ; this corresponds to a polarization with 95% of the nuclei in the lowest state. The sign and magnitude of this effect show that the γ-ray cannot be dipole : therefore it must be quadrupole with $I_1 = 2$. Furthermore, since the anisotropy is so large the K capture transition must carry away the minimum angular momentum compatible with the spins of the initial and final states :

$$i_\beta = I_\beta - I_1.$$

Thus if $I_\beta = 3$, $i_\beta = 1$ or if $I_\beta = 2$, $i_\beta = 0$. No other transitions can give anisotropies greater than 33%. If we assume that the anisotropy extrapolates to 100% we can conclude that ^{54}Mn has either spin 2, decaying by an allowed Fermi transition or spin 3, decaying by an allowed Gamow–Teller transition or a 1st forbidden Fermi transition. Although the experimental points of fig. 3 follow qualitatively the expected trend we could not obtain quantitative agreement with any existing theoretical curve. For this reason it is not possible to distinguish between the transitions mentioned above or to deduce a value for the magnetic moment of ^{54}Mn.

We are greatly indebted to Dr. J. M. Daniels for his generous advice and help during the early phases of this work, to Dr. H. Halban for his valuable cooperation and to Professor Sir Francis Simon for his interest and encouragement. Our grateful thanks are due to the Nuffield Cyclotron Group, Birmingham, for the irradiation of the iron target and to Dr. P. F. D. Shaw of this Laboratory for his great assistance in effecting a chemical separation of the activity.

REFERENCES

AMBLER, E., GRACE, M. A., HALBAN, H., KURTI, N., DURAND, H., JOHNSON, C. E., and LEMMER, H. R., 1953, *Phil. Mag.*, **44**, 216.
BLEANEY, B., DANIELS, J. M., GRACE, M. A., HALBAN, H., KURTI, N., ROBINSON, F. N. H., and SIMON, F. E., 1954, *Proc. Roy. Soc.* A, **221**, 170.
BLEANEY, B., and INGRAM, D. J. E., 1951, *Proc. Roy. Soc.* A, **205**, 336.
COLLINS, T. L., NIER, A. O., and JOHNSON, W. H., 1952, *Phys. Rev.*, **86**, 408.
COOKE, A. H., DUFFUS, J., and WOLF, W. P., 1953, *Phil. Mag.*, **44**, 623.
DANIELS, J. M., and ROBINSON, F. N. H., 1953, *Phil. Mag.*, **44**, 630.
DEUTSCH, M., and ELLIOTT, L. G., 1944, *Phys. Rev.*, **65**, 211.
GOLDHABER, M., and SUNYAR, A. W., 1951, *Phys. Rev.*, **83**, 906.
MOSZKOWSKI, S. A., 1951, *Phys. Rev.*, **82**, 35.
NORDHEIM, L. W., 1951, *Rev. Mod. Phys.*, **23**, 322.
SIMON, A., ROSE, M. E., and JAUCH, J. M., 1951, *Phys. Rev.*, **84**, 1155.
TRENAM, R. S., 1953, *Proc. Phys. Soc.* A, **66**, 118.

CXXXIII. *Polarized γ-Rays from Oriented* ^{54}Mn *Nuclei*

By G. R. Bishop, J. M. Daniels,* H. Durand, C. E. Johnson and J. Perez
Clarendon Laboratory, Oxford†

[Received July 3, 1954]

Abstract

The plane polarization of the γ-ray emitted in the decay of ^{54}Mn to ^{54}Cr has been measured using nuclei oriented by magnetic hyperfine structure at very low temperatures. It is found that the excited state of ^{54}Cr decays by an E2 transition, and it is furthermore concluded that this state has even parity.

In an earlier publication (Bishop, Daniels, Goldschmidt, Halban, Kurti and Robinson 1952) we have described the technique used in this laboratory to measure the plane polarization of the γ-rays emitted by oriented radioactive nuclei. The measurement of the electric or magnetic character of the radiation gives the relative parity of the nuclear states involved. We have recently measured the plane polarization of the γ-rays emitted in the decay of ^{54}Mn which we oriented by the two methods described in the preceding communication (I) (Grace, Johnson, Kurti, Lemmer and Robinson 1954).

The polarimeter was placed to receive γ-rays emitted in a direction at right angles to the single axis of orientation of the nuclei. For this direction a simple relation (Steenberg 1953) exists between the anisotropy ϵ defined in the preceding paper and the degree of plane polarization $p=(I_\sigma-I_\pi)/(I_\sigma+I_\pi)$. Here I_σ is the intensity of σ-radiation, i.e., radiation polarized with its electric vector perpendicular to the axis of nuclear orientation and I_π is the intensity of π radiation, i.e., the radiation polarized with its electric vector parallel to the axis. The measurements reported in (I) had established that the radiation was quadrupole and for this case $p=a\epsilon$, where $a=+1$ for electric and -1 for magnetic radiation. The ratio of the intensities of the σ and π radiation is therefore

$$\eta=\frac{I_\sigma}{I_\pi}=\frac{1+a\epsilon}{1-a\epsilon}$$

and the ratio of the coincidence counting rates parallel and perpendicular to the axis is

$$N_\parallel/N_\perp=(1+R\eta)/(R+\eta),$$

---

* Now at the University of British Columbia, Vancouver, B.C.

† Communicated by the Authors.

where R is the analyser efficiency ratio which may be calculated from the differential cross section for Compton Scattering and the geometry of the polarimeter.

In fig. 1 is plotted the observed ratio $N_{\parallel}/N_{\perp}$, normalized to the 'warm' rates, against $1/T^*$, the reciprocal of the magnetic temperature, for nuclei aligned by magnetic h.f.s. in the absence of an external field. Since ϵ is positive and $N_{\parallel}/N_{\perp}$ is greater than unity we see that a is positive and the radiation is electric in character.

Fig. 1

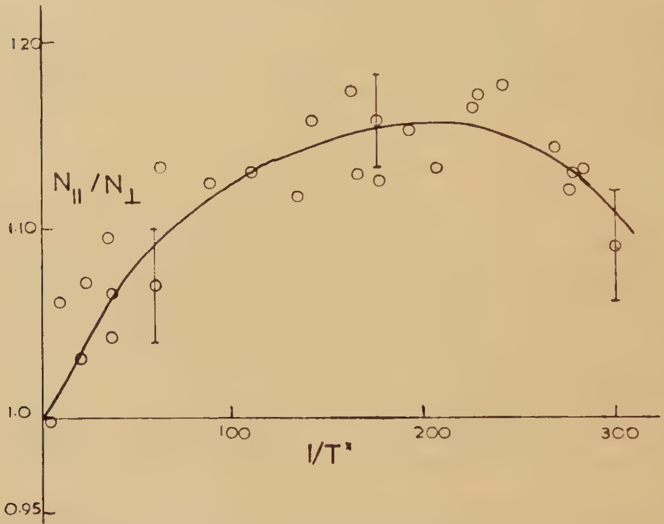

The ratio of counting rates $N_{\parallel}/N_{\perp}$ against $1/T^*$ for aligned nuclei.

In order to obtain a larger effect polarization of the ^{54}Mn nuclei was then produced by the application of a homogeneous magnetic field of 600 gauss. Owing to the restricted space between the magnetizing coils and the necessity of shielding the photo-multiplier tubes from the fringing magnetic field, the three scintillation phosphors constituting the polarimeter were placed at the end of perspex light guides. Curve A of fig. 2 shows $N_{\parallel}/N_{\perp}$ against $1/T^*$. Curve B shows the anisotropy ϵ for a magnetic field of 600 gauss. This had to be determined separately since the measurements mentioned in (I) were done with a field of 1000 gauss.

These results confirm those obtained with the aligned nuclei and prove conclusively that the excited state of ^{54}Cr decays to the ground state (even parity, spin 0) by the emission of electric quadrupole radiation. It follows that the excited state has even parity and spin 2.

We wish to thank Dr. H. Halban for his continued interest and encouragement.

Fig. 2

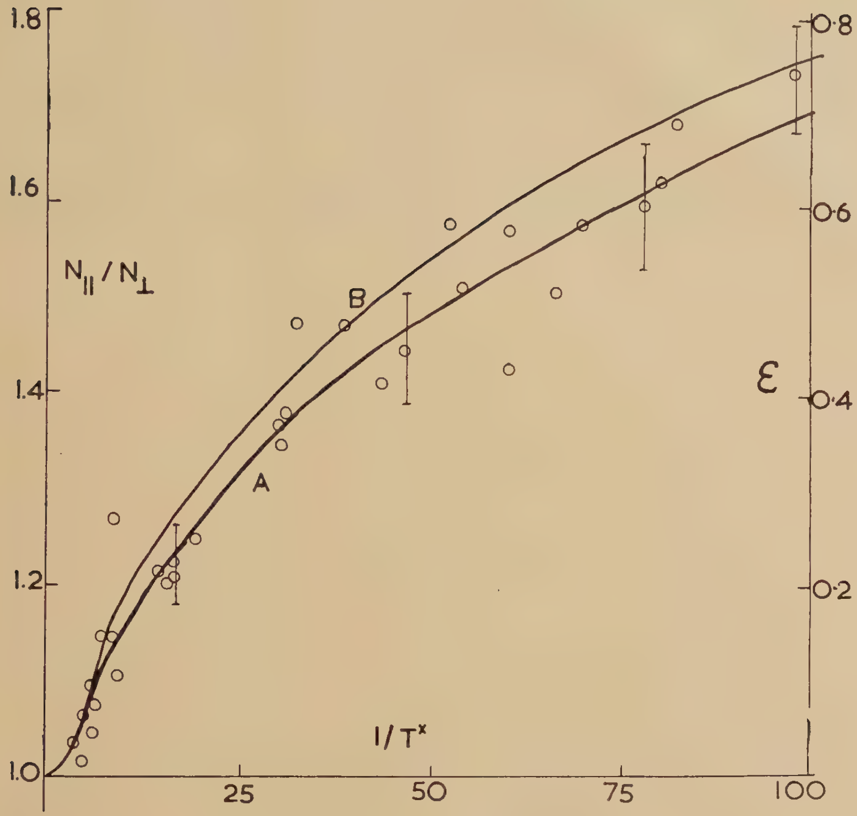

$N_{\parallel}/N_{\perp}$ (curve A) and ϵ (curve B) against $1/T^*$ for nuclei polarized by magnetic h.f.s. in a field of 600 gauss. The points refer to $N_{\parallel}/N_{\perp}$.

References

Bishop, G. R., Daniels, J. M., Goldschmidt, G., Halban, H., Kurti, N., and Robinson, F. N. H., 1952, *Phys. Rev.*, **88**, 1432.

Grace, M. A., Johnson, C. E., Kurti, N., Lemmer, H. R., and Robinson, F. N. H., 1954, *Phil. Mag.*, **54**, 1192.

Steenberg, N. R., 1953, *Proc. Phys. Soc.* A, **66**, 391.

CXXXIV. *Interaction of* 19 MeV *Deuterons with Carbon*

By R. G. Freemantle,* W. M. Gibson † and J. Rotblat ‡

[Received September 3, 1954]

The 19 MeV deuteron beam from the Birmingham cyclotron was used in a study of the nuclear reactions taking place at the bombardment of

Fig. 1

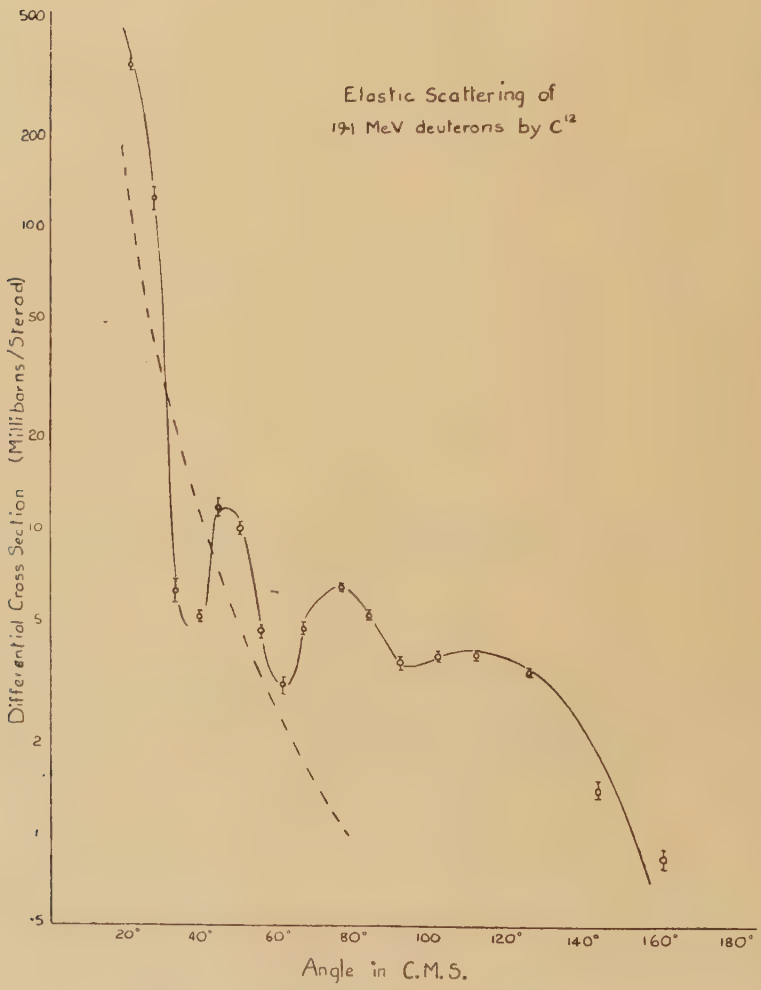

---

* University of Birmingham.
† The Queen's University of Belfast.
‡ St. Bartholomew's Hospital Medical College, London.
Communicated by the Authors.

carbon. The scattering camera described by Burrows, Powell and Rotblat (1951) was used, after slight modification. The target was acetylene gas at a pressure of 29·3 cm; the charged products of the reactions were recorded in photographic plates (Ilford C2, 400 microns thick).

Range experiments were carried out at a number of angles of emission of the particles. Histograms plotted for each angle showed the presence of a number of groups of particles, most of which could be identified from the measurement of the energy and its variation with angle. Apart from the group of protons due to the scattering by hydrogen, several other proton groups were identified as originating from the $^{12}C(d, p)$ reaction and corresponding to different energy states of ^{13}C. Three deuteron groups were identified: the elastic group, and two inelastic groups corresponding to the energy levels of ^{12}C at 4·43 and 9·61 MeV. No trace was found of the level reported at 7·5 or 7·68 MeV, which has been observed in

Fig. 2

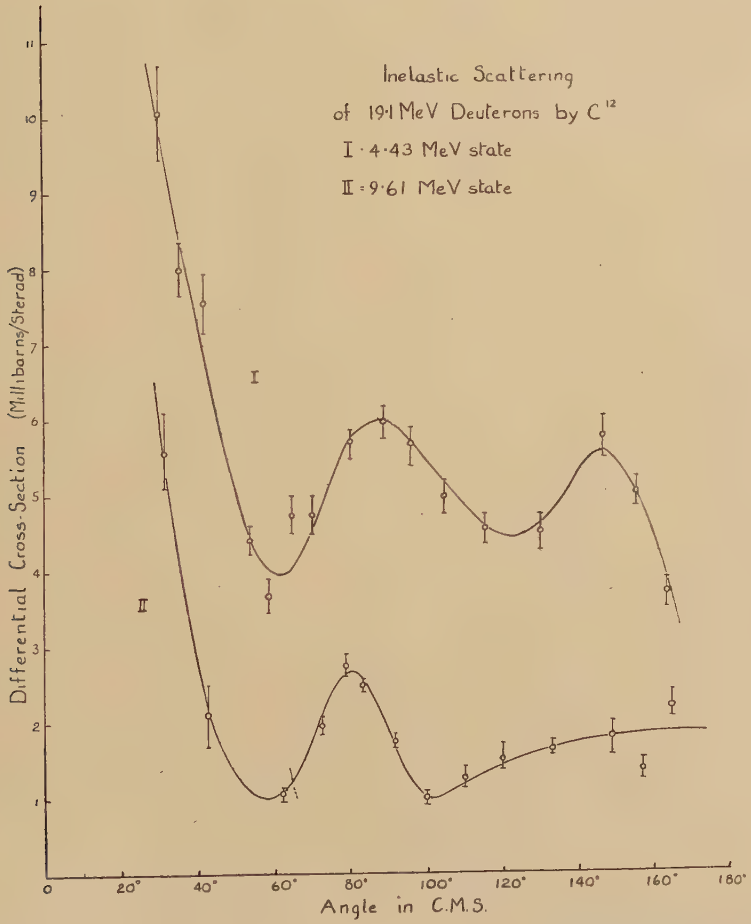

several reactions, i.e. ^{9}Be(α, n) (Guier *et al.* 1952) and ^{14}N(d, α) (Holloway and Moore 1940, Dunbar *et al.* 1953, Prowse 1954). The absence of this level in d, d scattering cannot be due to a selection rule for the isotopic spin, as the lowest level of ^{12}C with $T=1$ must lie much higher ; the fact that no sign of this level could be found must therefore be due to a different cause.

Fig. 3

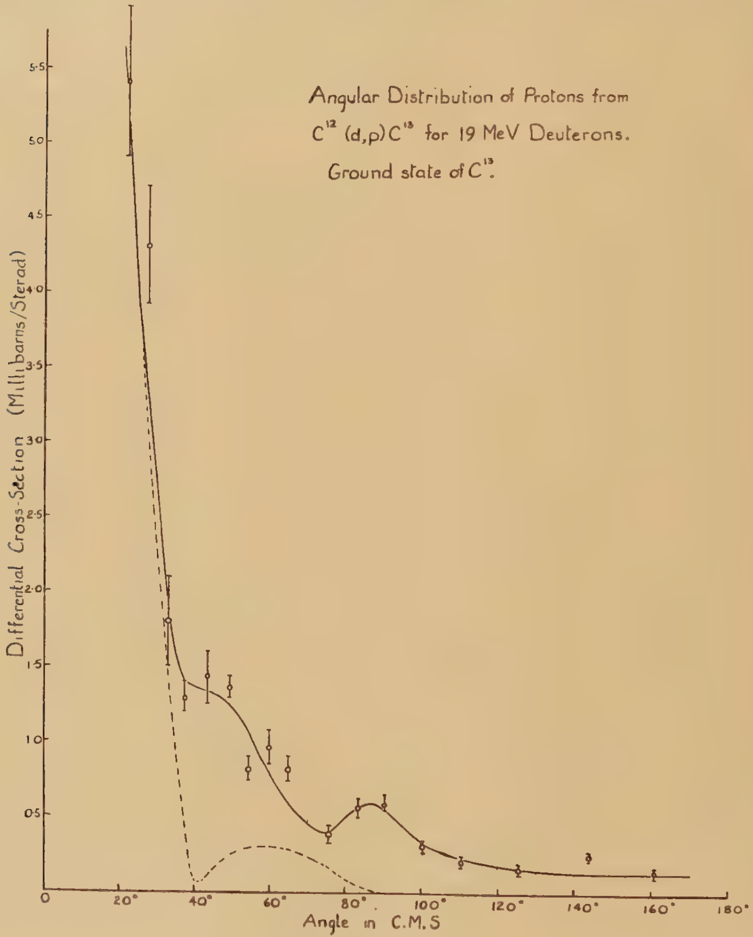

The angular distributions in the centre of mass system for the three groups of deuterons are shown in figs. 1 and 2 ; the ordinates give the differential cross section in millibarns per sterad. The errors indicated are statistical only, other relative errors are quite small. The absolute cross section may be too low by about 5% because of a possible systematic error in the beam integrating system. Figure 1 contains also the curve for Rutherford scattering. No analysis of these distributions has so far been carried out.

Figures 3 and 4 give the differential cross sections for the protons from the $^{12}C(d, p)$ reaction corresponding to ^{13}C being formed in the ground state, and in the 3·08 and 3·89 MeV states respectively. The latter group

Fig. 4

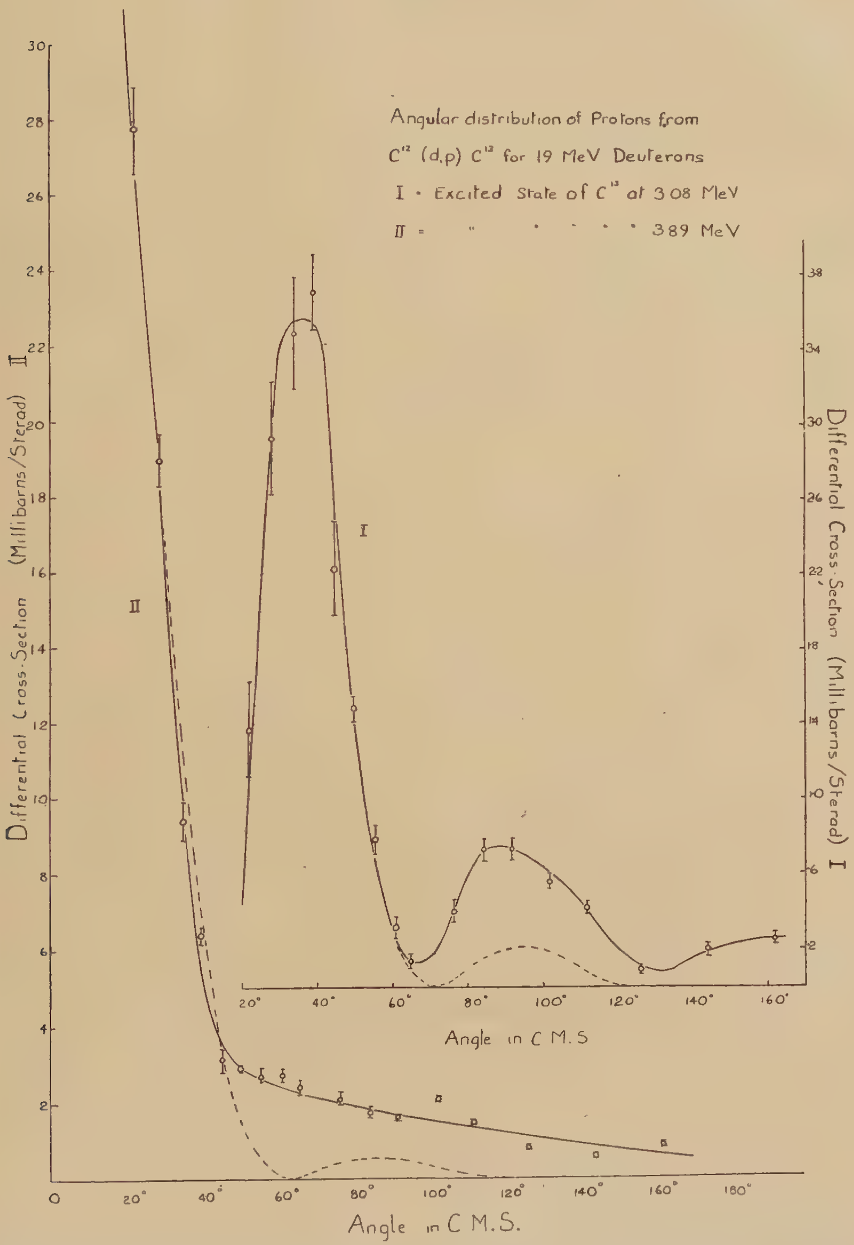

contains some protons from the 3·68 MeV state which was not resolved. These angular distributions are qualitatively similar to those observed with an 8 MEV deuteron beam (Rotblat 1951). An analysis of these curves, according to Butler's stripping theory and assuming a value $r_0=4\cdot5\times10^{-13}$ cm, was carried out by Mr. W. M. Fairbairn. The dashed curves in figs. 3 and 4 are the normalized curves calculated for $l_n=1$, 0 and 2 for the three states respectively. As is seen, the agreement is very good for the excited states, confirming the assignment of even parities and spin values of 1/2 to the 3·08 MEV state and 3/2 or 5/2 to the 3·89 MEV state. In the case of the ground state, however, the agreement is very poor, and experimental points at smaller angles would be necessary to confirm from this experiment the assignment of $l_n=1$ for the transition to this state.

REFERENCES

BURROWS, H. B., POWELL, C. F., and ROTBLAT, J., 1951, *Proc. Roy. Soc.*, **209**, 461.
DUNBAR, D. N. F., PIXLEY, R. E., WENZEL, W. A., and WHALING, W., 1953, *Phys. Rev.*, **92**, 649.
GUIER, W. H., BERTINE, H. W., and ROBERTS, J. H., 1952, *Phys. Rev.*, **85**, 426.
HOLLOWAY, M. G., and MOORE, B. L., 1940, *Phys. Rev.*, **58**, 847.
PROWSE, D. J., 1954, *Ph.D. Thesis* (Bristol).
ROTBLAT, J., 1951 a, *Nature, Lond.*, **167**, 1027; 1951 b, *Phys. Rev.*, **83**, 1271.

CXXXV. *Angular Distribution of Neutrons from the Reaction* ^{11}B(d, n)^{12}C *at* 0·85 MEV *Bombarding Energy*

By ARNFINN GRAUE
Fysisk Institutt, Norway *

[Revised MS. received August 19, 1954]

SUMMARY

Angular distributions and energy spectra of neutrons from ^{11}B(d, n)^{12}C have been measured at 0·85 MEV bombarding energy, using the photographic plate technique. Energy levels in ^{12}C are found at 4·4, 7·7, 9·6 and 12·7 MEV. The stripping process is suggested to be responsible for a large part of the neutron yield. The orbital angular momentum of the captured proton has been determined as $l_p=1$ and 2 for the 4·4 MEV and 9·6 MEV level respectively.

§ 1. INTRODUCTION

SEVERAL experiments have confirmed the existence of levels in ^{12}C at 4·4, 7·5 and 9·6 MEV. The ^{11}B(d, n)^{12}C reaction has been studied by Johnson (1952) and Gibson (1949). Johnson failed to observe the 7·5 MEV level whereas Gibson from his data concluded that this level could be confirmed less certainly than the 4·4 and 9·6 MEV levels.

Spin and parity assignments have been made only for the ground state and the 4·4 MEV level. Gibson (1953) has measured the angular distributions of neutrons leaving ^{12}C in its ground state and in its first excited state at a deuteron energy $E_d=8·1$ MEV. In both cases he found agreement with Butler's stripping theory (Butler 1951) for $l_p=1$.

Investigations regarding the competition between stripping and compound nucleus formation can be done at smaller bombarding energies. Burke *et al.* (1954) have measured the angular distribution of neutrons emitted in the ^{11}B(d, n)^{12}C reaction at bombarding energies 0·71, 1·06 and 1·43 MEV. The distribution curves had peaks in the forward direction. As, however, neutron groups of all energies were counted, further experiments with energy discrimination are desired. For the present measurements of the angular distributions of neutrons from ^{11}B(d, n)^{12}C the photographic plate technique has been used. At the moment this method seems to be the best one available for investigations of the more complicated neutron spectra.

§ 2. EXPERIMENTAL CONDITIONS

The deuterons were accelerated in the Van de Graaff generator at the University of Bergen. The target used was a separated ^{11}B target obtained from Dr. J. Koch, Institute of Theoretical Physics, Copenhagen. The target-thickness was approximately 25 kev for 0·85 Mev deuterons. Ilford C2 Nuclear Research Plates with emulsion thickness 200 μ were used. The plates received the neutrons at grazing incidence. They were arranged in such a way that they covered the range of the angle θ from 0°–160°, θ being the angle between deuteron and neutron directions. The distance between target and the scanned areas was 125–135 mm, the same for all angles θ. The total deuteron charge on the target was 100 μA-hours, which gave a suitable density of recoil-proton tracks in the emulsions. The methods for measurement and calculation of the neutron energy and the angular distribution have been described by many workers in previous papers (e.g. Trumpy *et al.* 1952 and 1953).

---

* Communicated by the Author.

Fig. 1

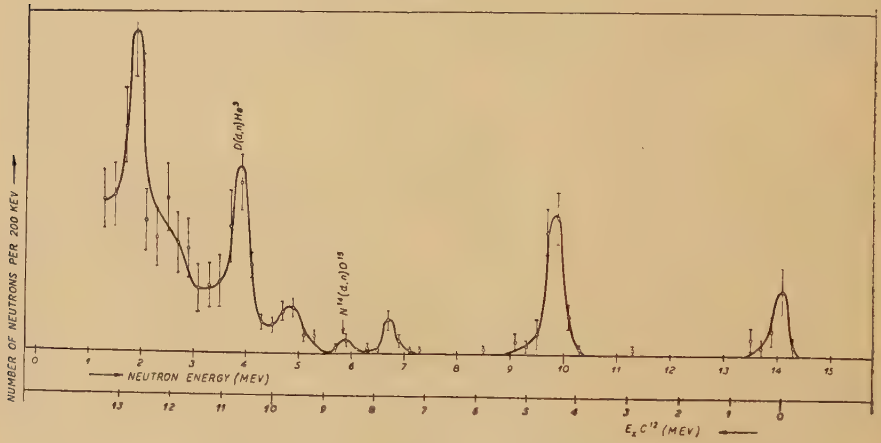

0° neutron spectrum from the $^{11}B(d, n)^{12}C$ reaction.

§ 3. The Neutron Energy Spectra

Neutron energy spectra have been measured at the following angles θ: 0°, 15°, 30°, 45°, 75°, 105°, 120°, 135° and 155°. A total of about 6000 tracks have been measured. Figure 1 shows one of these spectra. This spectrum is corrected for the variation with energy of the neutron–proton scattering cross section and for the escape of protons from the emulsion. The errors indicated are statistical errors only. Because of the lower intensity of the higher energy neutron groups, a greater area was scanned for measurements of these neutrons. This is the reason for the discontinuity in the statistical errors.

All the peaks shown in the spectrum correspond to levels in ^{12}C except those marked otherwise. In the lower part of the observed spectrum homogenous groups from $^{11}B(d, n)^{12}C$ reaction are superimposed upon the continuous spectrum from $^{11}B(d, n)3\alpha$ reaction.

All the neutron spectra have a high energy group corresponding to ^{12}C in its ground state. In accordance with previous measurements they also demonstrate the existence of energy levels in ^{12}C at 4·43, 9·67 and 12·67 MeV. The neutron spectra also indicate a level in ^{12}C at 7·67 MeV. This level was found at all angles. The existence of this neutron group has been less certain in previous measurements (Gibson 1949) on the $^{11}B(d, n)^{12}C$ reaction. It is, however, clearly resolved in fig. 1. The group can not be due to any contamination of the target because no conceivable contaminant gives rise to a neutron group of this energy. The only contamination groups observed in the spectra are from the $D(d, n)^3He$ and the $^{14}N(d, n)^{15}O$ reactions. Both D and ^{14}N have previously been observed to be picked up from the vacuum system during exposure (Enge 1952).

§ 4. ANGULAR DISTRIBUTION OF THE NEUTRONS

No theory for the angular distribution of the neutrons at low deuteron bombarding energies has so far been published. For energies higher than the Coulomb-barrier there are theories based on the stripping process. These theories, which predict a maximum in a forward direction, have also been successfully applied for deuteron energies lower than the Coulomb-barrier. However, in this region it is expected that compound nucleus formation also contributes appreciably to the reaction yield. Wolfenstein's theory (Wolfenstein 1951) for compound nucleus formation predicts a distribution symmetrical about 90° in the centre of mass system, and generally with maxima in the forward and backward directions.

Angular distributions of the neutron groups corresponding to the ground state, 4·4 MeV and 9·6 MeV levels are shown in fig. 2. Considering first the reaction forming ^{12}C in its ground state (fig. 2 (*a*)), we find a maximum in the forward direction. Such a distribution is characteristic for the stripping process, and theoretical curves were calculated, using the stripping theory in the form given by Bhatia *et al.* (1952). Two curves are plotted corresponding to l-values of the captured proton of 1 and 2. The nuclear radius used in the calculations was $R=6·4\times10^{-13}$ cm computed from the expression $R=(3·7+1·22\times A^{1/3})\times10^{-13}$ cm used by Bhatia *et al.* There is no good agreement between the experimental distribution and any of the theoretical curves. The l-value of the captured proton, however, is known from previous measurements at 8·1 MeV deuteron energy to be $l_p=1$ (Gibson 1953). Butler has reported some preliminary results about the influences of Coulomb forces on the deuteron stripping cross section (Butler 1954). He then finds that the maximum in the angular distribution curve is somewhat displaced towards larger angles. This would may be give a better agreement between the experimental results and a theoretical $l_p=1$ curve.

The reaction forming ^{12}C in its 4·4 MeV excited state also shows a distribution with a maximum in the forward direction (fig. 2 (*b*)). The curve with $l_p=1$ gives the best fit which is in accordance with Gibson's results at $E_d=8·1$ MeV. Since the ground state of ^{11}B has spin 3/2, and odd parity, the 4·4 MeV excited state of ^{12}C must have even parity and spin 0, 1, 2 or 3. The spin of this state is known to be 2 (Ajzenberg and Lauritsen 1952).

No parity assignment of the 9·6 MeV excited level of ^{12}C has so far been given. The distribution in fig. 2 (*c*) shows a minimum at 0° and a maximum at 80°. If the stripping process is responsible for this distribution the calculated curves show that protons with $l_p=2$ are captured. This leads to the results that the 9·6 MeV excited level of ^{12}C has odd parity and spin 0, 1, 2, 3 or 4.

Fig. 2

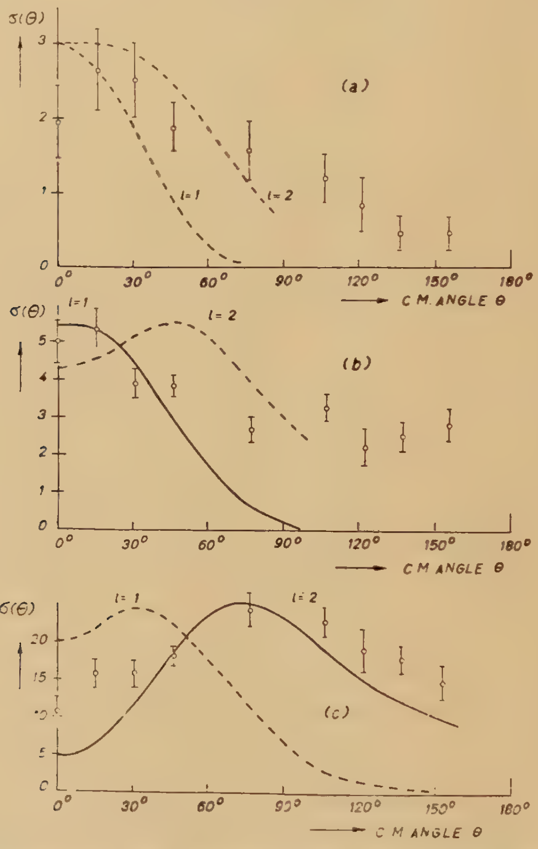

Angular distributions of the neutrons from the ^{11}B(d, n)^{12}C reaction and theoretical curves calculated from the stripping theory in the form given by Bhatia *et al.* (1952) for angular momentum transfers of 1 and 2. (*a*) ^{12}C formed in its ground state, (*b*) ^{12}C formed in the 4·4 MeV excited state, (*c*) ^{12}C formed in the 9·6 MeV excited state.

Because of the low intensity of the neutron group corresponding to the 7·7 MeV level of ^{12}C, the statistical errors in the experimental angular distribution for these neutrons are large. It can be stated, however, that the deviation from spherical symmetry in the centre of mass system is not more than 25%.

The agreement between the experimental curves and those calculated from the stripping theory is quite good for the 4·4 and 9·6 MeV levels. This is surprising because the theory takes no account of the Coulomb effects, and since contributions from the compound nucleus formation are expected. At large angles one should not expect the experimental and theoretical curves to agree.

The problem regarding the relative importance of the stripping process and the compound nucleus formation can only be solved on the basis of further experimental investigations and a theory for the stripping process valid also for low deuteron energies.

ACKNOWLEDGMENTS

The author wishes to express his best thanks to Professor B. Trumpy for proposing this work and to him, Mr. H. A. Enge and Mr. T. Grotdal for advice and assistance, to Dr. J. Koch for providing the separated ^{11}B target, to Mr. O. Tvedten for much of the microscope work and to Det Videnskapelige Forskningsfond av 1919 for valuable financial support to this work.

REFERENCES

AJZENBERG, F., and LAURITSEN, T., 1952, *Rev. Mod. Phys.*, **24,** 321.
BHATIA, A. B., KUN HUANG, HUBY, R., and NEWNS, H. C., 1952, *Phil. Mag.*, **43,** 485.
BUTLER, S. T., 1951, *Proc. Roy. Soc.* A, **208,** 559.
BUTLER, S. T., and AUSTERN, N., 1954, *Phys. Rev.*, **93,** 355.
BURKE, W. H., RISSER, J. R., and PHILLIPS, G. C., 1954, *Phys. Rev.*, **93,** 188.
ENGE, H. A., BUECHNER, W. W., and SPERDUTO, A., 1952, *Phys. Rev.*, **88,** 963.
GIBSON, W. M., 1949, *Proc. Phys. Soc.* A, **62,** 586 ; 1953, *Phil. Mag.*, **44,** 297.
JOHNSON, V. R., 1952, *Phys. Rev.*, **86,** 302.
TRUMPY, B., GROTDAL, T., and GRAUE, A., 1952, *Nature, Lond.*, **170,** 1118 ; 1953, *Universitetet i Bergen, Årbok* 1953, nr. 8.
WOLFENSTEIN, L., 1951, *Phys. Rev.*, **82,** 690.

CXXXVI. CORRESPONDENCE

On the Acceleration of Cosmic Ray Particles

By W. B. Thompson
Atomic Energy Research Establishment, Harwell*

[Received July 21, 1954]

A mechanism which seems capable of accelerating particles to cosmic ray energies has been proposed by Fermi (1949), and has recently been extended by Fermi, and by Morrison, Olbert and Rossi. Energetic charged particles are elastically scattered by magnetized clouds of partially ionized gas in interstellar space, and since head-on collisions are slightly more frequent than those in which the particle overtakes the cloud, a particle experiences a gradual increase in energy at a rate

$$\frac{1}{E}\frac{dE}{dt}\sim r\left(\frac{v}{c}\right)^2.$$

where v is the mean velocity of the gas clouds, c the velocity of light, E the energy of the charged particle, assumed relativistic, and r the rate at which the particle is scattered.

If particles have life-times which are distributed exponentially about a mean, this theory predicts the correct power law for the cosmic ray energy spectrum, the exponent in this fixing a relation between the mean life and the rate of energy increase. The mean life is determined by the presence of heavy nuclei in the primary cosmic rays, which implies that the time available for acceleration cannot be much greater than the average time between nuclear collisions involving cosmic ray particles, which is of order 10^7 years. Since the velocity of magnetized clouds v can be associated with the observed turbulent velocities of interstellar matter, about 30 km/sec, the theory determines a relation between the maximum energy for which the power law spectrum holds and the frequency of collisions between particles and clouds. Morrison, Olbert and Rossi conclude that the extension of the power law spectrum to 10^{15} ev implies scattering centres about a light year apart, an uncomfortably small separation. Recent air shower experiments (e.g. Cranshaw and Galbraith) have shown that the power law spectrum holds for energies of 10^{16} ev ; hence some more efficient accelerating mechanism must be found.

Fortunately such a mechanism is concealed in the Fermi theory. In the irregular magnetic field one expects to find fluctuations varying in diameter from several light years to small fractions of a light year ; and, while the small scale fluctuations by themselves do not seem sufficient to accelerate particles, they enable the large scale clouds to operate much

---

* Communicated by the Author.

more effectively. The scattering by these small irregularities changes the paths of the energetic particles from regular spirals to irregular diffusive tracks, and a particle undergoing such a motion can gain energy from a large scale fluctuation without being reflected. If, as a model of a large disturbance, we consider a region in which the field changes rather rapidly by an amount δH, remains constant for some space, then returns to its original value, one can approximate the solutions to the equations of motion by expanding in powers of $\delta H/H$. The first term in this expansion is enough to describe the reflections proposed by Fermi; while the second has associated with it an energy increase at a rate

$$\frac{1}{E}\frac{dE}{dt} \simeq Kr\left|\frac{v}{c}\right|\left(\frac{\delta H}{H}\right)^2,$$

where the constant K depends on the details of the model, and for a uniform distribution of particle velocities, and linearly varying fields is 9/4. Since $\delta H/H$, while assumed small, can easily be 10%, this acceleration rate may easily be 100 times that given by Fermi. This mechanism gives importance to relatively small variations in field strength, and more recent pictures of the galactic magnetic field (Chandrasekhar and Fermi 1953 a, b) suggest that the field is somewhat more uniform than had previously been supposed. If the galactic field has the regularity ascribed to it, and if the acceleration process described here is operative, it is possible to extend the theoretical range of the power law spectrum to about 10^{18} ev, but it is difficult to see how it can hold for much greater energies.

REFERENCES

CRANSHAW, T., and GALBRAITH, W., 1954, *Phil. Mag.* (to be published).
FERMI, E., 1949, *Phys. Rev.*, **75,** 1169; 1954, *Ap. J.*, **119,** 1.
FERMI, E., and CHANDRASEKHAR, S., 1953 a, *Ap. J.*, **118,** 113; 1953 b, *Ibid.*, **118,** 116.
MORRISON, P., OLBERT, S., and ROSSI, B., 1954, *Phys. Rev.*, **94,** 440.

On the Evaluation of Characteristic Temperatures for Cubic Crystals

By A. B. BHATIA and G. E. TAUBER
Division of Physics, National Research Council, Ottawa*

[Received June 21, 1954]

THE calculation of the Debye characteristic temperature Θ_D involves the evaluation of the integral

$$I=\int[\sum_i\{v_i(\theta,\phi)\}^{-3}]\,d\Omega, \quad . \quad . \quad . \quad . \quad . \quad . \quad . \quad . \quad (1)$$

---

* Communicated by the National Research Council, Ottawa.

where $v_i\ (\theta, \phi)$ $(i=1, 2, 3)$ are the velocities of the three elastic waves for a given direction (θ, ϕ) of propagation and integration is over all directions of propagation. In terms of elastic constants the v_i are given by the well-known Christoffel's equations of elasticity theory. Θ_D and I are related by the equation

$$\Theta_D=\frac{h}{k}\left(\frac{9s}{\Delta}\right)^{1/3}(I)^{-1/3}, \quad . \quad . \quad . \quad . \quad . \quad . \quad . \quad . \quad (2)$$

in which Δ is the cell-volume, s the number of atoms per cell, and other symbols have their usual meaning.

For elastically anisotropic crystals $[\eta=2c_{44}(c_{11}-c_{12})^{-1}\neq 1]$ I may either be evaluated numerically or by the Hopf–Lechner (1914) method ; both involve lengthy calculations. Recently Blackman (1951) has obtained a semi-theoretical formula for I valid for η sufficiently greater than unity. One of the constants occurring in this formula was fixed by fitting the value of Θ_D (obtained numerically) for Li.

The purpose of this note is to obtain an approximate formula for I in the following manner : since the integrand in (1) is invariant under the operations of the cubic symmetry group, we may expand it in terms of the appropriate *Kubic Harmonics* K_m introduced by Von der Lage and Bethe (1947).† Thus

$$I=\int\Big[\sum_{m=0}^{\infty}\alpha_m K_m\Big]\,d\Omega=4\pi\alpha_0. \quad . \quad . \quad . \quad . \quad . \quad . \quad . \quad . \quad (3)$$

The first three lowest order Kubic Harmonics, apart from normalization factors, are $(x^2+y^2+z^2=1)$

$$\left.\begin{array}{ll} & K_0=1, \qquad K_1=(x^4+y^4+z^4-\tfrac{3}{5}), \\ \text{and} & K_2=x^2y^2z^2+\tfrac{1}{22}K_1-\tfrac{1}{105}. \end{array}\right\} \quad . \quad . \quad . \quad . \quad . \quad (4)$$

Now if one assumes that the first three terms in the integrand of (3) give a reasonable approximation for (1), one may determine α_0, α_1 and α_2 analytically since for three directions in a cubic crystal, viz. (100), (110) and (111), the v_i can be easily obtained in terms of the elastic constants. This procedure gives for I the expression

$$\begin{aligned} I=\tfrac{4\pi}{35}[10c_{11}{}^{-3/2}&+16(c_{11}-\tfrac{1}{2}\epsilon)^{-3/2}+16(c_{44}+\tfrac{1}{2}\epsilon)^{-3/2} \\ &+9(c_{11}-\tfrac{2}{3}\epsilon)^{-3/2}+18(c_{44}+\tfrac{1}{3}\epsilon)^{-3/2}+36c_{44}{}^{-3/2}], \quad . \quad . \quad . \quad (5) \end{aligned}$$

with $\epsilon=c_{11}-c_{12}-2c_{44}$.

With the help of (5) and (2) we have evaluated Θ_D for several crystals. The results are given in table 1. Θ_D values calculated by other methods are also included. Since according to Blackman (1951) the latter estimates may be in error by several per cent, the Θ-values calculated here seem reasonable.

---

† It ought to be mentioned that the present method has been previously employed by W. V. Houston (1948, *Rev. Mod. Phys.*, **20,** 162), to obtain an approximate form for the frequency spectrum of crystals.

It should be noticed that (5) would be nearer to the correct value of (1), the closer η is to unity. A glance at the table shows that the formulae

	Li	Na	K	Cu	Ag	Au	Al	KCl	NaCl
$\Theta_D(P)$*	324	128	71	329	220	165	405	239·5	311
$\Theta_D(O)$	354	144	77	342	212	158	394	227	305
$\Theta_D(B)$	351	147	82	355	203	160	400	—	—
$\eta=\dfrac{2c_{44}}{c_{11}-c_{12}}$	7·8	8·2	8·4	3·2	2·9	2·9	1·2	0·52	0·74

* $\Theta_D(P)$=present calculation ; $\Theta_D(B)$=Blackman's values (loc. cit.) ; $\Theta_D(O)$=other calculations.

given here are approximately valid over a wide range of values of η. The accuracy in any particular case can of course only be estimated by calculating the influence of the next higher harmonic on α_0.

The authors are grateful to Mr. D. Patterson for many helpful discussions and to Miss C. de Chantigny for help with the numerical work.

References

Blackman, M., 1951, *Phil. Mag.*, **42,** 1441.
Hopf, L., and Lechner, G., 1914, *Verh. Deutsch. Phys. Ges.*, **16,** 643.
von der Lage, F. C., and Bethe, H. A., 1947, *Phys. Rev.*, **71,** 612.

The Elastic Scattering of Protons by Fluorine

By G. Dearnaley
Cavendish Laboratory, Cambridge

[Received August 20, 1954]

The differential elastic scattering cross section of fluorine for protons has been measured at four angles, with bombarding energies from 0·5 to 2·1 Mev. Anomalies were observed corresponding to the resonances in $^{19}F+p$ at 669, 831, 874, 935, 1355, 1381, 1431, 1690, 1940, and 2030 kev.

A beam of protons, monoenergetic to 1 kev and defined to 2 mm by 3 mm was provided by the Cavendish electrostatic generator. The target was 3 kev thick lithium fluoride evaporated on to a film of carbon a few hundred ångströms thick, made by the technique due to Bradley (1954). The scattered protons were analysed by a rotatable magnet analyser, and detected with a proportional counter ; protons scattered from ^{19}F, ^{12}C, ^{7}Li and ^{6}Li in the target were well resolved. The scattering angles chosen were those for which the respective Legendre polynomials of the angle in the centre-of-mass system are zero, i.e. 90°, 125·3°, 140·8°, 159·8°, since an anomaly due to resonance scattering of protons of angular momentum l disappears at an angle for which $P^{\circ}_{l}=0$. A Geiger counter detected gamma-rays from the target, and provided a voltage calibration of the generator. Monitoring was by integration of the beam current, after D.C. amplification.

Fig. 1

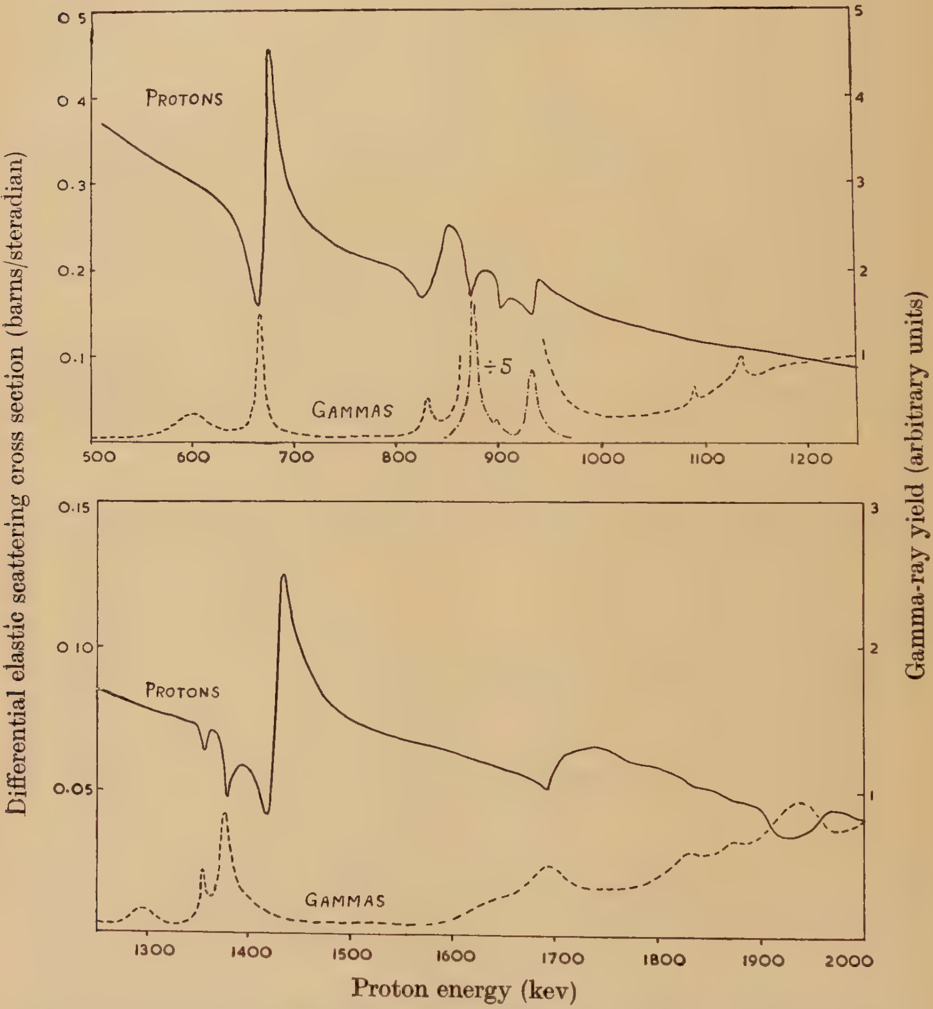

The ^{19}F(p, p) elastic cross section, at 140·8° in C.M. system, and gamma-ray excitation function.

Figure 1 shows the elastic scattering cross section curve obtained at 141°, together with the gamma-ray excitation function. The relative accuracy of the points on the curve is around 2%; the absolute cross section, obtained by comparison with ^{7}Li (Warters *et al.* 1953) is probably accurate to 10%.

Detailed analysis of the results is in progress, but certain features of the levels in ^{20}Ne are apparent. Thus, in the resonances for the reaction ^{19}F(p, $\alpha\gamma$)^{20}Ne, the alpha-particle yield (Chao 1950) gives a value for the ratio of proton to alpha partial widths, but does not indicate which is the larger. The marked scattering anomaly at 669 kev has been fitted, taking a value of proton partial width, Γ_p, equal to the total resonance width Γ which is 7·5 kev. The gamma-ray width is negligible. The alpha particle yield shows that $\Gamma_p=0{\cdot}98\Gamma$ or $0{\cdot}02\Gamma$, and so the present evidence leads to the conclusion that the proton width is larger, and some fifty times the alpha width. However, at the 935 kev resonance, which is also known to be (1, +) (Seed and French 1952), the scattering curve cannot be fitted by $\Gamma_p=\Gamma$, the observed anomaly being quite small. For this resonance, $\Gamma_p=0{\cdot}9\Gamma$ or $0{\cdot}1\Gamma$, and it therefore appears that the proton width takes the smaller value. The 669 kev level also differs from the other (1, +) resonances, at 340, 935 kev, in that some 2% of the transitions from it occur by gamma emission to the first excited level of ^{20}Ne (Devons and Hereward 1948, Rae *et al.* 1950, Carver and Wilkinson 1951).

Sinclair (1954) has observed three other resonances for the reaction ^{19}F(p, γ)^{20}Ne at 1092, 1324, and 1431 kev. The first corresponds to a resonance in ^{19}F(p, $\alpha\gamma$)^{16}O, whereas the last two do not. No appreciable variations in the proton scattering cross section occur at the first two of these levels, but at the third there is a large isotropic anomaly. The 1431 kev level is therefore formed by s-wave protons, allowing assignment (0, +) or (1, +), but not (0, −) as suggested by Sinclair. No alpha emission to levels in ^{16}O with even spin and parity are observed from this level (Chao 1950), so that it is probably (1, +).

For the levels formed at 874, 1355 and 1381 kev, the anomalies disappear at 90° and become more marked as the scattering angle increases, showing formation by p-wave protons. This agrees with the assignments, (2, −) for the 874 kev level (Seed and French 1952) and 1381 kev level (Sanders 1953). The spins and parities of the 1355 and 1381 kev levels deduced tentatively by Chao (1950) from the gamma-ray distribution and quoted by Ajzenberg and Lauritsen (1952) are incorrect. As (p, $\alpha\gamma$) transitions to levels in ^{16}O with odd spin and even parity occur from the 1355 kev level, the assignment must be (2, −). The small size of the 874 kev scattering anomaly in relation to the resonance cross section and width supports the argument of Wilkinson (1935) based on the radiative width, that the proton width is small. Similarly, at 598 kev, no appreciable anomaly occurs, though the resonance cross section is high, again indicating that Γ_p takes the smaller of the two possible values.

It remains unexplained why, of the four (1, +) levels at 340, 699, 935 and 1431 kev, two decay by alpha-emission, one by gamma-emission alone, and one by both processes.

I am indebted to Dr. A. P. French for suggesting this problem, to Mr. E. S. Shire for permitting the use of the electrostatic generator, and to the Department of Scientific and Industrial Research for a grant.

REFERENCES

AJZENBERG, F., and LAURITSEN, T., 1952, *Rev. Mod. Phys.*, **24**, 321.
BRADLEY, D. E., 1954, *Brit. Jour. App. Phys.*, **5**, 65.
CARVER, J. H., and WILKINSON, D. H., 1951, *Proc. Phys. Soc.* A, **64**, 199.
CHAO, C. Y., TOLLESTROP, A. V., FOWLER, W. A., and LAURITSEN, C. C., 1950, *Phys. Rev.*, **79**, 108.
CHAO, C. Y., 1950, *Phys. Rev.*, **80**, 1035.
DEVONS, S., and HEREWARD, H. G., 1948, *Nature, Lond.*, **162**, 331.
RAE, E. R., RUTHERGLEN, J. G., and SMITH, R. D., 1950, *Proc. Phys. Soc.* A, **63**, 775.
SANDERS, J. E., 1953, *Phil. Mag.*, **44**, 1302.
SEED, J., and FRENCH, A. P., 1952, *Phys. Rev.*, **88**, 1007.
SINCLAIR, R. M., 1954, *Phys. Rev.*, **93**, 1082.
WARTERS, W. D., FOWLER, W. A., and LAURITSEN, C. C., 1953, *Phys. Rev.*, **91**, 917.
WILKINSON, D. H., and CLEGG, A. B., 1953, *Phil. Mag.*, **44**, 1322.

On the Interaction of a Dislocation and a Charged Solute Ion

By ROLF LANDAUER
Research Department, International Business Machines Corporation,
Poughkeepsie, New York

[Received August 30, 1954]

COTTRELL, HUNTER AND NABARRO (1953) have pointed out that the electric field surrounding a dislocation in copper may exert an electrical force on a polyvalent substitutional solute atom. According to Friedel (1952) it is not likely that the polyvalent solute atom contributes more than two electrons to the conduction band of the copper matrix. The electrons which are not contributed to the conduction band, have an energy below the bottom of the conduction band, and are bound to the solute atom. This still leaves the possibility of having, for example, a Zn^{++} ion in solution, screened only by conduction electrons. Now if we consider motion of the Zn^{++} ion, the screening cloud must follow the ion, and the motion does not correspond to any net charge transfer. Therefore, there are no purely electrostatic energy changes, and consequently no net electrostatic forces. Cottrell, Hunter and Nabarro have only taken that part of the screening cloud which lies within the cell of the Zn^{++} ion as being effectively tied to the Zn^{++} ion in its motion, but it is not clear why this arbitrary cut-off can be introduced.

It should perhaps be pointed out that there is a great deal of evidence (Schwarz 1940) that an electric field in a conductor can move solute ions, despite the presence of screening electrons. However, this evidence deals with non-equilibrium situations in which there is an electronic current. One cannot talk in any simple way about the energy change of the screening cloud, as it is moved about, in the presence of the current.

Even if one discounts the direct electrostatic force on the Zn^{++} ion, it may still seem possible that a charged solute atom interacts with dilations, in a manner which is not satisfactorily represented by the usual picture (Cottrell 1953) of a misfitting atom, which produces elastic strains. After all, one does not convert a copper atom to a zinc atom, be inserting an extra layer of copper, as the usual elastic model presumes, but rather by adding an extra nuclear charge to a copper ion and simultaneously an extra electron to the conduction band. If this is to be represented by a classical elastic model, it seems more reasonable to consider the extra charges that have been added to the original copper matrix as providing localized body forces acting on the pure copper that was initially present.

We shall assume that these volume forces $\mathbf{f}(\mathbf{r})$, have radial symmetry about the solute ion, that the forces are directed radially, and exist in an isotropic medium with bulk modulus K. Then the change in volume of a finite sample, taking into account Eshelby's (1954) image terms can be shown to be

$$\delta V=\frac{1}{3K}\int \mathbf{f}(\mathbf{r})\cdot\mathbf{r}\,dV, \qquad . \quad . \quad . \quad . \quad (1)$$

where the range of integration can be limited to the small volume in which $\mathbf{f}(\mathbf{r})$ is appreciable. If we subject the copper matrix containing one set of these volume forces, to an externally applied dilation, $\varDelta_a$, then the work we do against the volume forces is

$$U_I=-\frac{\varDelta_a}{3}\int \mathbf{f}(\mathbf{r})\cdot\mathbf{r}\,dV=-\varDelta_a K(\delta V). \qquad . \quad . \quad . \quad . \quad (2)$$

In the more usual argument (Cottrell 1953) one pictures an inclusion which is too large for its cavity of radius r, by a factor $(1+\epsilon)$, where

$$\epsilon=\frac{1}{a}\frac{da}{dc}. \qquad . \quad . \quad . \quad . \quad . \quad . \quad . \quad . \quad (3)$$

In (3), a is the lattice constant of a dilute solution and c is the atomic concentration of solute atoms. The energy of interaction of this oversized atom with a hydrostatic pressure is then taken to be either

$$U_I=-4\pi\epsilon r^3 K\varDelta_a \qquad . \quad . \quad . \quad . \quad . \quad . \quad (4)$$

or else $3(1-\nu)/(1+\nu)$ times that value where ν is Poisson's ratio. The latter factor serves to include the strain energy in the solute atom. (3) combined with (4) yields

$$U_I=-\left(\frac{4}{3}\pi r^3 N\right)\left(\frac{3da}{aN\,dc}\right)\left(K\varDelta_a\right), \qquad . \quad . \quad . \quad (5)$$

where N is the total number of atoms in the specimen under consideration. The first factor in (5) is the volume under consideration. The second factor is the fractional change in volume that results from the addition of one solute atom. We therefore have $U_I=-K\varDelta_a\,(\delta V)$ in agreement with eqn. (2) which we found on the basis of the distributed force model.

The equation, $U_I = -K\Delta_a\ (\delta V)$, simply expresses the fact that if the energy of solution depends on the dilation of the lattice, then this energy dependence provides a force tending to change the crystal volume away from the value it has in the pure solvent. Consider a volume of copper into which the extra electron and nuclear charge are introduced to convert a Cu atom to Zn. Let this energy of conversion or solution be E_s, where E_s assumes that all copper nuclei are held in place. If we then permit the nuclear positions to relax, we can describe the relaxation by a set of coordinates β_i, in addition to a dilation Δ_r. The coordinates, β_i, are chosen so that in the pure copper matrix a dilation, Δ, does not simultaneously cause a change in the value of any of the β_i. Furthermore the β_i are taken to be zero in pure unstrained copper. The energy of a unit volume, containing n solute atoms can then be written

$$E = E_0 + nE_s + n\frac{\partial E_s}{\partial \Delta}\Delta_r + \sum_i n\frac{\partial E_s}{\partial \beta_i}\beta_i + \frac{1}{2}K\Delta_r^2 + \sum_{i,j}\omega_{ij}\beta_i\beta_i . \quad . \quad . \quad (6)$$

Here E_0 is the energy of the initial state, before the conversion. The last term gives the elastic energy associated with the β_i. If we permit relaxation we must have

$$\frac{\partial E}{\partial \Delta_r} = n\frac{\partial E_s}{\partial \Delta} + K\Delta_r = 0, \quad . \quad . \quad . \quad . \quad . \quad (7)$$

or

$$\frac{\partial E_s}{\partial \Delta} = -\frac{K\Delta_r}{n} = -K(\delta V). \quad . \quad . \quad . \quad . \quad . \quad (8)$$

Here, as before, δV is the volume change produced by a single conversion of copper to zinc. The interaction with an externally enforced dilation, Δ_a, is

$$U_I = \Delta_a\frac{\partial E_s}{\partial \Delta} = -\Delta_a K(\delta V) \quad . \quad . \quad . \quad . \quad (9)$$

in agreement with eqn. (2).

REFERENCES

COTTRELL, A. H., 1953, *Dislocations and Plastic Flow in Crystals* (Oxford: Clarendon Press), p. 56.

COTTRELL, A. H., HUNTER, S. C., and NABARRO, F. R. N., 1953, *Phil. Mag.*, **44**, 1064.

ESHELBY, J. D., 1954, *J. Appl. Phys.*, **25**, 255.

FRIEDEL, J., 1952, *Phil. Mag.*, **43**, 153.

SCHWARZ, K., 1940, *Elektrolytische Wanderung in flüssigen und festen Metallen* (Leipzig: Johann Ambrosius Barth).

Further Evidence for the β-Decay of K-Mesons

By C. Dahanayake,* P. E. Francois, Y. Fujimoto,† P. Iredale,
C. J. Waddington and M. Yasin
H. H. Wills Physical Laboratory, University of Bristol‡

[Received September 15, 1954]

An event has recently been reported from this laboratory which appears to be due to the decay of a K-meson into an electron of ∼ 90 Mev (Friedlander *et al.* 1954). In this letter we report a similar event in which the secondary electron has an energy of only 50 Mev. This event was found in the course of an investigation, currently proceeding in this laboratory, in which K-mesons emitted from stars are detected in stacks of stripped emulsions (Dahanayake *et al.* 1954, see also Report of Padua Conference 1954).

The primary particle, K_{46}, was emitted from a star of type 19+6p, and traversed five plates with a total range of 11·79 mm before coming to rest. All other tracks associated with the parent star, with grain-densities above plateau, have been examined and appear to be due to stable particles. The mass of the K-meson, measured by ionization-range is $970 \pm 100\, m_e$; by scattering-range (Menon and Rochat 1951, Menon and O'Ceallaigh 1954) $690 \pm 160\, m_e$; and by scattering-range using the constant sagitta method (Dilworth *et al.* 1954, Fay *et al.* 1954), $760 \pm 110\, m_e$.

The secondary particle, which has an ionization indistinguishable from the plateau value, traverses 23 plates with a total range of 25·6 mm before leaving the stack. Initially the length per plate of the secondary track is about 2 mm, but it becomes steeper, and just before leaving the stack the length per plate is only 0·8 mm.

For convenience the track was divided into 5 segments and blob density-scattering measurements were made on each. These results are shown in the table.

Scattering and Blob Density Measurement

Segment	Length/plate mm	Normalized blob density	Multiple scattering angle per 100 μ		$p\beta$ in Mev/c from $\alpha^{(3)}$
			$\alpha^{(2)}$	$\alpha^{(3)}$	
1	6·35/4 plates	1·00 ± 0·04	0·52 ± 0·04	0·46 ± 0·04	49 ± 4
2	5·36/4 plates	1·03 ± 0·08	0·64 ± 0·05	0·71 ± 0·06	31 ± 3
3	5·68/5 plates	1·06 ± 0·09	0·82 ± 0·06	0·70 ± 0·05	31 ± 2
4	3·96/5 plates	∼ 1	0·82 ± 0·08	0·70 ± 0·07	31 ± 3
5	3·76/5 plates	∼ 1	0·82 ± 0·09	1·26 ± 0·15	17 ± 2

$\bar{\alpha}^{(2)}$ is obtained from the second differences of coordinates, and $\bar{\alpha}^{(3)}$ from the third differences to eliminate distortion. The value of $p\beta$ is obtained from $\bar{\alpha}^{(3)}$.

---

* On leave of absence from the University of Ceylon.

† On leave of absence from the University of Kyoto.

‡ Communicated by Professor C. F. Powell, F.R.S.

Values of $\bar{\alpha}^{(2)}$ were obtained by noise-elimination, using the procedure of Daniel and Perkins. Values of $\bar{\alpha}^{(3)}$ obtained by the method of third differences are also quoted, as an indication of the comparative lack of distortion in the plates. A rigorous $4\bar{D}$-‘ cut off ’ was employed. The errors quoted are purely statistical.

Extensive measurements in the present stack of plates (Fowler and Perkins 1954) indicate that a μ-meson with an ionization near the plateau value must have a value of $p\beta$ greater than about 120 Mev/c. It therefore appears from the results obtained in the first segment alone, which provides the most favourable conditions for measurements, that the secondary particle is most probably an electron. This identification is supported by the results obtained from the other segments.

Since the observed track-length of 2·56 cm is $\sim$ 0·9 cascade units, we may expect an appreciable decrease in the value of $p\beta$ due to *bremsstrahlung* if the track is indeed due to an electron. The values of $p\beta$ obtained in the five segments of track are plotted in fig. 1 and may be compared with the expected variations due to (*a*) ionization loss alone, and (*b*) to ionization loss together with average *bremsstrahlung* losses. It appears that the particle has in fact suffered some *bremsstrahlung* loss.

Fig. 1

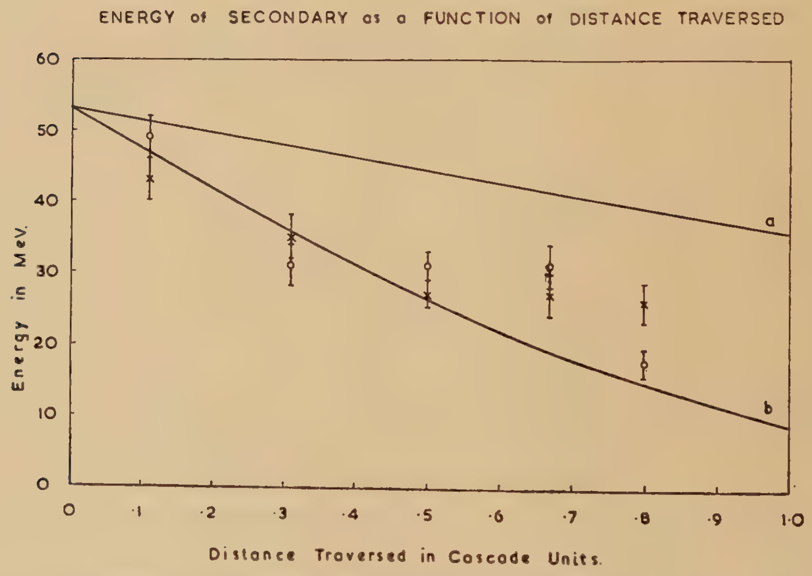

Plot of the energy of the secondary as a function of the distance traversed in cascade units. (*a*) shows the expected variation due to ionization loss alone, and (*b*) that due to ionization loss together with average *bremsstrahlung* losses. Points marked × show values calculated from 2nd differences, and those marked ○ values from 3rd differences.

The present event increases to four the number of heavy mesons which apparently undergo β-decay (Friedlander *et al.* 1954, O'Ceallaigh 1954). The spread of the $p\beta$ values in these events suggests that the β-decay of the K-meson is probably a three-body process. Since a secondary particle can be identified as an electron only if the initial value of $p\beta$ is very low, or if there is considerable *bremsstrahlung* loss, the results suggest that K-mesons not infrequently decay in this mode.

REFERENCES

DAHANAYAKE, FRANCOIS, FUJIMOTO, IREDALE, WADDINGTON, and YASIN, 1954, *Phil. Mag.*, **45**, 855.
DANIEL, and PERKINS, 1954, *Proc. Roy. Soc.*, **221**, 351.
DILWORTH, GOLDSACK, and HIRSCHBERG, 1954, *Nuovo Cim.*, **11**, 113.
FAY, GOTTSTEIN, and HAIN, 1954, *Nuovo Cim.*, Suppl. **11**, 235.
FOWLER, and PERKINS, 1954, private communication.
FRIEDLANDER, KEEFE, MENON, and VAN ROSSUM, 1954, *Phil. Mag.*, **45**, 1043.
MENON, and O'CEALLAIGH, 1954, *Proc. Roy. Soc.*, **221**, 292.
MENON, and ROCHAT, 1951, *Phil. Mag.*, **42**, 1232.
O'CEALLAIGH, private communication.
REPORT PADUA CONFERENCE, 1954, *Nuovo Cim.*, Suppl. to Vol. XII., in the press.

Paramagnetic Resonance at Radio Frequencies in Low Temperature Carbons

By D. J. E. INGRAM and J. G. TAPLEY
Department of Electronics, University of Southampton

[Received September 21, 1954]

IN order to confirm (Ingram and Bennett 1954, Castle 1954 a, Bennett *et al.* 1954) that two distinct types of paramagnetic resonance absorption occur in different kinds of carbon we have now made measurements in the radio frequency region of 25–50 Mc/s. The apparatus used is a modification of Pound and Knight's nuclear spectrometer (1950), the carbon samples filling the inductive coil, which has a volume of about 0·5 cm^3. The magnetic field is obtained from a Helmholtz coil-pair fed with current at 50 c/s, no steady d.c. field being produced. Since the magnetic field strength required for resonance at these frequencies is only of the order of 15 gauss, the modulating field, of some ±20 gauss amplitude, will go through resonance at each side of zero, and hence two absorption lines are obtained on the oscilloscope screen, as seen in the figure. The frequency of the absorbed radiation (ν) is measured by a crystal-controlled wavemeter. This determination also acts as a direct calibration of the magnetic field, since the spectroscopic splitting factor of the carbon samples is the same as that of the hydrazyl marker to within ±0·001, and hence the separation between the centres of the two resonant lines is given by $2h\nu/g\beta$ ($=7{\cdot}178\times10^{-7}\nu$ gauss).

The photographs shown in the figure are the resonances obtained from (i) diphenyl trinitrophenyl hydrazyl, (ii) powdered, activated, decolourizing charcoal, (iii) coal carbonized at 550°C, this being the carbonizing temperature which produces the highest free-radical concentration (Ingram *et al.* 1954). The different widths of all three samples can be clearly seen, and the measured values for full width at half-power are (i) $2{\cdot}5 \pm 0{\cdot}5$ gauss, (ii) $4{\cdot}5 \pm 2{\cdot}0$ gauss and (iii) $8 \pm 2{\cdot}0$ gauss. The fact that the widths of the resonances from the two different carbon samples are still the same as those observed at microwave frequencies (Bennett *et al.* 1954) is in striking contrast to the results obtained by Henning *et al.* (1954) on graphites; where the width changed from the 8 to 40 gauss, observed by Castle (1953, 1954 b) at 9000 Mc/s, to 0·1 gauss at radio frequencies. Any increase in width due to random size, or orientation, of the particles is ruled out by the fact that both carbon samples have the same range of particle size, and previous measurements on graded sizes have shown no change in width (Bennett *et al.* 1954).

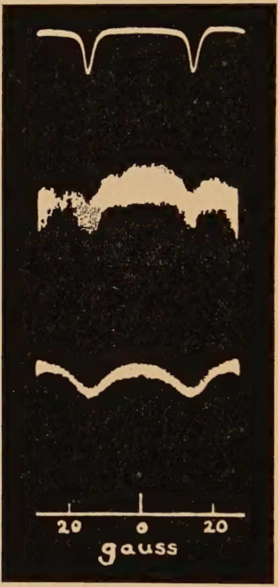

Paramagnetic Resonance Absorptions at 40 Mc/s.
Top: Diphenyl trinitrophenyl hydrazyl
Centre: Activated, decolourizing charcoal
Bottom: Coal, carbonized at 550°C

These low frequency measurements therefore confirm the suggestion (Bennett *et al.* 1954) that there are two different mechanisms responsible for paramagnetic absorption in carbon. (i) In carbons which have not been heated above 650°C there is a resonance due to free radicals, or 'broken bonds', in the carbon structure, this normally having a width of 8 gauss, independent of frequency of absorption ; and (ii) in graphites, formed above 1200°C, there is a resonance from the conduction electrons in the two-dimensional plane, the width of this absorption varying markedly with frequency. This difference is also supported by the recent measurements of signal strength against carbonizing temperature (Ingram *et al.* 1954).

The reason for the reduced line width in the decolourizing charcoal is still not clear, but is thought to be due to the presence of adsorbed oxygen, and further measurements are in progress to clarify this point.

REFERENCES

BENNETT, J. E., INGRAM, D. J. E., and TAPLEY, J. G., 1954, *Report of Bristol Conference on Defects in Solid State* (London : Physical Society).

CASTLE, J. G., 1953, *Phys. Rev.*, **92,** 1063 ; 1954 a, *Ibid.*, **94,** 1410 ; 1954 b, *Ibid.*, **95,** 846.

HENNING, F. R., SMALLER, B., and YASAITIS, E. L., 1954, *Phys. Rev.*, **95,** 1088.

INGRAM, D. J. E., and BENNETT, J. E., 1954, *Phil. Mag.*, **45,** 545.

INGRAM, D. J. E., TAPLEY, J. G., JACKSON, R., BOND, R. L., and MURNAGHAN, A. R., 1954, *Nature, Lond.* (in the press).

POUND, R. V., and KNIGHT, W. D., 1950, *Rev. Sci. Instrum.*, **21,** 219.

CXXXVII. *Notices of New Books and Periodicals received*

The Concise History of Mathematics. By Dirk J. Struik. (G. Bell and Sons Ltd.) [Pp. xix+299.] Price 14*s.*

This book gives a short account of the history of mathematics from the earliest times to the year 1900. The work is based on sound scholarship and is likely to become the standard book on the subject. The author has managed to give a balanced account of all the important periods in the development of mathematical thought. Owing to limitations of space the author is not in a position to discuss controversial questions at great length, or to point out the large number of unsolved problems which may offer scope for successful research.

Though the author displays sound judgement in most places, the reviewer is not convinced by his arguments on the relatively undeveloped state of formal algebra in classical Greece. In particular the sentence " If the classical authors had been interested in algebra they would have created the appropriate symbolism with which Diophantos actually made a beginning " (p. 80) appears to be highly dogmatic. The author tries to point out relations between social changes and changes in the trend of mathematical research in various communities. As he has not the space at his disposal to develop these difficult problems in greater detail, these passages do not enlighten the reader to a considerable extent.

At the end of each chapter the author gives a good bibliography. The value of the book is further enhanced by a carefully compiled index.

H. H.

Optical Aberration Coefficients. By H. A. Buchdahl. (Oxford: University Press.) [Pp. 336.] Price 50*s.*

Royal Society Mathematical Tables. 3. *Binomial Coefficients.* (Cambridge: University Press.) [Pp. 162.] Price 35*s.*

Royal Society Shorter Mathematical Tables. 3. *Bessel Functions of Integer Orders and Large Arguments.* By L. Fox. (Cambridge: University Press.) Price 6*s.* 6*d.*

Elements of Statistical Mechanics. By D. ter Haar. (Rinehart & Company Inc.) [Pp. 468.] Price $8.50.

Atomphysik III and IV. By K. Bechert. (Berlin: Walter de Gruyter.) Price D.M. 4.80 each.

Statistical Analysis in Chemistry and the Chemical Industry. By Carl A. Bennett and Norman L. Franklin. (Wiley Publications in Statistics.) Price 58*s.*

Sound. By R. C. Brown. (Longmans, Green and Co.)

The Method of Trigonometrical Sums in the Theory of Numbers. By I. M. Vinogradov. (Interscience Publishers, Ltd.) Price 33*s.*

Gas Dynamics of Thin Bodies. By F. I. Frankl and E. A. Karpovich. (Interscience Publishers, Ltd.) Price 38*s.*

A Selection of Graphs for Use in Calculations of Compressible Airflow by the Compressible Flow Tables Panel. (Oxford: University Press.) Price 84*s.*

[*The Editors do not hold themselves responsible for the views expressed by their correspondents.*]